Identification of the Functional Mechanisms of Alcohol–Wnt Signaling Pathway Interactions in Taste Sensory Organ Development: Insight from the Mexican Tetra (*Astyanax mexicanus*)

By
Gandhrav Goel

A Thesis submitted to the Faculty of Graduate and
Postdoctoral Studies of The University of Manitoba
in partial fulfillment of the requirements of the degree
of Master of Science

Department of Oral Biology
Dr. Gerald Niznick College of Dentistry
Rady Faculty of Health Sciences
University of Manitoba
Winnipeg

Abstract

Animal models provide critical insight into conserved mechanisms underlying development and disease. The Mexican tetra (*Astyanax mexicanus*), which exists as both surface and cave morphs, offers a powerful system to study craniofacial and sensory development. Canonical Wingless/Integrated beta-catenin (Wnt/β-catenin) signaling is an important cell signaling pathway in early embryonic development and its disruption is implicated in various birth defects. Prenatal alcohol exposure (PAE) has been consistently associated with characteristic birth defects, categorized as Fetal Alcohol Spectrum Disorders (FASD). Alcohol exposure during embryogenesis suppresses both canonical and non-canonical Wnt signaling, associated with craniofacial abnormalities, while folic acid has been shown to minimise the early developmental defects.

This study examined how alcohol exposure affects taste bud formation and gustatory associated chemoattractive behaviour, and whether modulation of Wnt signaling or folic acid supplementation alters these outcomes in surface fish (SF) and cavefish (CF) morphs. Embryos were exposed to ethanol (EtOH), Lithium chloride (LiCl) (Wnt activator), Wnt-C59 (WC-59) (Wnt inhibitor), or folic acid 10 hours post-fertilization (hpf). Taste bud patterning and distribution was assessed across larval stages at 8, 15 and 30 days post-fertilization (dpf) using live whole mount Ponceau S stain. The chemosensory attractive behaviour was assessed using the various taste stimulants in DanioVision observation system.

CF consistently exhibited increased taste bud size and broader spatial distribution compared to SF, with divergence becoming more pronounced over development. Regional analysis revealed

sequential emergence of taste bud subtypes, with T1, T3, and T4 appearing earlier, while T2 emerged later and was observed exclusively in CF within the stages examined. These findings suggest that differences in developmental timing and spatial organization underlie morph-specific sensory architectures. Across both surface and cave morphs of Mexican tetra, chemical perturbation of canonical Wnt signaling resulted in only limited and inconsistent effects on gustatory morphology. Although minor stage-specific differences were detected, these changes were not maintained across developmental stages or anatomical regions. Behavioral responses were similarly resilient to treatment, as chemoattractive behavior showed no consistent alterations in time spent near feed, distance to feed, or locomotor activity. Together, these findings suggest that modulation of canonical Wnt signaling has a minimal impact on taste bud development and feeding-related behavior in either morph under the conditions tested. Instead, behavioral outcomes were strongly morph-dependent: SF exhibited more variable and exploratory movement patterns, whereas CF demonstrated more consistent feed engagement and elevated locomotor activity.

Overall, intrinsic differences between morphs were the dominant factor shaping both gustatory morphology and chemoattractive behaviour, indicating that these traits are robust to short-term developmental perturbation. These results suggest that sensory system organization in *Astyanax mexicanus* is primarily governed by developmental programming and evolutionary adaptation rather than acute modulation of signaling pathways under the conditions tested.

Acknowledgments

I would like to express my deepest gratitude to my supervisor, Dr. Devi Atukorallaya, for the opportunity to pursue my passion for children's health. Her guidance, encouragement, and patience over the past two and a half years were invaluable. Even during challenging moments, she remained supportive and ensured my project stayed on the right path. This work would not have been possible without her mentorship.

I sincerely thank my committee members, Dr. Prashen Chelikani and Dr. Samantha Pauls, for their insightful feedback and guidance. Their expertise and support have strengthened this research and contributed significantly to my development as a researcher.

I also extend my gratitude to the Head of the Department, Dr. James Gilchrist, and the academic staff for their support throughout my studies.

I am grateful to my lab mates Zheng Fang, Nafees Zahra Rizvi, Sophie Chen, Tanzelela Ahmed, and Rosa Iranpour for their scientific input, assistance, and support. Their collaboration not only contributed to this work but also made the lab an enjoyable and welcoming environment.

I would also like to thank Nisha for her help with laboratory work and equipment, and Mahamudul, Arian, Bukky, and Mani for the memorable experiences and friendships that made this journey meaningful.

Lastly, I acknowledge the University of Manitoba and the Natural Sciences and Engineering Research Council of Canada (NSERC) for their financial support.

Dedication

I dedicate this thesis to my family and loved ones for their unwavering support and understanding throughout my academic journey. I am also grateful to my friends for their constant encouragement, for keeping me focused on my goals, and for supporting me every step of the way.

Especially, this thesis is dedicated to my dear sister, Ria Goel, for her unwavering support, encouragement, and belief in me throughout this journey.

I would like to offer a special dedication to my mother, Siloni Goel, and father Rajesh Kumar Gupta for their financial support and for easing the burdens that made this achievement possible.

TABLE OF CONTENTS

ABSTRACT ii

ACKNOWLEDGEMENT iv

DEDICATION v

TABLE OF CONTENTS vi

LIST OF FIGURES viii

LIST OF ABBREVIATIONS xiv

CHAPTER 1: INTRODUCTION 1

1.1 Animal Models and *Astyanax mexicanus* 2

1.2 Fetal Alcohol Spectrum Disorder 3

1.3 Taste Bud Development 4

1.4 Alcohol Teratogenicity 6

1.5 Wnt Signaling Pathway 7

1.6 Mechanisms of Wnt Modulators (LiCl, WC-59, Folic Acid) 10

CHAPTER 2: HYPOTHESIS, OBJECTIVES, AND RATIONALE 11

2.1 Hypothesis 12

2.2 Objectives and Rationale 12

CHAPTER 3: MATERIALS AND METHODS 15

3.1 Fish Husbandry and Breeding – Astyanax mexicanus 16

3.1.1 Maintenance 16

3.1.2 Feeding and Priming 16

3.1.3 Breeding and Embryo Collection 17

3.1.4 Larval Rearing and Experimental Use 18

3.2 Fish Rearing and Chemical Treatments – *Astyanax mexicanus* 18

3.2.1 Chemical Treatment Protocol 18

3.2.2 Larval Rearing Conditions 19

3.2.3 Sample Collection and Experimental Timepoints 20

3.3 Morphological Assays 21
3.3.1 Ponceau S Staining Protocol 21
3.3.2 Taste Bud Quantification and Spatial Analysis 22
3.3.3 Behavioural Analysis 25
3.3.3.1 Locomotor Activity 26
3.3.3.2 Gustatory Behaviour 26
3.4 Statistical Analysis 28
CHAPTER 4: RESULTS 29
4.1 Whole Mount Taste Bud Ponceau S Staining 30
4.2 Taste Bud Count 33
4.3 Taste Bud Diameter 36
4.4 Regional Taste Bud Analysis (T1–T4) 39
4.5 Spatial Distribution and Bilateral Symmetry Analysis 50
4.6 Behavioral Assay – Locomotor Activity and Feeding Behaviour 60
CHAPTER 5: DISCUSSION 92
CHAPTER 6: CONCLUSION 106
Appendix 109
References 114

List of FIGUREs

FIGURE 1.1: Schematic representation of canonical Wnt- β-catenin Signaling pathway...... 9

FIGURE 3.1: Schematic representation of the ventral mandible of *Astyanax mexicanus* following Ponceau S staining, illustrating the standardized regions used for taste bud analysis...... 24

FIGURE 3.2: Behavioral setup for 30 days post fertilization *Astyanax mexicanus* within 9 cm petri dish containing 1 cm cubic agar feeding blocks submerged within standardized system water. 27

FIGURE 4.1: Live Ponceau S staining of the ventral mandibular surface in cavefish across developmental stages and treatment conditions. 31

FIGURE 4.2: Live Ponceau S staining of the ventral mandibular surface in surface fish across developmental stages and treatment conditions. 32

FIGURE 4.3 Mandibular taste bud counts across treatment conditions in Pachón cavefish compared to surface fish controls during larval development. 34

FIGURE 4.4: Mandibular taste bud counts across treatment conditions in surface fish compared to Pachón cavefish controls during larval development. 35

FIGURE 4.5: Mandibular taste bud diameter across treatment conditions in Pachón cavefish compared to surface fish controls during larval development. 37

FIGURE 4.6: Mandibular taste bud diameter across treatment conditions in surface fish compared to Pachón cavefish controls during larval development. 38

FIGURE 4.7: T1 taste bud diameter across treatment conditions in Surface fish compared to Pachón cavefish control during larval development. 40

FIGURE 4.8: T1 taste bud diameter across treatment conditions in Pachón cavefish compared to Surface fish control during larval development. 41

FIGURE 4.9: T2 taste bud diameter across treatment conditions in Pachón cavefish during larval development. 43

FIGURE 4.10: T3 taste bud diameter across treatment conditions in Surface fish compared to Pachón cavefish control during larval development. 45

FIGURE 4.11: T3 taste bud diameter across treatment conditions in Pachón cavefish compared to Surface fish control during larval development. 46

FIGURE 4.12: T4 taste bud diameter across treatment conditions in Surface fish compared to Pachón cavefish control during larval development. 48

FIGURE 4.13: T4 taste bud diameter across treatment conditions in Pachón cavefish compared to Surface fish control during larval development. 49

FIGURE 4.14: Bilateral distance between left and right T1 taste bud regions across treatment conditions in Surface fish compared to Pachón cavefish control during larval development. .51

FIGURE 4.15: Bilateral distance between left and right T1 taste bud regions across treatment conditions in Pachón cavefish compared to Surface fish control during larval development. .52

FIGURE 4.16: Bilateral distance between T1-T2 taste bud regions across treatment conditions in Pachón cavefish during larval development. 54

FIGURE 4.17: Bilateral distance between T2-T3 taste bud regions across treatment conditions in Pachón cavefish during larval development. 56

FIGURE 4.18: Bilateral distance between T3-T4 taste bud regions across treatment conditions in Surface fish compared to Pachón cavefish control during larval development. 58

FIGURE 4.19: Bilateral distance between T3-T4 taste bud regions across treatment conditions in Pachón cavefish compared to Surface fish control during larval development. 59

FIGURE 4.20: Behavioral heatmaps showing swimming patterns of Pachón cavefish and surface fish. 61

FIGURE 4.21: Chemosensory feeding behavior associated with average distance from feed for untreated surface and cavefish larvae. 63

FIGURE 4.22: Chemosensory feeding behavior associated with average distance from feed for EtOH treated surface and cavefish larvae. 64

FIGURE 4.23: Chemosensory feeding behavior associated with average distance from feed for folic acid treated surface and cavefish larvae. 65

FIGURE 4.24: Chemosensory feeding behavior associated with average distance from feed for LiCl treated surface and cavefish larvae. 66

FIGURE 4.25: Chemosensory feeding behavior associated with average distance from control feed across treatment conditions in surface and cave morph larvae. 68

FIGURE 4.26: Chemosensory feeding behavior associated with average distance from EtOH feed across treatment conditions in surface and cave morph larvae. 69

FIGURE 4.27: Chemosensory feeding behavior associated with average distance from quinine feed across treatment conditions in surface and cave morph larvae. 70

FIGURE 4.28: Chemosensory feeding behavior associated with average distance from sucrose feed across treatment conditions in surface and cave morph larvae. 71

FIGURE 4.29: Chemosensory feeding behavior associated with average time near feed for untreated surface and cavefish larvae. …… 73

FIGURE 4.30: Chemosensory feeding behavior associated with average time near feed for EtOH treated surface and cavefish larvae. …… 74

FIGURE 4.31: Chemosensory feeding behavior associated with average time near feed for folic acid treated surface and cavefish larvae. …… 75

FIGURE 4.32: Chemosensory feeding behavior associated with average time near feed for LiCl treated surface and cavefish larvae. …… 76

FIGURE 4.33: Chemosensory feeding behavior associated with average time near control feed across treatment conditions in surface and cave morph larvae. …… 78

FIGURE 4.34: Chemosensory feeding behavior associated with average time near EtOH feed across treatment conditions in surface and cave morph larvae. …… 79

FIGURE 4.35: Chemosensory feeding behavior associated with average time near quinine feed across treatment conditions in surface and cave morph larvae. …… 80

FIGURE 4.36: Chemosensory feeding behavior associated with average time near sucrose feed across treatment conditions in surface and cave morph larvae. …… 81

FIGURE 4.37: Chemosensory feeding behavior associated with average velocity of untreated surface and cavefish larvae. …… 83

FIGURE 4.38: Chemosensory feeding behavior associated with average velocity of EtOH treated surface and cavefish larvae. …… 84

FIGURE 4.39: Chemosensory feeding behavior associated with average velocity of folic acid treated surface and cave morph larvae. …… 85

FIGURE 4.40: Chemosensory feeding behavior associated with average velocity of LiCl treated surface and cavefish larvae. …… 86

FIGURE 4.41: Chemosensory feeding behavior associated with average velocity within control feed across treatment conditions in surface and cave morph larvae. …… 88

FIGURE 4.42: Chemosensory feeding behavior associated with average velocity within EtOH feed across treatment conditions in surface and cave morph larvae. …… 89

FIGURE 4.43: Chemosensory feeding behavior associated with average velocity within quinine feed across treatment conditions in surface and cave morph larvae. …… 90

FIGURE 4.44: Chemosensory feeding behavior associated with average velocity within sucrose feed across treatment conditions in surface and cave morph larvae. …… 91

List of Abbreviations

PAE – Prenatal Alcohol Exposure

FASD – Fetal Alcohol Spectrum Disorder

Wnt – Wingless/Integrated signaling pathway

β-catenin – Beta-catenin

CNCC – Cranial Neural Crest Cells

hpf – Hours Post-Fertilization

dpf – Days Post-Fertilization

SF – Surface Fish

CF – Cavefish

LiCl – Lithium Chloride

PORCN – Porcupine (O-acyltransferase enzyme)

GSK3β – Glycogen Synthase Kinase 3 Beta

APC – Adenomatous Polyposis Coli

CK1 – Casein Kinase 1

LRP5/6 – Low-Density Lipoprotein Receptor-Related Protein 5/6

TCF/LEF – T-cell Factor / Lymphoid Enhancer Factor

PCP – Planar Cell Polarity

Shh – Sonic Hedgehog

BMP – Bone Morphogenetic Protein

FGF – Fibroblast Growth Factor

T1R – Taste Receptor Type 1

T2R – Taste Receptor Type 2

OTOP1 – Otopetrin 1

SAM – S-adenosylmethionine

EtOH – Ethanol

MS-222 – Tricaine Methanesulfonate

TCA – Trichloroacetic Acid

μS – Microsiemens

pH – Potential of Hydrogen

CAS – Chemical Abstracts Service

FDR – False Discovery Rate

Chapter 1: Introduction

1.1 Animal Models and *Astyanax mexicanus*

Animal-based research has a long and influential history, extending back more than 2,400 years, forming the foundation of our understanding of human biology and disease[1]. The comparative approach, later formalized by August Krogh, established that specific biological problems are best studied in the most suitable organism[1]. This principle continues to guide modern biomedical research, where animal models are widely used due to their conserved genetic, anatomical, and physiological similarities to humans[2].

Commonly used systems such as murine models provide substantial genetic homology and experimental accessibility; however, limitations remain, as interspecies differences in gene regulation, metabolism, and environmental adaptation can affect disease progression and translational outcomes[3–8]. Advances in genetic technologies, including CRISPR-Cas9, have strengthened the utility of animal models by enabling precise genetic manipulation and the development of transgenic or humanized systems[1,9]. At the same time, ethical and practical constraints particularly in studying human embryonic development have encouraged the integration of alternative approaches such as in vitro and computational models, in line with the principles of replacement, reduction, and refinement[4,6,10,11].

Despite the widespread use of traditional mammalian systems, increasing emphasis has been placed on incorporating evolutionarily diverse organisms to better capture conserved biological processes and uncover novel disease mechanisms[36]. Teleost models, including zebrafish, demonstrate broad utility across developmental, metabolic, immune, and neurobehavioral studies and are particularly well suited for high throughput genetic and chemical screening[8,9,12].

This diversification of model organisms expands the comparative framework and enhances the ability to investigate complex developmental pathways.

More recently, the Mexican tetra (*Astyanax mexicanus*) has emerged as a powerful evolutionary model organism. *Astyanax mexicanus* consists of two distinct subtypes, the surface fish (SF) and the cavefish (CF). CF being further distinguished by the specific cave systems that they inhabit examples such as Molino, Pachón and Tinaja caves[13]. Due to the years of being in separate environments, SF and CF have evolved separate phenotypic traits to better suit their environment[14–16,]. SF are found within fresh water and are characterized with silver and gray pigmentation. CF on the other hand are found within Mexican cave systems characterized as unpigmented, eyeless or blind[14–16]. Both of which in the recent years has started to become an established popular choice for developmental studies, specifically craniofacial birth defects and bone diseases[14].

For example, CF skull morphology and craniofacial asymmetries have been characterized as analogs to human craniofacial anomalies, demonstrating the organism's utility for studying bone patterning and skeletal development[17]. Genetic mapping has further identified loci associated with jaw shape, bite differences and tooth number between morphs, providing insight into genetic regulation of orofacial traits[18]. In addition to craniofacial differences, sensory system adaptations have also been extensively characterized between morphs, with CF exhibiting enhanced mechanosensory lateral line neuromast structures compared to SF, reflecting compensatory evolution in the absence of vision[19]. Due to the conserved nature of craniofacial developmental processes between vertebrates, the *Astyanax mexicanus* can be considered a

valid model to study craniofacial bone diseases such as cleft palate and cranial development as a whole[14,20].

In addition to craniofacial traits, differences in sensory systems have also been observed between morphs. CF show accelerated development and increased distribution of taste buds compared to SF making them a relevant model for taste system development[17]. In addition prior findings have reported CF possessing a greater repertoire of bitter taste receptors, suggesting chemosensory adaptation beyond the oral cavity, and broader shifts in chemosensory traits between the two morphs[18,21].

1.2 Taste Bud Development

Taste buds are specialized neurosensory organs that are utilized in the perception of foods and survival, through detection of essential nutrients such as carbohydrates for energy (sweet receptors), amino acids (umami receptors), maintenance of electrolytic balance (salt perception), and avoidance of harmful substances through perception of bitterness and sour. In humans, they are organized within onion shaped structures called papillae classified into fungiform, circumvallate, and foliate papillae[22,23].

Fungiform papillae are distributed mainly on the anterior two thirds of the tongue and contain taste buds sensitive to sweet, salty, and umami tastes. Circumvallate papillae form a V-shaped row at the posterior tongue and have a high density of taste buds primarily tuned to bitter stimuli[18]. Foliate papillae are located on the lateral aspects of the posterior tongue and contribute to sour and bitter taste detection[23].

Unlike other sensory structures, taste buds retain their regenerative capacity throughout life, with basal epithelial propagation occurring approximately every 10–14 days[23,24]. Dysregulation

of taste bud development or maintenance can influence appetite, food preference, and feeding behaviour, contributing to taste dysfunction such as dysgeusia or ageusia[25].

Taste bud formation begins during embryogenesis with the appearance of epithelial placodes on the dorsal tongue, which give rise to fungiform papillae and establish spatial patterning[26,27]. While taste receptor cells arise from local epithelium, cranial neural crest cell (CNCC) derived mesenchyme contributes to tongue connective tissue and interacts with epithelial domains to regulate papilla positioning and morphogenesis[28,29].

It has long been thought that taste buds arise exclusively from local epithelium; however, newer work has identified indirect roles of CNCCs through epithelial–mesenchymal interactions[22,30,31]. These interactions are mediated by conserved developmental pathways such as Sonic hedgehog (Shh), Bone Morphogenetic Protein (BMP), Fibroblast Growth Factor (FGF), and Wingless/Integrated β-catenin (Wnt) signaling pathway [26,27].

Mechanistically, taste perception is mediated by receptor types present within taste buds. Sweet and umami compounds are detected by Taste Receptor Type 1 (T1R) heterodimeric G protein-coupled receptors, while bitter compounds are detected by Taste Receptor Type 2 (T2R) receptors[22]. Sour taste perception is mediated by Otopetrin 1 (OTOP1) proton channels, and sodium ion channels are associated with salt detection[32,33].

Prior literature has shown shared developmental signaling pathways between taste bud patterning and craniofacial structures, particularly involving Wnt/β-catenin signaling[26,28].

In teleost models such as *Astyanax mexicanus*, taste bud development exhibits divergence between morphs, where CF display increased taste bud number and accelerated development

relative to SF[17]. CF also possess an expanded repertoire of bitter taste receptors, suggesting enhanced chemosensory adaptation[18,21].

1.3 Fetal Alcohol Spectrum Disorder

Fetal alcohol spectrum disorder (FASD) encompasses a range of developmental abnormalities resulting from prenatal alcohol exposure (PAE), including growth restriction, craniofacial malformations, neurodevelopmental deficits, and long-term behavioral impairments[34–36]. Alcohol readily crosses the placenta and accumulates in the amniotic fluid due to the limited metabolic capacity of the fetus, prolonging embryonic exposure during critical windows of development[34]. The severity and spectrum of outcomes are influenced by factors such as timing, dosage, and genetic susceptibility.

A hallmark feature of FASD is the disruption of craniofacial development, which is largely mediated through impairment of CNCC survival, migration, and differentiation. Experimental studies have demonstrated that EtOH exposure interferes with key developmental signaling pathways, particularly canonical Wnt/β-catenin signaling, resulting in increased apoptosis of neural crest progenitors and subsequent craniofacial abnormalities[37,38]. This disruption contributes to characteristic phenotypes such as midfacial hypoplasia, cleft palate, and dental defects observed in organisms such as the zebrafish[39–43].

Beyond structural abnormalities, emerging evidence indicates that PAE also affects sensory system development, including chemosensory pathways involved in taste and olfaction. Mammalian studies have shown that PAE alters neural processing of taste and odor cues, leading to increased postnatal acceptance and preference for EtOH[44]. Similarly, human cohort studies

report that individuals with documented PAE exhibit altered perception of alcohol related odors and increased likelihood of alcohol use later in life[45,46].

At the molecular level, EtOH exerts its teratogenic effects through multiple mechanisms, including oxidative stress, mitochondrial dysfunction, disruption of retinoic acid signaling, and epigenetic modifications[34,36]. Importantly, suppression of Wnt/β-catenin signaling represents a critical mechanistic link between EtOH exposure and impaired craniofacial and sensory development.

1.4 Alcohol's teratogenicity

Alcohol and its primary metabolite acetaldehyde act as teratogens. Alcohol readily crosses the placenta and accumulates in the amniotic fluid due to the limited metabolic capacity of the fetus[47].

EtOH exerts teratogenic effects through multiple mechanisms, including oxidative stress, mitochondrial dysfunction, disruption of retinoic acid metabolism, protein synthesis, and epigenetic dysregulation[47,48].

Importantly, alcohol suppresses canonical Wnt/β-catenin signaling during early embryogenesis. In chick embryos, alcohol exposure triggers intracellular Ca^{2+} release in pre-migratory neural crest progenitors, leading to depletion of nuclear β-catenin and apoptosis of neural crest cells[38]. Stabilization of β-catenin rescues neural crest survival, directly implicating Wnt suppression as a mechanistic driver of alcohol induced craniofacial defects[38].

Because neural crest cells are critical for craniofacial and oral development, alcohol mediated suppression of Wnt signaling provides a mechanistic link between PAE and craniofacial anomalies.

1.5 Wnt signaling pathway.

The Wnt signaling pathways consist of a family of glycoproteins that are highly evolutionarily conserved, governing cell proliferation, and migration during embryonic development[49]. Disruption in Wnt signalling has been shown to lead to bone diseases [50,51]. In vertebrate craniofacial development, precise spatial and temporal regulation of Wnt activity is essential for neural crest induction, maintenance, and differentiation, as well as for coordinated epithelial–mesenchymal interactions that shape the facial primordia[52,53].

Wnt signaling functions through two major branches: the canonical (β-catenin dependent) and non-canonical (β-catenin independent) pathway.

Canonical Wnt signaling operates through stabilization of β-catenin, primarily regulates gene transcription and cell fate decisions. In the absence of Wnt ligand β-catenin is phosphorylated by a destruction complex composed of Axin, Adenomatous Polyposis Coli (APC), Casein Kinase 1 (CK1), and glycogen synthase kinase 3β (GSK3β), targeting it for ubiquitin mediated degradation. Ligand binding to frizzled receptors and Low-Density Lipoprotein Receptor-Related Protein 5/6 (LRP5/6) co-receptors disrupts this complex, permitting β-catenin accumulation and nuclear translocation, where it interacts with T-cell Factor / Lymphoid Enhancer Factor (TCF/LEF) transcription factors to regulate gene expression critical for lineage specification (FIGURE 1.1)[51,54–56].

Non-canonical Wnt signaling (β-catenin-independent) pathways include the planar cell polarity (PCP) and Wnt/Ca^{2+} pathways, which regulate cellular processes independently of β-catenin-mediated transcription[54]. The PCP pathway is activated through Frizzled receptors and downstream effectors such as Dishevelled (Dvl), RhoA, Rac1, and c-Jun N-terminal kinase (JNK), resulting in cytoskeletal reorganization and the establishment of cellular polarity within tissues[54]. In contrast, the Wnt/Ca^{2+} pathway promotes intracellular calcium release, activating calcium-sensitive signaling molecules including protein kinase C (PKC), calcium/calmodulin-dependent protein kinase II (CaMKII), and calcineurin[54]. Through these downstream effectors, non-canonical Wnt signaling regulates cell migration, tissue morphogenesis, and coordinated cellular movements during embryonic development, particularly important during neural crest cell migration, where precise control is required for craniofacial and sensory organ development[52,54–56].

During craniofacial development, Wnt signaling is critical for the induction, migration, and differentiation of neural crest cells, a transient multipotent cell population that gives rise to much of the craniofacial mesenchyme, including bone, cartilage, connective tissue, and components of the oral cavity[53,57,58]. Disruption of these processes leads to abnormal facial patterning and structural defects.

Wnt signaling is also required for epithelial placode formation and taste papilla patterning. Canonical Wnt/β catenin signaling initiates fungiform papilla development and regulates papilla number and spacing[26,28].

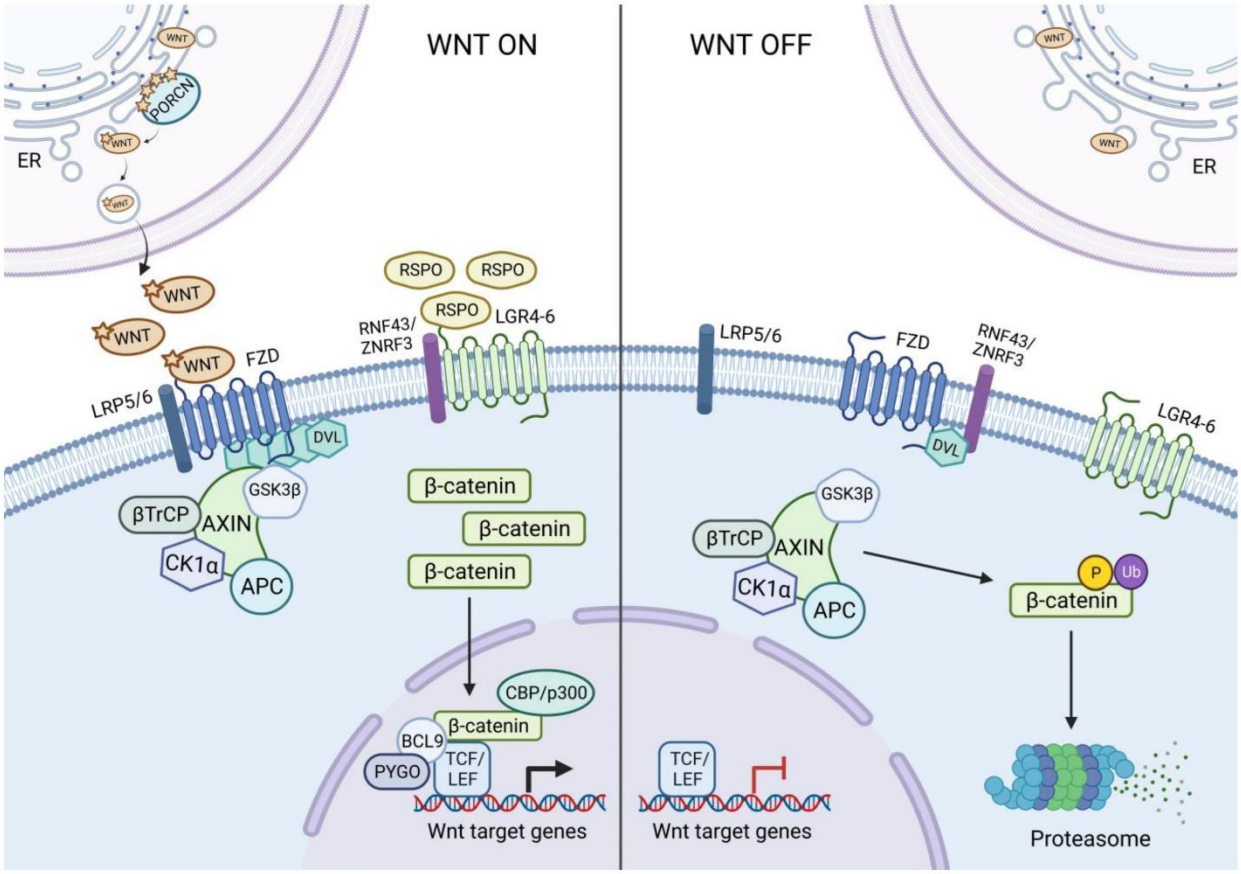

FIGURE 1.1: Schematic representation of canonical Wnt- β-catenin Signaling pathway. Active and inactive states of canonical Wnt signaling pathway. Canonical pathway activation can be seen through Wnt ligand secretion via PORCN induced release, and ligand binding through frizzled receptors (FZD) inducing cytoplasmic release from degradation of β-catenin leading to downstream Wnt target gene transcription (Left Panel). As well as ligand inhibited deactivation of the pathway (right panel). Illustrating overall areas of pharmacological interventions and effects upon Wnt pathway regulated genes[59].

1.6 Mechanisms of Wnt Modulators (LiCl, WC-59, Folic Acid)

Lithium Chloride (LiCl) is a pharmacological activator of the canonical Wnt signaling pathway. Mechanistically LiCl acts by inhibiting GSK3β (FIGURE 1.1), preventing β-catenin phosphorylation and degradation, thereby stabilizing β-catenin and enhancing transcription of Wnt target genes[60].

In opposition, Wnt-C59 (WC-59) inhibits porcupine (PORCN), an acyltransferase required for palmitoylation and secretion of the Wnt ligand (FIGURE 1.1). Therefore due to the blockage Wnt ligand secretion, WC-59 directly supresses canonical Wnt signaling and downstream transcription[61].

Folic Acid (Vitamin B9) plays a central role in metabolism, supporting nucleotide synthesis and generation of S-adenosylmethionine (SAM), the universal methyl donor required for DNA and histone methylation[62]. Because canonical Wnt signaling depends on transcriptional regulation, epigenetic modulation of Wnt pathway genes through altered folate availability[63]. Because alcohol can alter DNA methylation patterns, folic acid supplementation may provide partial rescue by restoring epigenetic mechanisms that regulate Wnt pathway gene expression[48].

Chapter 2: Hypothesis, Objectives and Rationale

2.1. Hypothesis

Astyanax mexicanus the SF and CF display differences in taste bud formation and development, perturbation of the canonical Wnt signaling pathway through chemical modulation, including EtOH is expected to distinctly affect taste bud formation and gustatory perception between the two morphs.

2.2. Objectives and Rationales

2.2.1 Objective 1

To analysis the effects of canonical wnt modulation upon taste bud development between surface and cave *Astyanax mexicanus*.

2.2.1.1 Rational

Due to the presence of two distinct morphs, *Astyanax mexicanus* has emerged as a valuable model for examining evolutionary differences in taste bud development, with previous studies reporting divergence between SF and CF[64]. While canonical Wnt/β-catenin signaling has been implicated in taste papilla formation, its role in regulating taste bud development between morphs remains unclear[26]. EtOH exposure provides a means to disrupt this pathway, while folic acid offers a complementary approach to assess modulation of this pathway through epigenetic regulation. Although both have been studied in the context of developmental defects, their impact on taste bud formation has not been investigated. Therefore, I will perform a comparative analysis of taste bud development between SF and CF under conditions of canonical Wnt

pathway modulation by quantifying taste bud number, diameter, and spatial distribution following treatment with Wnt activators and inhibitors.

2.2.1.2 Sub-objectives:

1) To define morph-specific differences in taste bud development between SF and CF across developmental time points.
2) To evaluate the impact of canonical Wnt pathway modulation on taste bud number, morphology, and growth dynamics in both morphs.
3) To investigate regional patterning and spatial organization of taste buds (T1–T4) in response to Wnt pathway perturbation.

2.2.2 Objective 2

Characterize the perceptual changes associated within gustatory processing following canonical wnt signaling modulation within CF and SF.

2.2.2.1 Rationale

In *Astyanax mexicanus*, CF exhibit enhanced chemosensory capabilities and increased reliance on non-visual feeding strategies compared to SF. These behavioural adaptations are thought to be associated with differences in taste bud development and sensory processing[39]. Canonical Wnt/β-catenin signaling plays a key role in craniofacial and sensory organ development; however, its functional impact on chemoattractive behaviour remains unclear[26,50]. EtOH exposure and folic acid supplementation provide complementary but independent approaches to modulate this pathway, allowing for the assessment of how disruption or alteration of

developmental signaling influences gustatory driven behaviour. Although both have been studied in the context of developmental defects, their effects on chemosensory and attraction behaviour remain unclear. Therefore, I aim to assess chemosensory responses in SF and CF following pharmacological modulation of canonical Wnt signaling. Behavioural responses will be quantified by measuring average distance from and time spent near different feeding types, as well as total average velocity within each feeding type and treatment conditions.

2.2.2.2 Sub-objectives

1) To determine whether differences in chemoattractive behaviour exist between SF and CF under varying feeding conditions following canonical Wnt pathway modulation.
2) To evaluate treatment specific effects of Wnt pathway modulation on chemoattractive behaviour within SF.
3) To evaluate treatment specific effects of Wnt pathway modulation on chemoattractive behaviour within CF.

Chapter 3: Materials and Methods

3.1 Fish Husbandry and Breeding – *Astyanax mexicanus*

3.1.1 Maintenance

All wild type male and female SF and Pachón CF were originally obtained from Dr. Richard Borowsky (New York University) and Dr. William Jeffery (University of Maryland). Recent SF colony was obtained from Dr. Tamara Franz Odendaal from Mount Saint Vincent University, Halifax, Nova Scoita. Fish were maintained and bred at the Bannatyne Campus, University of Manitoba, using a Tecniplast recirculating rack system under a 12-hour light/12-hour dark photoperiod at 21 °C.

Water physicochemical parameters were automatically regulated within the system, with conductivity maintained at 900 µS and pH at 7.2. Water quality was routinely monitored to ensure stable environmental conditions and optimal fish health.

All experimental procedures were conducted in accordance with the guidelines of the Canadian Council on Animal Care (CCAC) Protocol # 2022-038 and were approved by the University of Manitoba animal care committee.

3.1.2 Feeding and Priming

Adult fish were maintained on Tetra min flake food and fed twice daily.

To promote spawning, fish were conditioned (primed) for two weeks prior to breeding. Adult fish were maintained on a standardized high nutrient diet (Ziegler® Zebrafish Feed) and fed twice daily at 10:00 and 16:00 hours.

During this period, feeding was consistent and controlled to ensure optimal reproductive readiness and to minimize variability between breeding groups.

3.1.3 Breeding and Embryo Collection

Breeding groups were established using a ratio of one female to two males of comparable size and age. Fish were transferred to spawning tanks containing fresh system water maintained at 25.5–26.5 °C and fitted with egg collection tray inserts to prevent predation.

Breeding groups were maintained under these conditions for up to 48 hours and monitored daily for egg production after 10:00. If spawning did not occur within the first 24 hours, individuals were reassorted into new breeding groups to improve spawning success.

Following spawning, fertilized eggs were collected immediately using a transfer pipette and rinsed with system water to remove debris. Eggs were then transferred to petri dishes containing fresh embryo medium containing 1 ml of 0.1% methylene blue (Fisher Scientific CAS:7220-79-3) in 1L of system water and maintained at 26 °C for subsequent experimental use. Embryos were staged and monitored regularly to ensure normal development prior to downstream analyses. Larvae were maintained in Petri dishes within an incubator at 26 °C until 5 days post-fertilization (dpf). At 5 dpf, larvae were transferred to a portable incubator set to 26 °C and housed in plastic containers for continued development. During this stage, larvae were fed freshly prepared brine shrimp daily. Containers were monitored and cleaned each day to remove debris and deceased individuals, ensuring stable rearing conditions.

After approximately two weeks, larvae were transferred to a recirculating rack system once they reached sufficient size and swimming capacity to tolerate increased water flow associated with system water exchange. Fish were subsequently maintained under standard housing conditions.

Adult breeders were returned to standard housing conditions (21–22 °C) and reconditioned prior to future breeding attempts.

3.1.4 Larval Rearing and Experimental Use

Following successful spawning, fertilized embryos were collected within 2–4 hours post-fertilization (hpf) using a plastic transfer pipette to minimize mechanical damage. Embryos were rinsed with system water to remove debris and unfertilized eggs.

Collected embryos were transferred into sterile Petri dishes containing embryonic medium composed of system water supplemented with methylene blue (approximately 0.00003%) to inhibit fungal growth. Embryos were maintained at a density of 20–30 embryos per dish to reduce crowding, ensure adequate oxygenation, and minimize developmental variability.

All embryos were incubated at 26 °C under controlled laboratory conditions and monitored regularly to confirm normal development prior to experimental manipulation.

Embryos were maintained in embryo medium at 26 °C under controlled conditions until the desired developmental stages were reached. Larvae were monitored daily for viability and normal morphology, and non-viable individuals were removed.

3.2 Fish Rearing and Chemical Treatments – *Astyanax mexicanus*

3.2.2 Chemical Treatment Protocol

At 10 hpf, corresponding to a critical window of early craniofacial and sensory development, embryos were exposed to pharmacological treatments targeting canonical Wnt signaling pathways[65,66].

The following treatment groups were established:

- 1% EtOH (Catalog: 036935)
- 10 nM WC-59 (Sigma-Aldrich, Cas. No. 500496)
- 2 nM LiCl (TCI America, Cat 866405-64-3)
- 100 µM folic acid (ThermoFisher Cas 59-30-3)
- untreated control

Embryos were exposed to treatment solutions for a duration of 12 hours. All treatments were prepared in Tecniplast system water and administered under identical environmental conditions to ensure consistency across groups.

After 12 hours following treatment, embryos were rinsed three times with fresh embryonic medium to remove residual compounds and were subsequently transferred to clean Petri dishes containing fresh embryonic medium for continued development.

3.2.3 Larval Rearing Conditions

Post-treatment, larvae were maintained at 26 °C under a 12-hour light/12-hour dark cycle to ensure consistent developmental progression. Embryonic medium was replaced daily to maintain water quality and to prevent accumulation of waste products and microbial contamination.

Larvae were carefully monitored for viability, developmental progression, and morphological abnormalities. Dead or non-viable individuals were removed promptly to prevent contamination of the culture environment.

At 5 dpf, once yolk reserves were depleted and active feeding began, larvae were transferred to glass rearing containers containing fresh embryonic medium. From 5 dpf onwards, larvae were fed live brine shrimp (*Artemia nauplii*) twice daily to support normal growth and development.

Feeding quantities were adjusted to avoid overfeeding, and uneaten food and debris were removed daily by gentle pipetting. Rearing containers were cleaned and replenished with fresh embryonic medium as needed to maintain optimal conditions.

3.2.4 Sample Collection and Experimental Timepoints

Larvae were collected at defined developmental stages of 8, 15, and 30 dpf for downstream analyses. At each timepoint, individuals were selected randomly from each treatment group to minimize sampling bias.

For behavioural assays, larvae were collected and assessed live under controlled experimental conditions. For morphological analyses, larvae were euthanized prior to fixation and staining at 8, 15 and 30 DPF.

Euthanasia was performed using 0.1% tricaine methanesulfonate (MS-222) (ACROS ORGANIC CAS: 886-86-2), and death was confirmed by cessation of opercular movement. Following euthanasia, specimens were processed immediately for staining or preserved for further analysis as required.

3.3 Morphological Assays

3.3.1 Staining Protocol

Following euthanasia, samples were transferred using a plastic pipette into staining solution containing 0.5% Ponceau S (CAS: 6226-79-5) prepared in 0.3 M trichloroacetic acid (TCA) (Sigma Aldrich Cas 76-03-9), adjusted to pH 0.9 using the Fisher Scientific ABISO pH/mV pH meter. The staining solution was prepared fresh and maintained at room temperature.

Individual larvae were immersed in the staining solution for 20 seconds to allow rapid labeling of external structures. Staining was performed in small volumes to ensure consistent exposure across samples. Following staining, samples were immediately rinsed in distilled water to remove excess dye. Washing was performed for 20 seconds with gentle agitation to reduce background staining while preserving contrast. After washing, specimens were transferred to a 1% agar medium prepared in distilled water. Larvae were carefully oriented using fine forceps to ensure consistent lateral or ventral positioning for imaging. Samples were imaged immediately using a Leica V8 stereomicroscope under consistent lighting and magnification settings. All imaging was performed within a standardized timeframe following staining to minimize variability in signal intensity. To ensure consistency across experimental groups, staining duration, washing time, and imaging conditions were strictly controlled for all samples.

3.3.2 Taste Bud quantification and Spatial Analysis

Following whole-mount staining, larvae of *Astyanax mexicanus* were imaged using the Leica V8 stereomicroscope.

Taste buds were identified based on morphological features and were quantified on the external craniofacial surface, with particular focus on the ventral region of the mandible. Additional observations were made in surrounding facial regions, including the perioral and periocular areas where applicable.

To ensure consistency in quantification, anatomical orientation and region boundaries were standardized prior to analysis. The ventral mandibular surface was selected as the region of interest based on the characteristic distribution of taste buds in *Astyanax mexicanus*. Quantification was restricted to a defined area extending along the external mandible, beginning at the anterior oral region and terminating immediately prior to the branchial (gill) region. This boundary was established based on observed patterns of taste bud localization to ensure consistent and comparable measurements across all samples seen in FIGURE 3.1. All measurements were performed using ZEN 2011 Blue imaging software (Zeiss), which was used for both counting and morphometric analysis.

Taste bud number was quantified manually for each specimen within defined regions of interest. Taste bud diameter was measured as the maximum visible width of each structure, and measurements were collected across developmental timepoints of 8, 15, and 30 dpf.

Spatial distribution was assessed by measuring inter bud distances, defined as the distance between the centers of adjacent taste buds. These measurements were used to evaluate changes in patterning and organization over 8, 15, and 30 dpf.

All analyses were performed using consistent criteria across samples to minimize observer bias and ensure reproducibility.

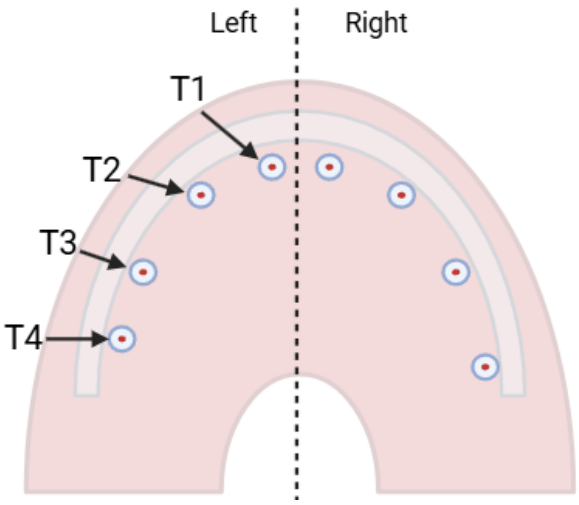

FIGURE 3.1: Schematic representation of the ventral mandible of *Astyanax mexicanus* following Ponceau S staining, illustrating the standardized regions used for taste bud analysis. Taste bud distribution was assessed by quantifying the total number of taste buds beneath the mandible, average taste bud diameter, and spatial distribution across regions T1–T4. Bilateral symmetry was evaluated by measuring the distance between the left and right T1 positions, as well as the distances between sequential taste bud regions (T1–T2, T2–T3, and T3–T4). These measurements were used to analyze developmental changes in taste bud patterning at 8, 15, and 30 dpf.

3.3.3 Behavioural Analysis

Behavioral assays were conducted following established automated video tracking methodologies for larval fish using a DanioVision observation system and EthoVision XT software Noldus Information Technology[67].

Post chemical exposure, 3–5 larvae per treatment group were reared until 30 dpf. To standardize motivational state meaning encouraging chemosensory driven feeding behaviour, larvae were food deprived for 24 h prior to testing. Behavioral assays were conducted at 10:00 under controlled environmental conditions to minimize circadian effects.

Individual *Astyanax mexicanus* larvae were placed in 9 cm circular Petri dish arenas within a DanioVision observation chamber under constant illumination. Petri dishes were filled with system water sourced from a recirculating aquarium system to maintain stable physicochemical conditions.

Behavioral trials were conducted in a repeated measures design, where each individual sample was exposed to all feeding conditions (sucrose (Fisher Scientific CAS: 57-50-1), quinine (Fisher Scientific CAS: 130-95-0), EtOH, and control agar (Fisher Scientific CAS: 9002-18-0). Conditions were tested on separate days with a minimum 24 h interval between trials to prevent carry over effects. Prior to each recording, larvae were acclimated in the arena for 15 min. Each trial consisted of a 5 min recording period, and each larva completed three independent trials per condition.

Behavioral recordings were obtained using EthoVision XT 3.1 (Noldus Information Technology). Movement was quantified using centroid based tracking of each larva, capturing whole body displacement over time.

3.3.3.1 Gustatory Chemosensory Attraction Behavior Assay

Agar based food blocks were prepared at 1% agar concentration. Chemical stimuli (sucrose [1 M], quinine [3 mM], EtOH [1%]) were incorporated into molten agar prior to solidification to ensure uniform distribution throughout each block. Control blocks consisted of unflavoured 1% agar prepared under identical conditions.

Solidified agar was cut into 1 cm^3 cubes and placed at a fixed position along the edge of each Petri dish.

A feeding zone was defined as a 1 cm diameter circular area surrounding each food block (FIGURE 3.2). Behavioral outputs included time spent within the feeding zone and average centroid distance from the feeding zone centre across each 5 min trial.

These variables were used to quantify stimulus dependent feeding responses[68,69].

3.3.3.2 Locomotor Activity Assay

Locomotor activity was quantified using centroid derived movement outputs. Total distance travelled and swimming velocity were extracted for each 5 min trial using EthoVision tracking data.

Velocity was calculated as total distance travelled divided by trial duration. These measures were used as indices of general locomotor activity independent of feeding stimuli.

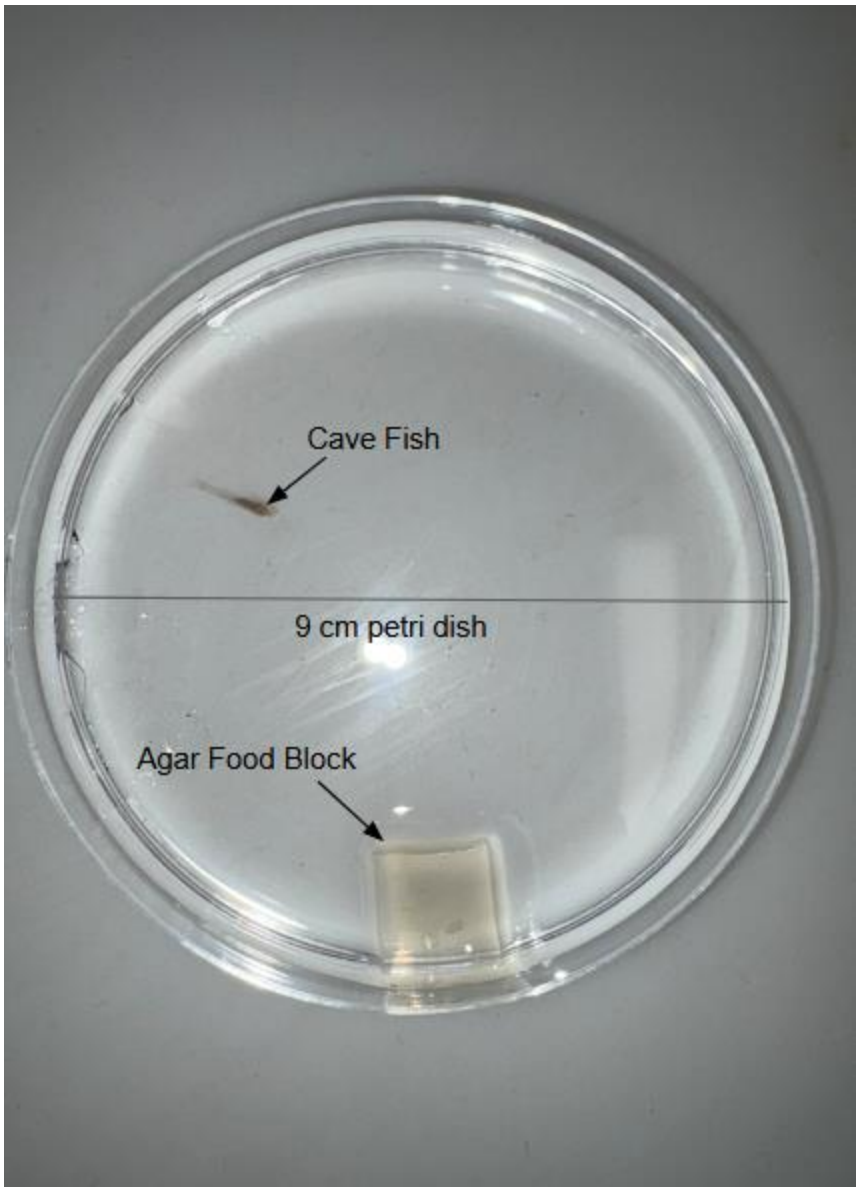

FIGURE 3.2: Behavioral setup for 30 days post fertilization *Astyanax mexicanus* within 9 cm petri dish containing 1 cm cubic agar feeding blocks submerged within standardized system water. Cave fish within a 9 cm petri dish containing fish rearing system water as well as agar feeding block for assessing chem attractive behaviour as well as locomotive movement.

3.4 Statistical Analysis

All statistical analyses were performed using R (R Core Team). Behavioral data were imported from Microsoft Excel spreadsheets using the *readxl* package and processed using *dplyr*. Data visualization was performed using *ggplot2*, and statistical testing was conducted using the *rstatix* and *ggpubr* packages.

Behavioral datasets were analyzed using non-parametric statistical methods due to violations of normality assumptions. Because behavioral assays were conducted in a repeated measures design, differences in feeding conditions were evaluated using the Friedman test for within individual comparisons across conditions.

Where significant effects were detected, post-hoc pairwise comparisons between feeding conditions were performed using Wilcoxon signed rank tests with multiple comparisons correction.

To control for false discovery rate across multiple pairwise tests, Benjamini–Hochberg (FDR) correction was applied to adjusted p-values. Statistical significance was defined as $\alpha = 0.05$.

Chapter 4: Results

Whole Mount Taste Bud Ponceau S staining

Stereomicroscopy was used initially to examine changes on the external ventral mandible of both SF and Pachón CF prior Ponceau S staining (FIGURE 4.1, FIGURE 4.2 respectively). Generating a hypothetical generalized schematic towards normal taste bud formation and distribution prior to chemical perturbation with LiCl, EtOH, WC-59 and folic acid (FIGURE 3.1). Therefore, creating and outline used as the baseline towards morphological analysis towards changes in normal taste bud distribution, morphology and patterning, through analysis of total taste bud count, taste bud diameter and distance between taste bud containing regions on the external ventral mandible of both morphs.

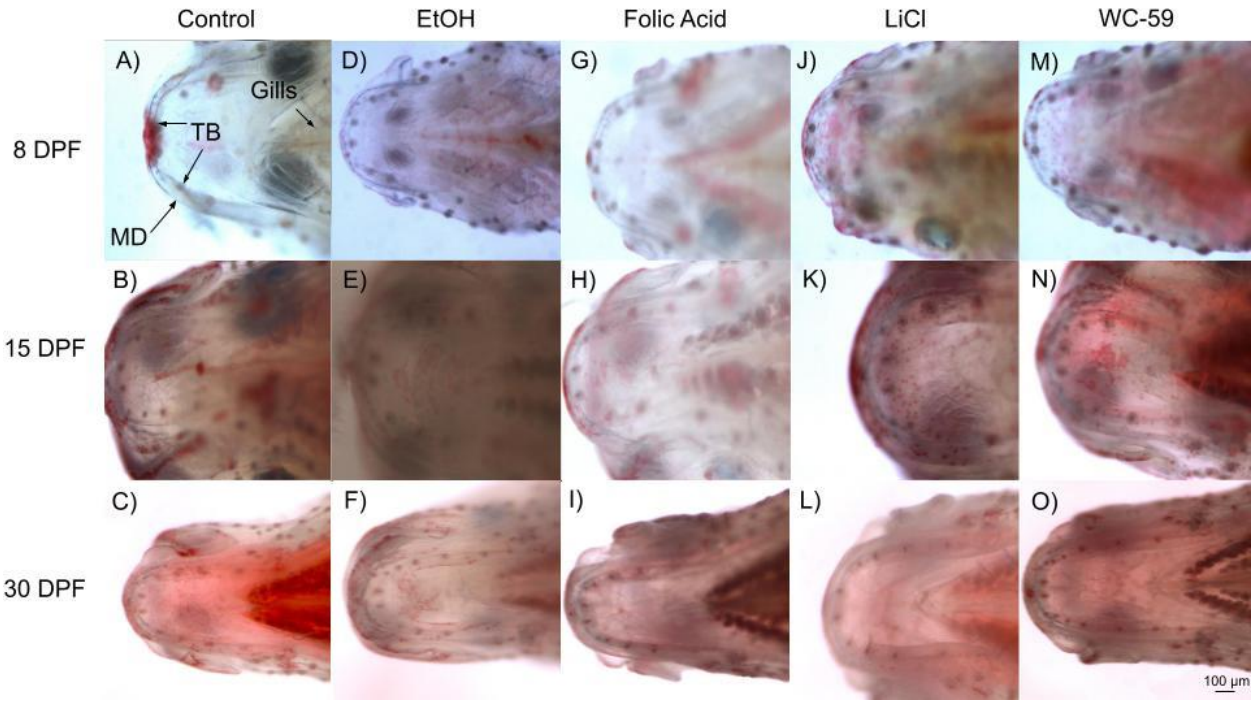

FIGURE 4.1: Live Ponceau S staining of the ventral mandibular surface in cavefish across developmental stages and treatment conditions. Panels show representative images at 8, 15, and 30 days post-fertilization (dpf). **A–C:** Control (8, 15, 30 dpf). **D–F:** EtOH (8, 15, 30 dpf). **G–I:** Folic acid (8, 15, 30 dpf). **J–L:** LiCl (8, 15, 30 dpf). **M–O:** WC-59 (8, 15, 30 dpf). External mandibular structures are shown for juvenile *Astyanax mexicanus*, with taste buds (TB) visible as discrete, circular protrusions on the epithelial surface on the mandible (MD) and gill rakers (Gills) indicated by black arrows in panel A. Representative larvae demonstrate the progressive expansion of taste bud containing regions over developmental time, with treatment groups exhibiting deviations from control patterns. Scale bar = 100 µm

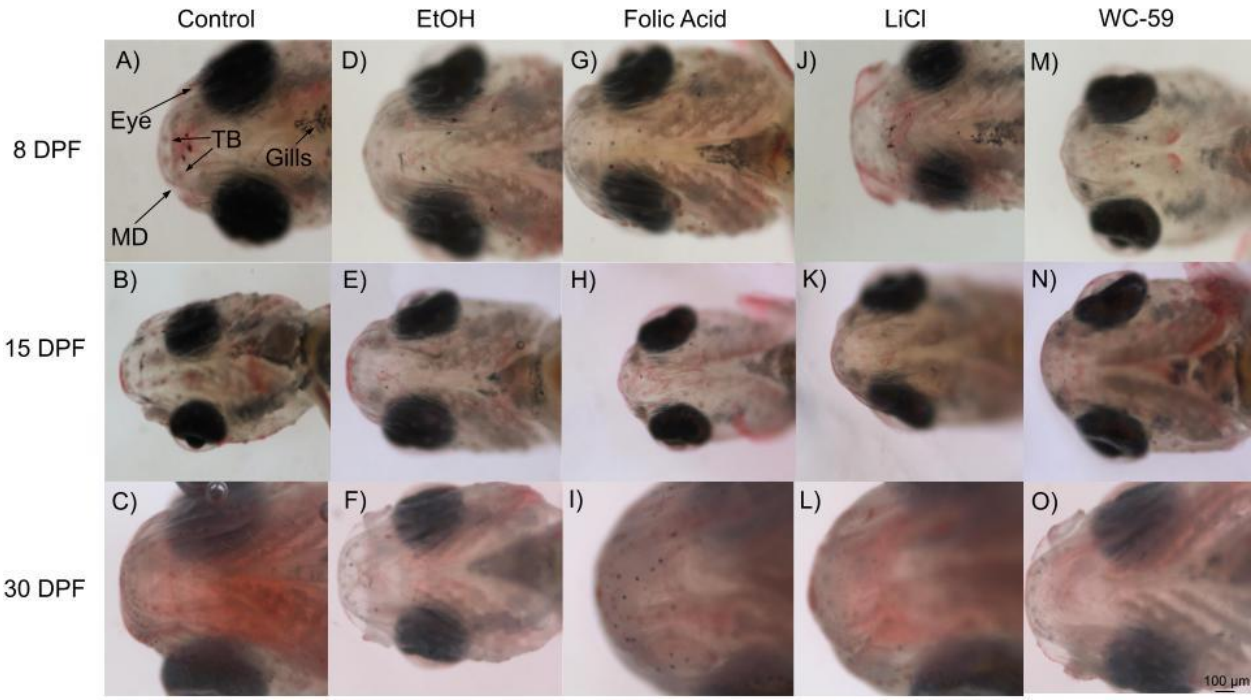

FIGURE 4.2: Live Ponceau S staining of the ventral mandibular surface in surface fish across developmental stages and treatment conditions. Panels show representative images at 8, 15, and 30 days post-fertilization (dpf). **A–C:** Control (8, 15, 30 dpf). **D–F:** EtOH (8, 15, 30 dpf). **G–I:** Folic acid (8, 15, 30 dpf). **J–L:** LiCl (8, 15, 30 dpf). **M–O:** WC-59 (8, 15, 30 dpf). External mandibular structures are shown for juvenile *Astyanax mexicanus*, with taste buds (TB) visible as discrete, circular protrusions on the epithelial surface, mandible (MD), gill rakers (Gills) and the eye indicated by black arrows in panel A. Representative larvae demonstrate the progressive expansion of taste bud containing regions over developmental time. Scale bar = 200 µm.

Taste Bud Count

Total taste bud counts were quantified on the external surface of the mandible in SF and Pachón CF morphs at 8, 15, and 30 dpf.

No statistically significant differences were detected at either 8 or 15 dpf. At 8 dpf, all treatment groups exhibited an average of approximately six taste buds. By 15 dpf, slight variation among treatments was observed: LiCl treated fish showed a modest increase in taste bud number with greater variance, whereas EtOH and folic acid treatments showed a slight decrease relative to the surface control, which remained consistent at six taste buds.

At 30 dpf, differences among treatments became more apparent. While mean taste bud numbers varied across EtOH, folic acid, LiCl, and WC-59 treatments, statistically significant differences were detected between the SF control and Pachón CF treated with WC-59, as well as between the SF control and Pachón CF treated with EtOH ($p \leq 0.05$; FIGURE 4.3).

Comparison of all SF treatments with the Pachón CF control (FIGURE 4.4) showed that at 8 dpf all conditions exhibited approximately six taste buds on the external mandible. At 15 dpf, SF treatments remained at approximately six taste buds, which was significantly lower than the Pachón CF control average of seven taste buds ($p \leq 0.01$). By 30 dpf, the difference in taste bud number between groups decreased but remained statistically significant ($p \leq 0.05$) when comparing Pachón CF controls with all SF treatments, including control, EtOH, LiCl, and folic acid conditions. Additionally, a similar level of significance ($p \leq 0.05$) was observed when comparing SF treated with WC-59 to other surface treatments, including surface control, EtOH, LiCl, and folic acid.

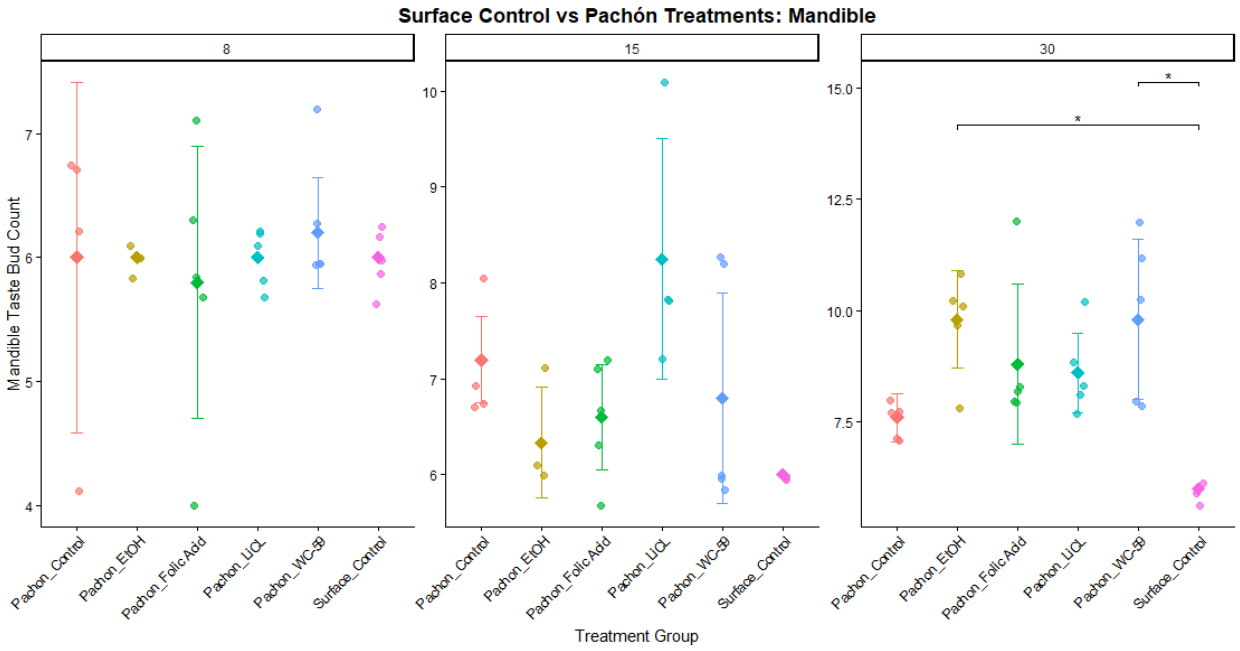

FIGURE 4.3: Mandibular taste bud counts across treatment conditions in Pachón cavefish compared to surface fish controls during larval development. Mandibular taste bud number was quantified in Pachón cavefish larvae following different treatment conditions (Control, EtOH, folic acid, LiCl, and WC-59) and compared with untreated surface fish controls. Measurements were collected at developmental timepoints of 8, 15, and 30 days post-fertilization. Individual points represent taste bud counts from individual larvae, diamonds indicate the mean, and error bars represent ± standard deviation. Pairwise comparisons were conducted between treatment groups within each developmental stage to assess treatment associated differences in mandibular taste bud development.

Significance levels: $p \leq 0.05$ (*), $p \leq 0.01$ (**), $p \leq 0.001$ (***), $p \leq 0.0001$ (****).

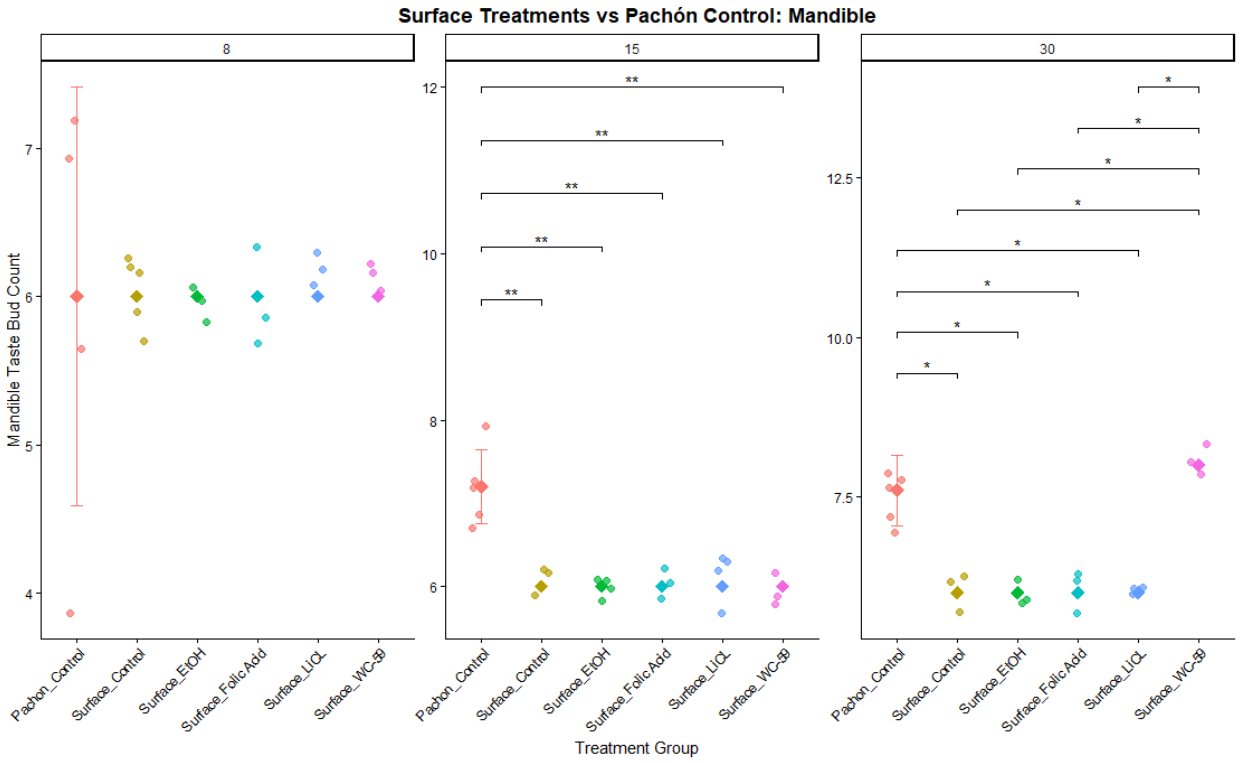

FIGURE 4.4: Mandibular taste bud counts across treatment conditions in surface fish compared to Pachón cavefish controls during larval development. Mandibular taste bud number was quantified in surface fish larvae following different treatment conditions (Control, EtOH, folic acid, LiCl, and WC-59) and compared with untreated Pachón cavefish controls. Measurements were collected at developmental timepoints of 8, 15, and 30 days post-fertilization. Individual points represent taste bud counts from individual larvae, diamonds indicate the mean, and error bars represent ± standard deviation. Pairwise comparisons were conducted between treatment groups within each developmental stage to assess treatment associated differences in mandibular taste bud development.

Significance levels: $p \leq 0.05$ (*), $p \leq 0.01$ (**), $p \leq 0.001$ (***), $p \leq 0.0001$ (****).

Taste Bud Diameter

Total taste bud diameters were quantified on the external surface of the mandible in SF and Pachón CF morphs at 8, 15, and 30 dpf.

When comparing all SF treatments to the Pachón CF control (FIGURE 4.5), a significant difference was detected at 8 dpf, where Pachón CF exhibited a larger average taste bud diameter than LiCl treated SF ($p \leq 0.05$, *). While other treatment comparisons were not statistically significant, SF treatments generally displayed reduced taste bud diameters relative to the Pachón CF control. At 15 dpf, these differences were reduced and no statistically significant differences were observed. By 30 dpf, average taste bud diameter had increased relative to 8 dpf across groups, with a significant difference observed between Pachón CF control and WC-59 treated SF ($p \leq 0.01$, **).

Comparison of SF control with all Pachón CF treatments (FIGURE 4.6) revealed a significant difference at 8 dpf ($p \leq 0.001$, ***), where Pachón CF treatment groups exhibited smaller taste bud diameters relative to the SF control. At later developmental stages (15 and 30 dpf), variation in taste bud diameter increased across groups and no statistically significant differences were detected. At 15 dpf, Pachón CF treatment groups showed slightly larger mean diameters relative to both SF and Pachón CF controls, although these differences were not statistically significant. By 30 dpf, Pachón CF controls again exhibited the largest average diameters relative to treatment groups and surface controls, though these differences remained non-significant.

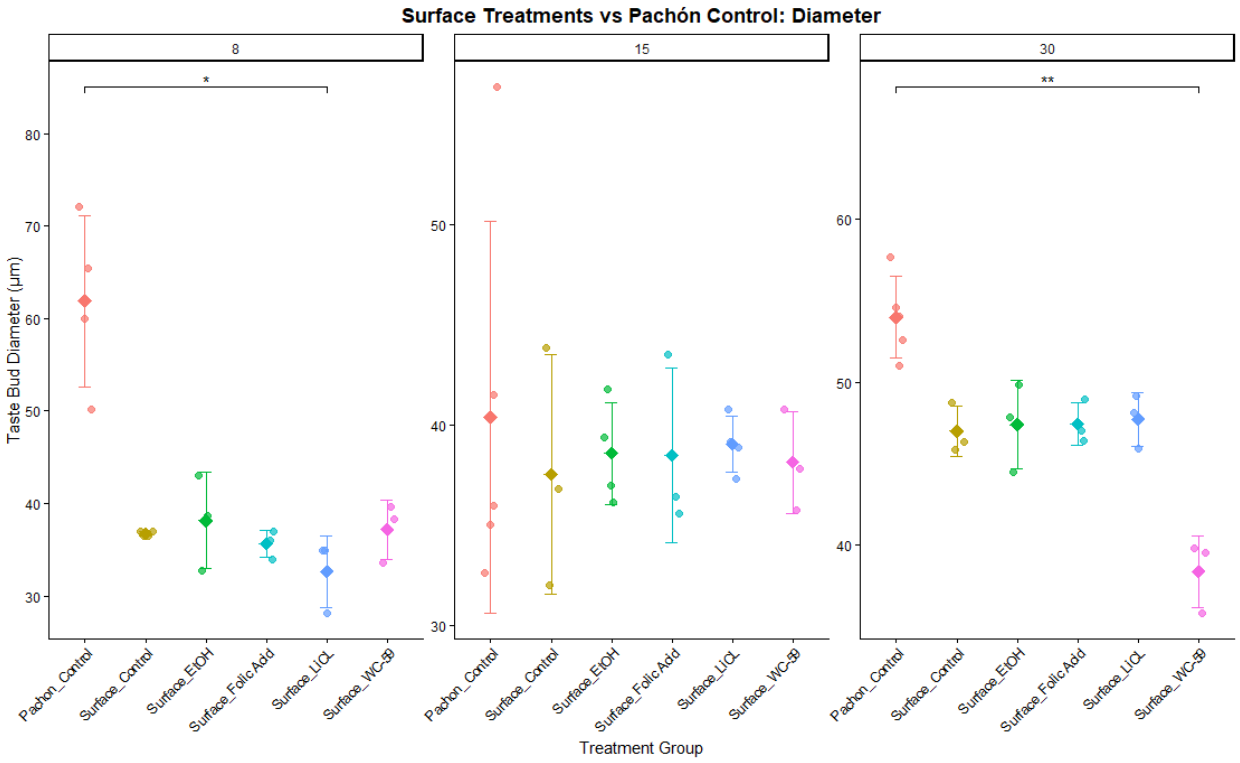

FIGURE 4.5: Mandibular taste bud diameter across treatment conditions in Pachón cavefish compared to surface fish controls during larval development. Mandibular taste bud diameter was quantified in Pachón cavefish larvae following different treatment conditions (Control, EtOH, folic acid, LiCl, and WC-59) and compared with untreated surface fish controls. Measurements were collected at developmental timepoints of 8, 15, and 30 days post-fertilization. Individual points represent taste bud counts from individual larvae, diamonds indicate the mean, and error bars represent ± standard deviation. Pairwise comparisons were conducted between treatment groups within each developmental stage to assess treatment associated differences in mandibular taste bud development.

Significance levels: $p \leq 0.05$ (*), $p \leq 0.01$ (**), $p \leq 0.001$ (***), $p \leq 0.0001$ (****).

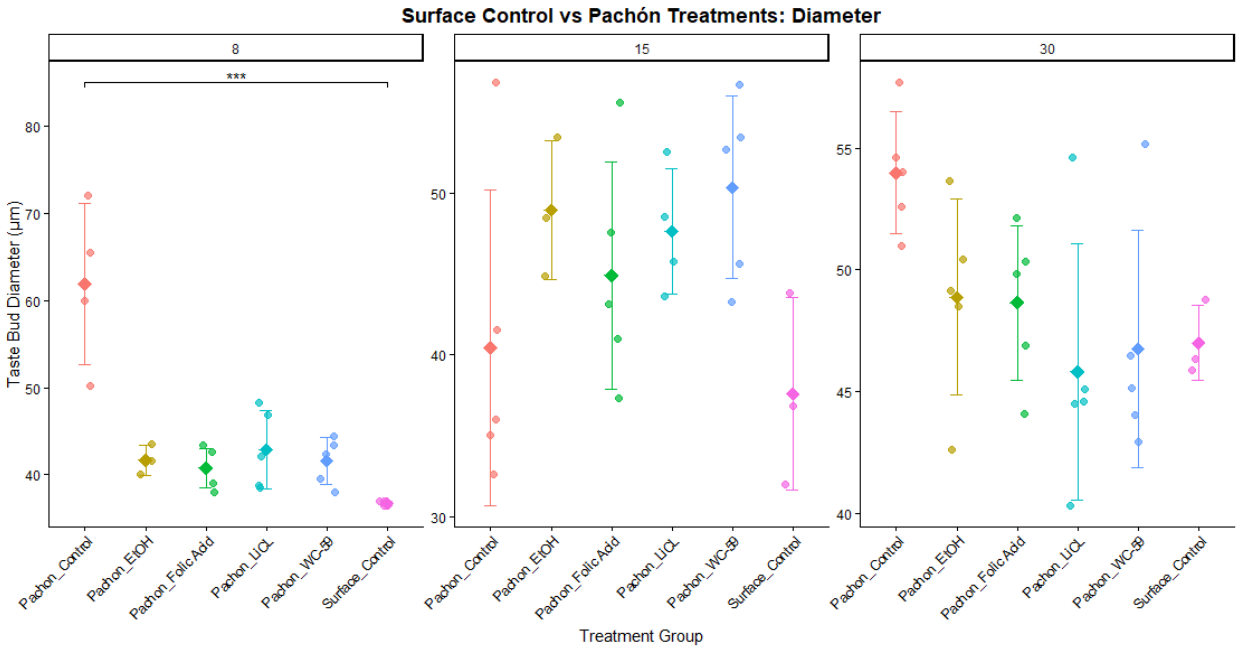

FIGURE 4.6: Mandibular taste bud diameter across treatment conditions in surface fish compared to Pachón cavefish controls during larval development. Mandibular taste bud diameter was quantified in Surface fish larvae following different treatment conditions (Control, EtOH, folic acid, LiCl, and WC-59) and compared with untreated Pachón cavefish controls. Measurements were collected at developmental timepoints of 8, 15, and 30 days post-fertilization. Individual points represent taste bud counts from individual larvae, diamonds indicate the mean, and error bars represent ± standard deviation. Pairwise comparisons were conducted between treatment groups within each developmental stage to assess treatment associated differences in mandibular taste bud development.

Significance levels: $p \leq 0.05$ (*), $p \leq 0.01$ (**), $p \leq 0.001$ (***), $p \leq 0.0001$ (****).

Regional Taste Bud Analysis (T1–T4)

T1 Region:

Average taste bud diameter was quantified within taste bud containing T1 regions on the external surface of the mandible in SF and Pachón CF morphs at 8, 15, and 30 dpf.

When comparing all SF treatments to the Pachón CF control, no statistically significant differences in taste bud diameter were observed at 8 dpf (FIGURE 4.7). However, Pachón CF controls exhibited the largest average taste bud diameter at this developmental stage, with greater variance relative to all other groups.

At 15 dpf, average taste bud diameter within the T1 region remained relatively consistent across treatment groups. A slight reduction in diameter was observed within the Pachón CF control compared to the previous developmental stage, resulting in values comparable to those observed in other Pachón treatments and the SF control. At 30 dpf, an overall increase in taste bud diameter within the T1 region was observed across all conditions. At this developmental stage, a statistically significant difference was detected between Pachón CF control and WC-59 treated SF ($p \leq 0.05$).

Comparison of SF control with all Pachón CF treatment groups showed no significant differences at 8 dpf, although the largest mean diameter was again observed in the Pachón CF control. At 15 dpf, taste bud diameters increased slightly across all treatment groups, with SF control exhibiting the smallest average diameter. Similar patterns were observed at 30 dpf, although these differences were not statistically significant (FIGURE 4.8).

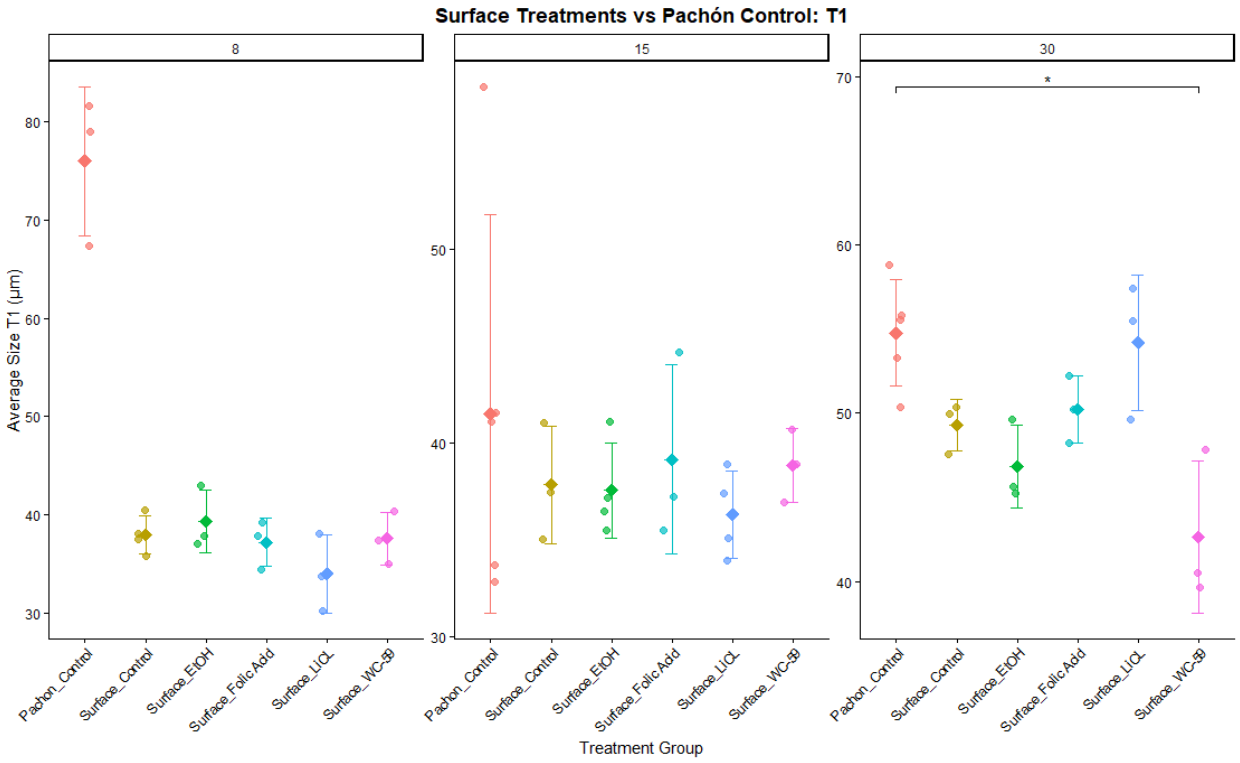

FIGURE 4.7: T1 taste bud diameter across treatment conditions in Surface fish compared to Pachón cavefish control during larval development. Average T1 taste bud diameter was quantified in Surface fish larvae following different treatment conditions (Control, EtOH, folic acid, LiCl, and WC-59) and compared to untreated Pachón cavefish control. Measurements were collected at developmental timepoints of 8, 15, and 30 days post-fertilization. Individual points represent measurements from individual larvae, diamonds indicate the mean, and error bars represent ± standard deviation. Pairwise comparisons were conducted between treatment groups within each developmental stage to assess treatment associated differences in T1 taste bud diameter**.**

Significance levels: p ≤ 0.05 (*), *p ≤ 0.01 (**), p ≤ 0.001 (***)*, p ≤ 0.0001 (****).

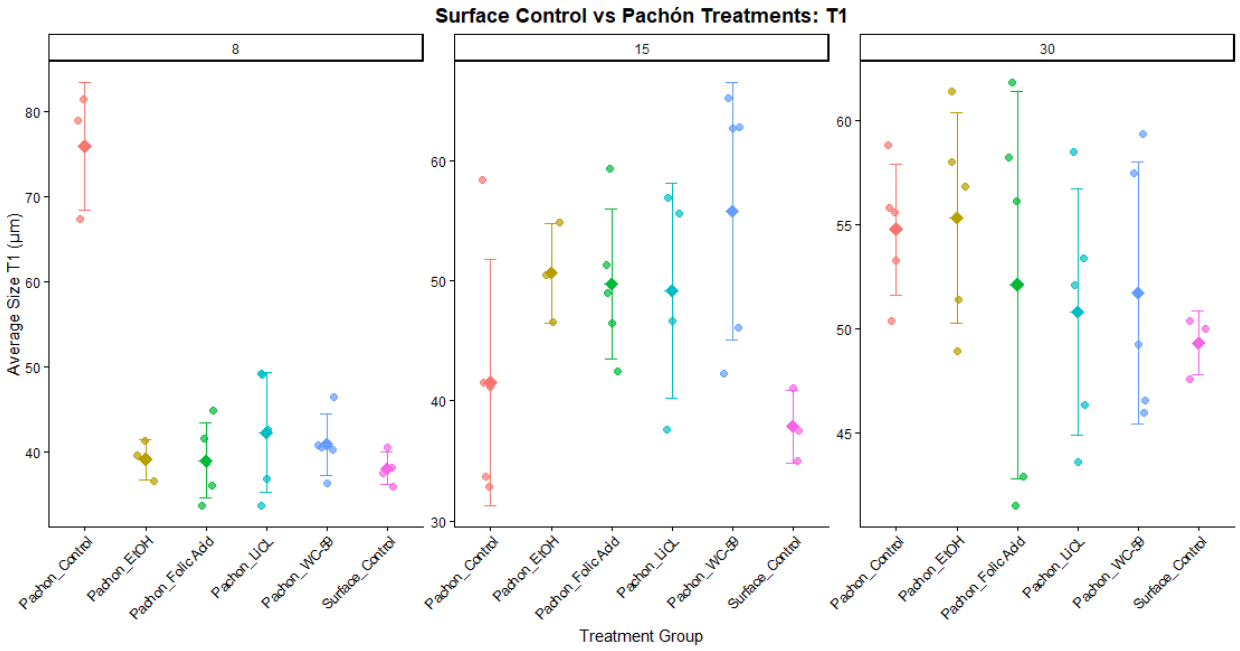

FIGURE 4.8: T1 taste bud diameter across treatment conditions in Pachón cavefish compared to Surface fish control during larval development. Average T1 taste bud diameter was quantified in Pachón cavefish larvae following different treatment conditions (Control, EtOH, folic acid, LiCl, and WC-59) and compared to untreated surface fish control. Measurements were collected at developmental timepoints of 8, 15, and 30 days post-fertilization. Individual points represent measurements from individual larvae, diamonds indicate the mean, and error bars represent ± standard deviation. Pairwise comparisons were conducted between treatment groups within each developmental stage to assess treatment associated differences in T1 taste bud diameter**.**

Significance levels: p ≤ 0.05 (*), *p ≤ 0.01 (**), p ≤ 0.001 (***)*, p ≤ 0.0001 (****)

T2 Region:

Average taste bud diameter was quantified within taste bud containing T2 regions on the external surface of the mandible in SF and Pachón CF morphs at 8, 15, and 30 dpf.

T2 taste buds were observed to develop in Pachón CF by 15 dpf, whereas SF did not exhibit taste bud development in this region at the developmental stages examined. As a result, T2 region analysis was restricted to Pachón CF treatments across the 8, 15, and 30 dpf developmental stages (FIGURE 4.9).

Because SF did not develop taste buds in the T2 region, comparisons between SF control and Pachón treatments could not be performed. At 8 dpf, although no statistically significant differences were detected among Pachón CF groups, the control group exhibited the largest average taste bud diameter. Reduced diameters were observed in some treatment groups, particularly folic acid and WC-59 treatments, while other treatment conditions showed minimal or no detectable taste bud development within this region.

At 15 dpf, significant differences in taste bud diameter were observed within the T2 region. Pachón CF treated with EtOH exhibited a significantly larger average diameter compared to Pachón CF control ($p \leq 0.05$, *). Additionally, EtOH treated Pachón CF showed significantly larger diameters compared to the folic acid treatment group ($p \leq 0.05$, *).

By 30 dpf, average taste bud diameters within the T2 region became more comparable across treatment groups. However, statistically significant differences were observed between Pachón CF control and both LiCl treated and WC-59 treated Pachón CF ($p \leq 0.05$, *, $p \leq 0.01$ ** respectively).

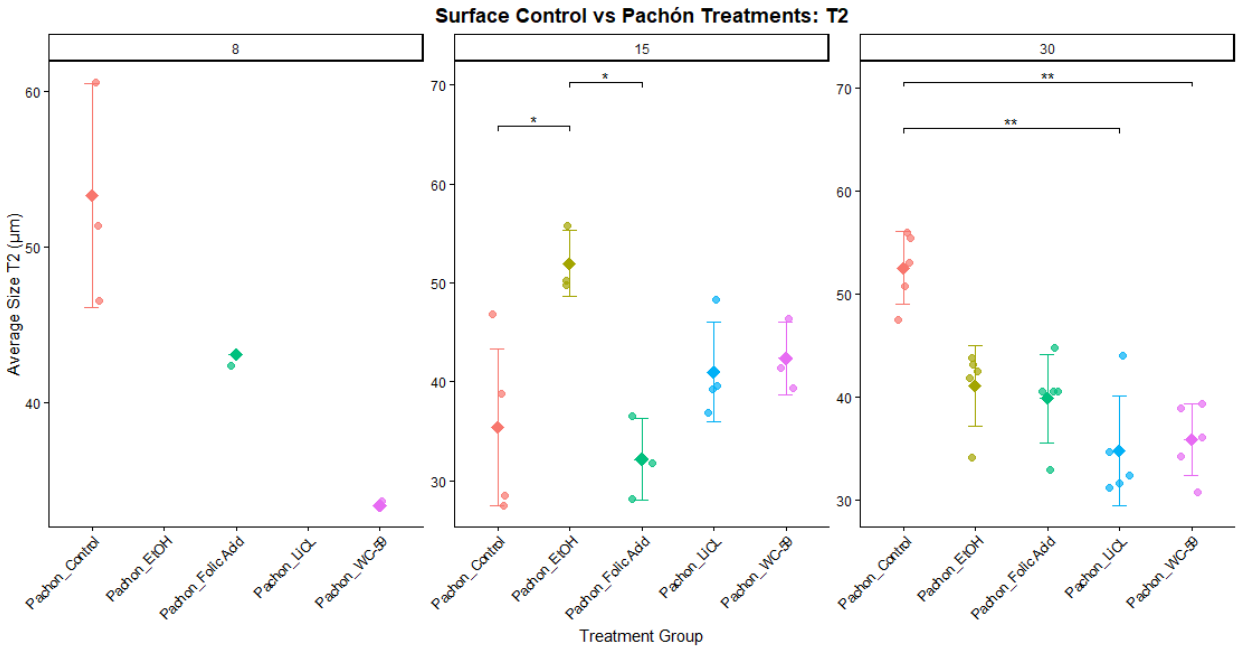

FIGURE 4.9: T2 taste bud diameter across treatment conditions in Pachón cavefish during larval development. Average T2 taste bud diameter was quantified in Pachón cavefish larvae following different treatment conditions (Control, EtOH, folic acid, LiCl, and WC-59). Measurements were collected at developmental timepoints of 8, 15, and 30 days post-fertilization. Individual points represent measurements from individual larvae, diamonds indicate the mean, and error bars represent ± standard deviation. Pairwise comparisons were conducted between treatment groups within each developmental stage to assess treatment associated differences in T2 taste bud diameter**.**

Significance levels: p ≤ 0.05 (*), *p ≤ 0.01 (**), p ≤ 0.001 (***)*, p ≤ 0.0001 (****).

T3 Region:

Average taste bud diameter was quantified within taste bud containing T3 regions on the external surface of the mandible in SF and Pachón CF morphs at 8, 15, and 30 dpf.

When comparing SF treatments to the Pachón CF control at 8 dpf, Pachón CF control exhibited larger average T3 taste bud diameters relative to all SF treatments (FIGURE 4.10). Statistically significant differences were observed between Pachón CF control and SF treated with folic acid as well as LiCl ($p \leq 0.05$, *). At 15 dpf, average taste bud diameters across groups became more comparable. Both Pachón CF and SF controls exhibited the greatest variance in taste bud diameter at this developmental stage. By 30 dpf, overall variance between groups decreased. Pachón CF control again exhibited the largest average diameter within T3 regions. Significant differences were observed between Pachón CF control and SF treated with LiCl ($p \leq 0.05$, *) as well as WC-59 ($p \leq 0.01$, **).

When comparing all Pachón CF treatments to SF control, similar patterns were observed. At 8 dpf, Pachón CF control exhibited the largest taste bud diameters, with a significant difference observed between Pachón CF control and SF control ($p \leq 0.05$, *; FIGURE 4.11). At 15 dpf, differences among groups were reduced, with an overall increase in average taste bud diameter across treatments and greater variance among measurements. By 30 dpf, Pachón CF control again exhibited the largest diameters within T3 regions, while treatment groups showed comparatively reduced diameters.

.

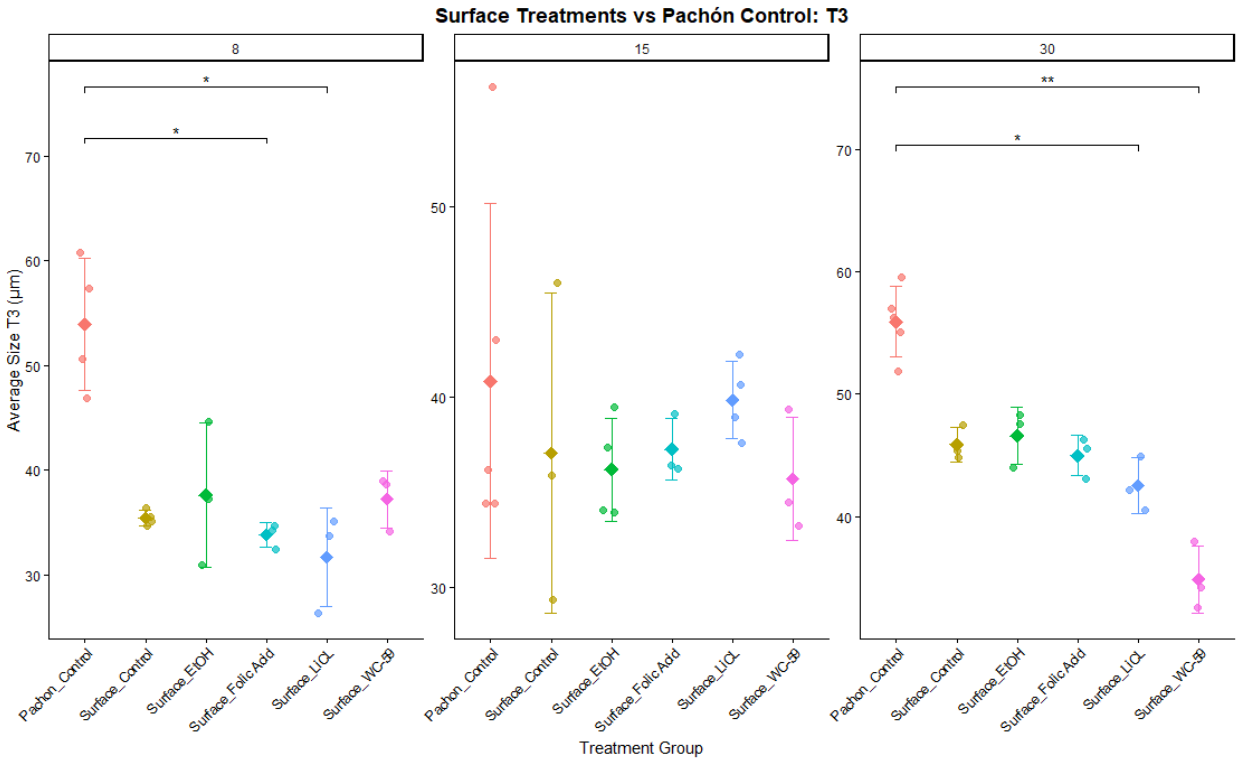

FIGURE 4.10: T3 taste bud diameter across treatment conditions in Surface fish compared to Pachón cavefish control during larval development. Average T3 taste bud diameter was quantified in Surface fish larvae following different treatment conditions (Control, EtOH, folic acid, LiCl, and WC-59) and compared to untreated Pachón cavefish control. Measurements were collected at developmental timepoints of 8, 15, and 30 days post-fertilization. Individual points represent measurements from individual larvae, diamonds indicate the mean, and error bars represent ± standard deviation. Pairwise comparisons were conducted between treatment groups within each developmental stage to assess treatment associated differences in T3 taste bud diameter**.**

Significance levels: p ≤ 0.05 (*), *p ≤ 0.01 (**), p ≤ 0.001 (***)*, p ≤ 0.0001 (****).

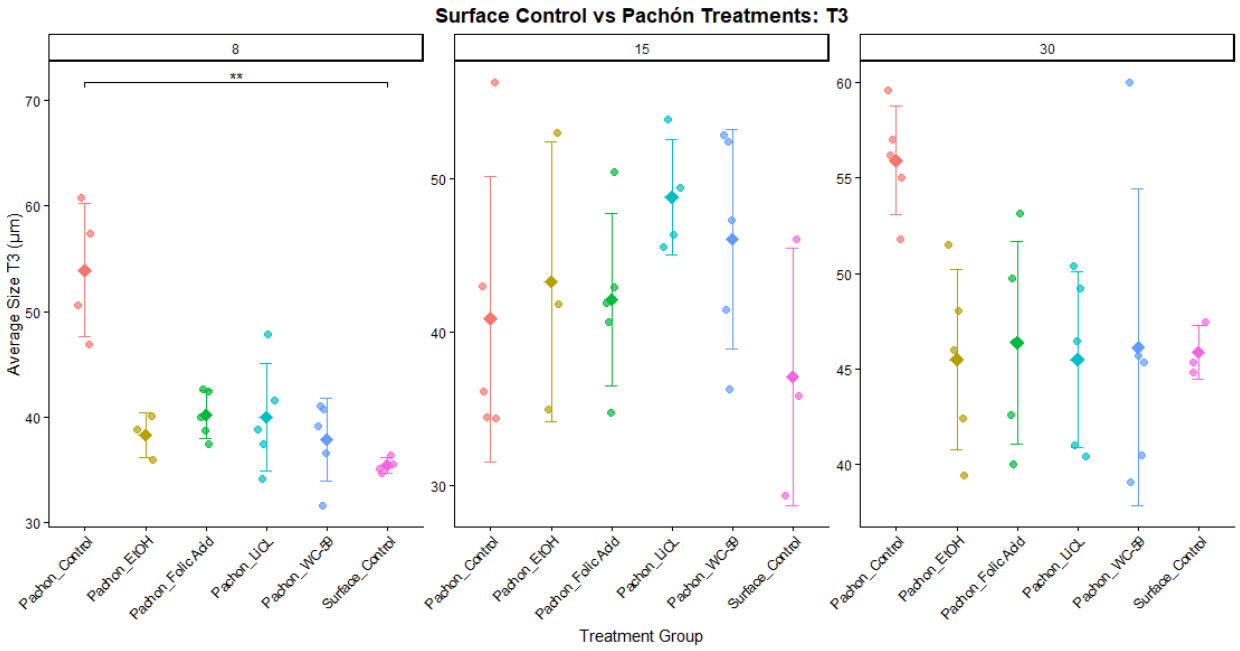

FIGURE 4.11: T3 taste bud diameter across treatment conditions in Pachón cavefish compared to Surface fish control during larval development. Average T3 taste bud diameter was quantified in Pachón cavefish larvae following different treatment conditions (Control, EtOH, folic acid, LiCl, and WC-59) and compared to untreated surface fish control. Measurements were collected at developmental timepoints of 8, 15, and 30 days post-fertilization. Individual points represent measurements from individual larvae, diamonds indicate the mean, and error bars represent ± standard deviation. Pairwise comparisons were conducted between treatment groups within each developmental stage to assess treatment associated differences in T3 taste bud diameter**.**

Significance levels: p ≤ 0.05 (*), *p ≤ 0.01 (**), p ≤ 0.001 (***), p ≤ 0.0001 (****).

T4 Regions:

Average taste bud diameter was quantified within taste bud containing T4 regions on the external surface of the mandible in SF and Pachón CF morphs at 8, 15, and 30 dpf.

When comparing SF treatments to the Pachón CF control, no statistically significant differences were observed at either 8 or 15 dpf (FIGURE 4.12). At 8 dpf, Pachón CF control exhibited the largest average taste bud diameter among all groups. This diameter was reduced at 15 dpf, resulting in values that were more comparable across treatments. By 30 dpf, taste bud diameters across groups became more closely clustered, indicating reduced variance between treatments. However, a statistically significant difference was observed between Pachón CF control and WC-59treated SF ($p \leq 0.05$, *), with Pachón CF control still exhibiting the largest average diameter.

When comparing SF control to all Pachón CF treatments, Pachón CF control exhibited the largest average diameter at 8 dpf. A statistically significant difference was observed between SF control and Pachón CF control ($p \leq 0.01$, **; FIGURE 4.13). At 15 and 30 dpf, no statistically significant differences were detected. However, taste bud diameters within the T4 region of Pachón CF were slightly reduced compared to earlier developmental stages and were more comparable to treatment groups, while remaining larger than those observed in the SF control.

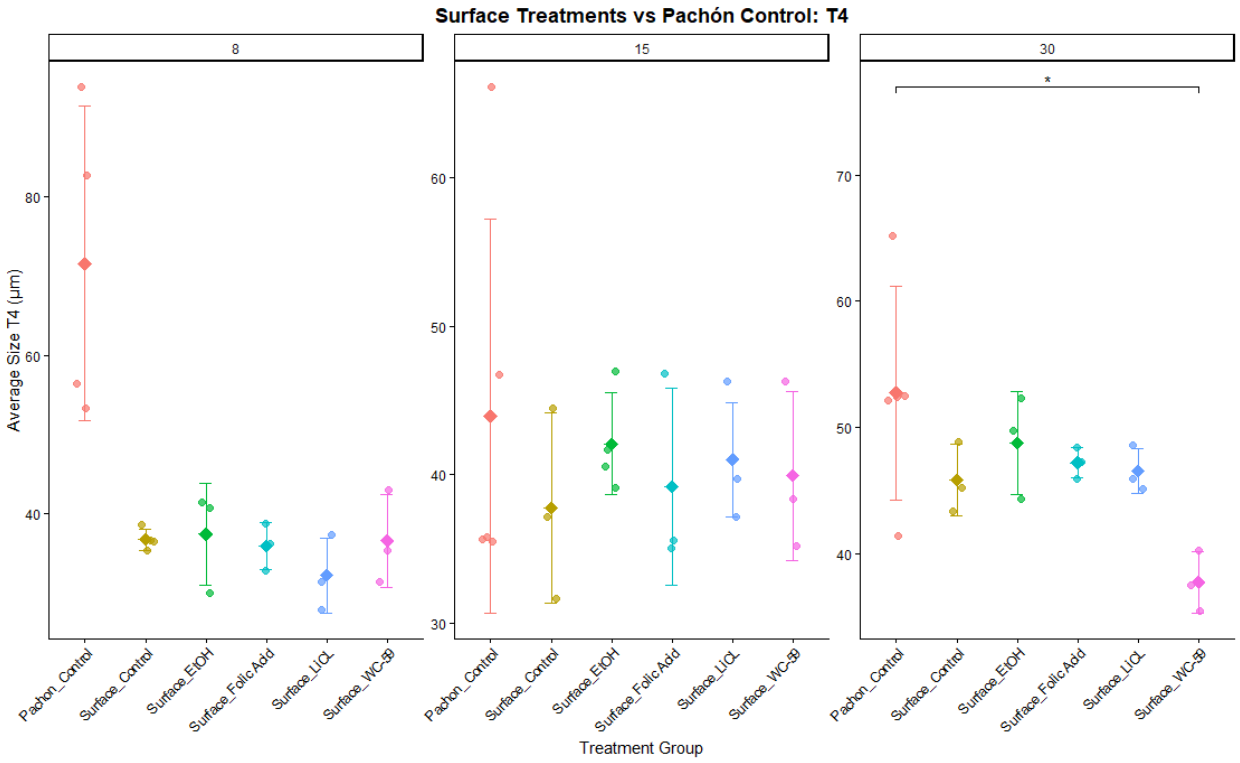

FIGURE 4.12: T4 taste bud diameter across treatment conditions in Surface fish compared to Pachón cavefish control during larval development. Average T4 taste bud diameter was quantified in Surface fish larvae following different treatment conditions (Control, EtOH, folic acid, LiCl, and WC-59) and compared to untreated Pachón cavefish control. Measurements were collected at developmental timepoints of 8, 15, and 30 days post-fertilization. Individual points represent measurements from individual larvae, diamonds indicate the mean, and error bars represent ± standard deviation. Pairwise comparisons were conducted between treatment groups within each developmental stage to assess treatment associated differences in T4 taste bud diameter**.**

Significance levels: p ≤ 0.05 (*), *p ≤ 0.01 (**), p ≤ 0.001 (***)*, p ≤ 0.0001 (****).

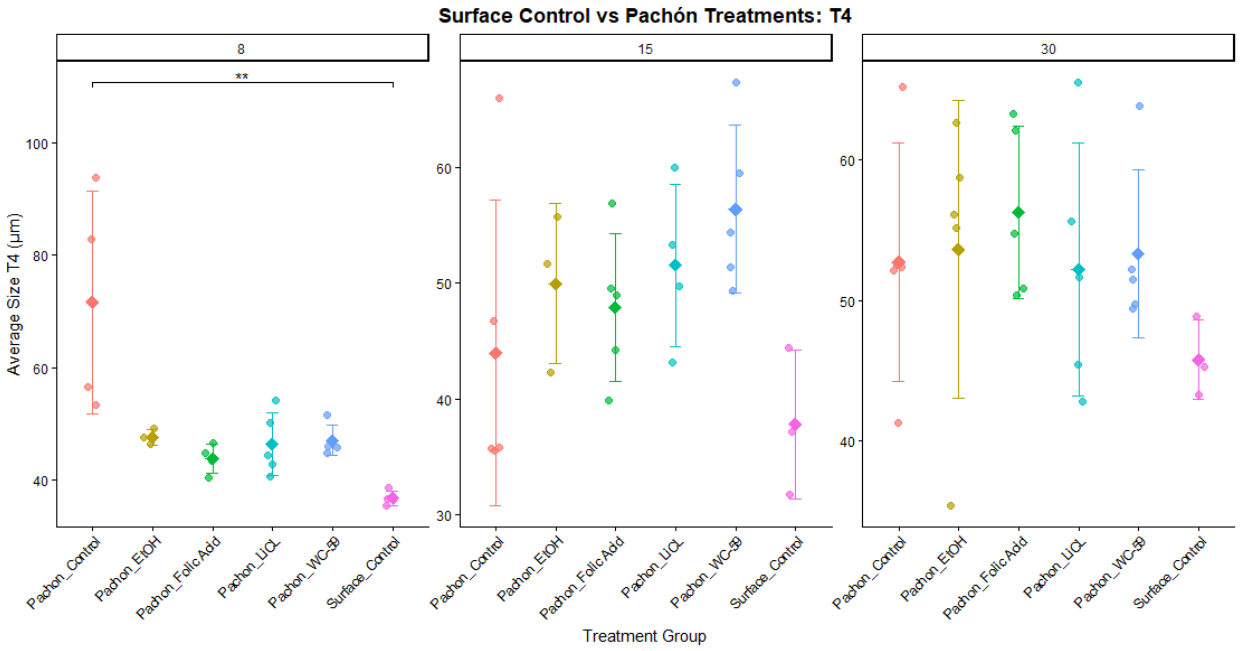

FIGURE 4.13: T4 taste bud diameter across treatment conditions in Pachón cavefish compared to Surface fish control during larval development. Average T4 taste bud diameter was quantified in Pachón cavefish larvae following different treatment conditions (Control, EtOH, folic acid, LiCl, and WC-59) and compared to untreated surface fish control. Measurements were collected at developmental timepoints of 8, 15, and 30 days post-fertilization. Individual points represent measurements from individual larvae, diamonds indicate the mean, and error bars represent ± standard deviation. Pairwise comparisons were conducted between treatment groups within each developmental stage to assess treatment associated differences in T4 taste bud diameter**.**

Significance levels: p ≤ 0.05 (*), *p ≤ 0.01 (**), p ≤ 0.001 (***), p ≤ 0.0001 (****).

Spatial Distribution and Bilateral Symmetry Analysis

T1 Bilateral length:

Average bilateral distance between T1 taste bud containing regions was measured between the left and right sides of the external mandible in SF and Pachón CF at 8, 15, and 30 dpf.

When comparing all SF treatments to the Pachón CF control, no statistically significant differences were observed at 8, 15, or 30 dpf (FIGURE 4.14). However, Pachón CF control exhibited the greatest average bilateral distance between T1 taste bud containing regions across the developmental stages examined.

When comparing Pachón CF treatments to SF control, no statistically significant differences were observed at 8 or 15 dpf. Despite the lack of statistical significance, Pachón CF treatments generally exhibited greater average distances between T1 taste bud containing regions relative to SF control, with Pachón CF control showing the largest average distance at 8 dpf (FIGURE 4.15). At 30 dpf, a statistically significant difference was detected between SF control and WC-59 treated Pachón CF ($p \leq 0.05$, *). Overall, a similar trend was observed across developmental stages, with Pachón CF exhibiting greater bilateral spacing between T1 taste bud containing regions compared to SF.

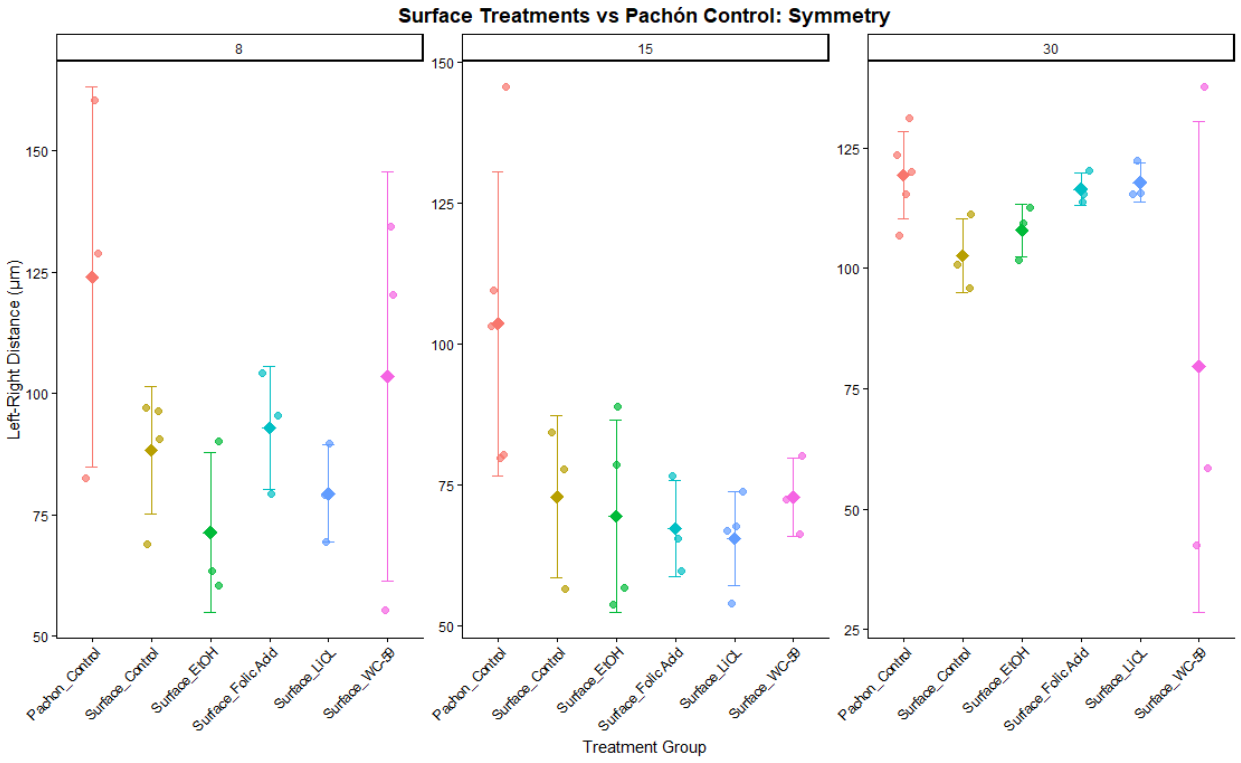

FIGURE 4.14: Bilateral distance between left and right T1 taste bud regions across treatment conditions in Surface fish compared to Pachón cavefish control during larval development. Bilateral distance between left and right T1 taste bud regions was quantified in Surface fish larvae following different treatment conditions (Control, EtOH, folic acid, LiCl, and WC-59) and compared to untreated Pachón cavefish control. Measurements were collected at developmental timepoints of 8, 15, and 30 days post-fertilization. Individual points represent measurements from individual larvae, diamonds indicate the mean, and error bars represent ± standard deviation. Pairwise comparisons were conducted between treatment groups within each developmental stage to assess treatment associated differences in bilateral distance between left and right T1 taste bud regions

Significance levels: p ≤ 0.05 (*), *p ≤ 0.01 (**), p ≤ 0.001 (***)*, p ≤ 0.0001 (****).

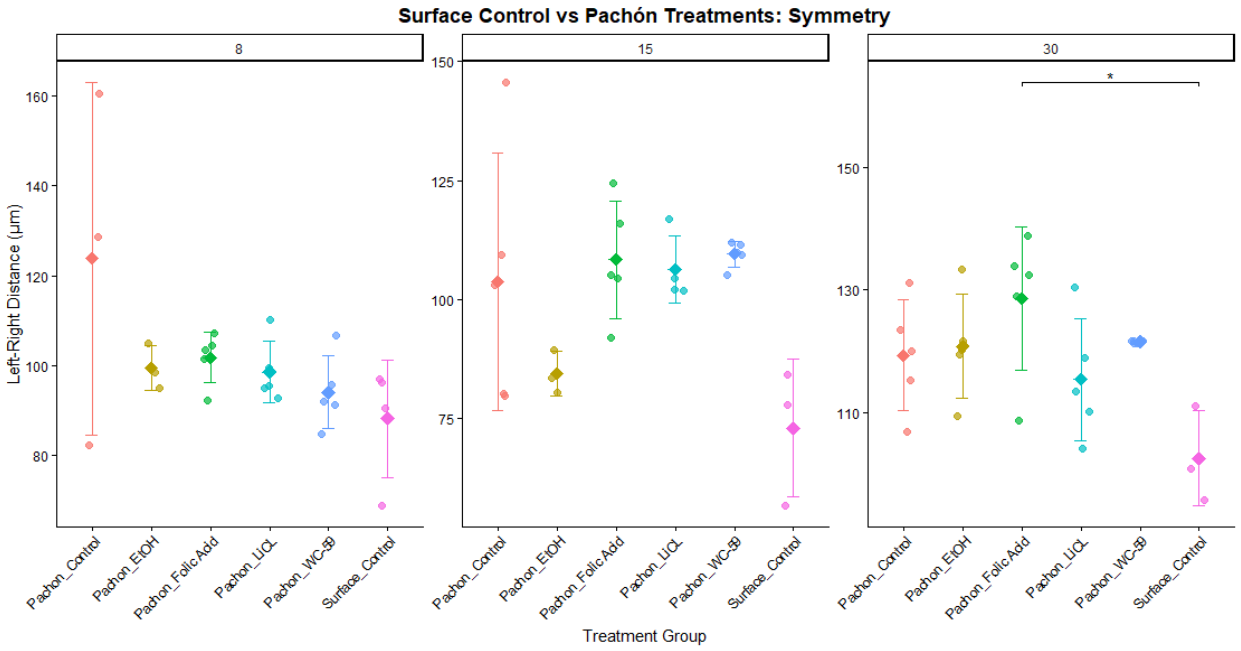

FIGURE 4.15: Bilateral distance between left and right T1 taste bud regions across treatment conditions in Pachón cavefish compared to Surface fish control during larval development. Bilateral distance between left and right T1 taste bud regions was quantified in Pachón cavefish larvae following different treatment conditions (Control, EtOH, folic acid, LiCl, and WC-59) and compared to untreated surface fish control. Measurements were collected at developmental timepoints of 8, 15, and 30 days post-fertilization. Individual points represent measurements from individual larvae, diamonds indicate the mean, and error bars represent ± standard deviation. Pairwise comparisons were conducted between treatment groups within each developmental stage to assess treatment associated differences in bilateral distance between left and right T1 taste bud regions

Significance levels: p ≤ 0.05 (*), *p ≤ 0.01 (**), p ≤ 0.001 (***)*, p ≤ 0.0001 (****).

T1-T2 Bilateral length:

Average bilateral distance between T1 and T2 taste bud containing regions was measured on individual sides of the external mandible in SF and Pachón CF at 8, 15, and 30 dpf.

Due to the lack of T2 taste bud development in SF, measurements and comparisons were conducted solely within Pachón CF treatment groups (FIGURE 4.16).

At 8 dpf, most treatment groups did not exhibit fully developed taste buds within the T2 region. However, limited early onset development was observed in a small number of samples within the Pachón CF control, folic acid, and WC-59 treatment groups. As a result, measurements at this developmental stage were limited and no statistically significant differences were detected between groups.

At later developmental stages, T2 taste buds became more consistently detectable across treatment groups. While no statistically significant differences were observed between Pachón CF treatments, a relatively high degree of variance was noted across samples. By 30 dpf, most treatment groups exhibited slightly reduced average T1–T2 distances compared to Pachón CF controls, although these differences were not statistically significant.

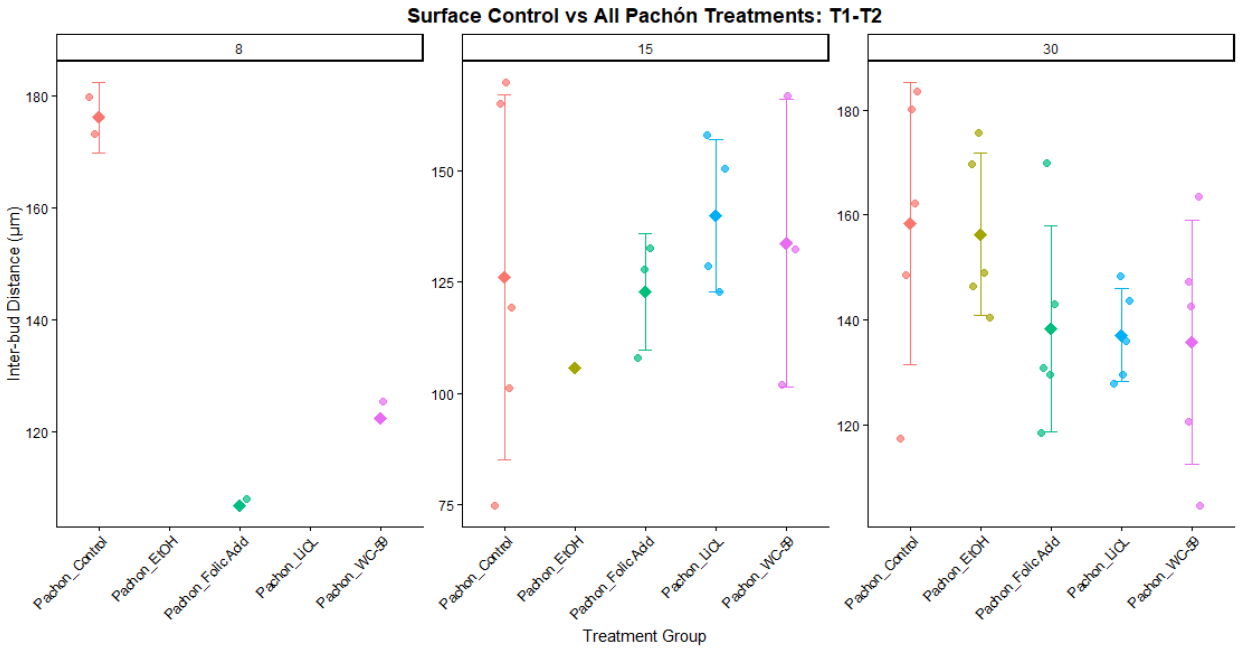

FIGURE 4.16: Bilateral distance between T1-T2 taste bud regions across treatment conditions in Pachón cavefish during larval development. Bilateral distance between T1-T2 taste bud regions was quantified in Pachón cavefish larvae following different treatment conditions (Control, EtOH, folic acid, LiCl, and WC-59). Measurements were collected at developmental timepoints of 8, 15, and 30 days post-fertilization. Individual points represent measurements from individual larvae, diamonds indicate the mean, and error bars represent ± standard deviation. Pairwise comparisons were conducted between treatment groups within each developmental stage to assess treatment associated differences in bilateral distance between T1-T2 taste bud regions.

Significance levels: p ≤ 0.05 (*), *p ≤ 0.01 (**), p ≤ 0.001 (***)*, p ≤ 0.0001 (****).

T2-T3 Bilateral length:

Average bilateral distance between T2 and T3 taste bud containing regions was measured on individual sides of the external mandible in SF and Pachón CF at 8, 15, and 30 dpf.

Due to the lack of T2 taste bud development in SF, measurements and comparisons were conducted solely within Pachón CF treatment groups (FIGURE 4.17).

At 8 dpf, most samples across treatment groups did not exhibit fully developed taste buds within the T2 region. However, limited early onset development was observed in a small number of samples within the Pachón CF control, folic acid, and WC-59 treatment groups. As a result, measurements at this developmental stage were limited.

Across all developmental time points, no statistically significant differences in T2–T3 distance were observed between Pachón CF treatment groups. Although measurements became more consistent as development progressed, distances between T2 and T3 regions remained comparable across treatments.

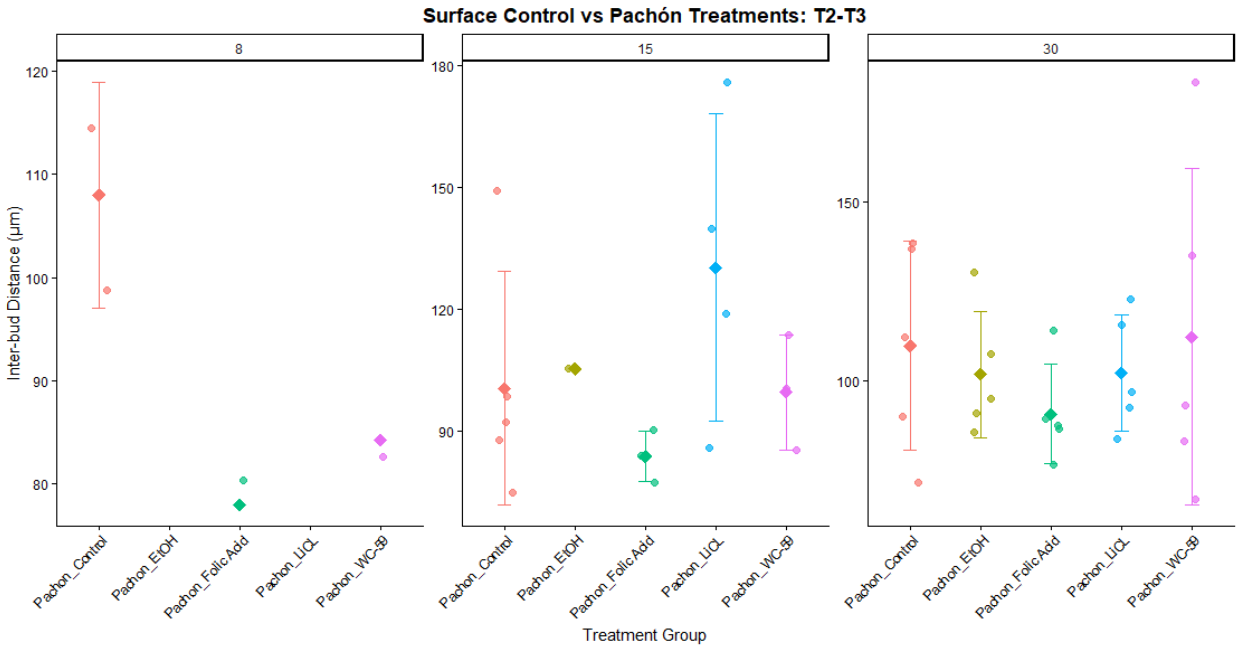

FIGURE 4.17: Bilateral distance between T2-T3 taste bud regions across treatment conditions in Pachón cavefish during larval development. Bilateral distance between T2-T3 taste bud regions was quantified in Pachón cavefish larvae following different treatment conditions (Control, EtOH, folic acid, LiCl, and WC-59). Measurements were collected at developmental timepoints of 8, 15, and 30 days post-fertilization. Individual points represent measurements from individual larvae, diamonds indicate the mean, and error bars represent ± standard deviation. Pairwise comparisons were conducted between treatment groups within each developmental stage to assess treatment associated differences in bilateral distance between T2-T3 taste bud regions.

Significance levels: $p \leq 0.05$ (*), $p \leq 0.01$ (**), $p \leq 0.001$ (***), $p \leq 0.0001$ (****).

T3-T4 Bilateral length:

Average bilateral distance between T3 and T4 taste bud containing regions was measured on individual sides of the external mandible in SF and Pachón CF at 8, 15, and 30 dpf.

When comparing all SF treatments to the Pachón CF control, no statistically significant differences were observed in the average T3–T4 distance at either 8 or 15 dpf (FIGURE 4.18). At 8 dpf, Pachón CF control exhibited slightly larger average distances relative to all other treatment groups, although these differences were not statistically significant. At 30 dpf, average distances across SF treatments remained comparable. However, a statistically significant reduction in T3–T4 distance was observed when comparing Pachón CF control to WC-59 treated SF ($p \leq 0.05$, *).

When comparing SF control with all Pachón CF treatments (FIGURE 4.19), no statistically significant differences were detected at any developmental stage. Despite this, Pachón CF groups generally exhibited slightly greater average distances between T3 and T4 taste bud containing regions compared to SF control, particularly at 8 and 30 dpf.

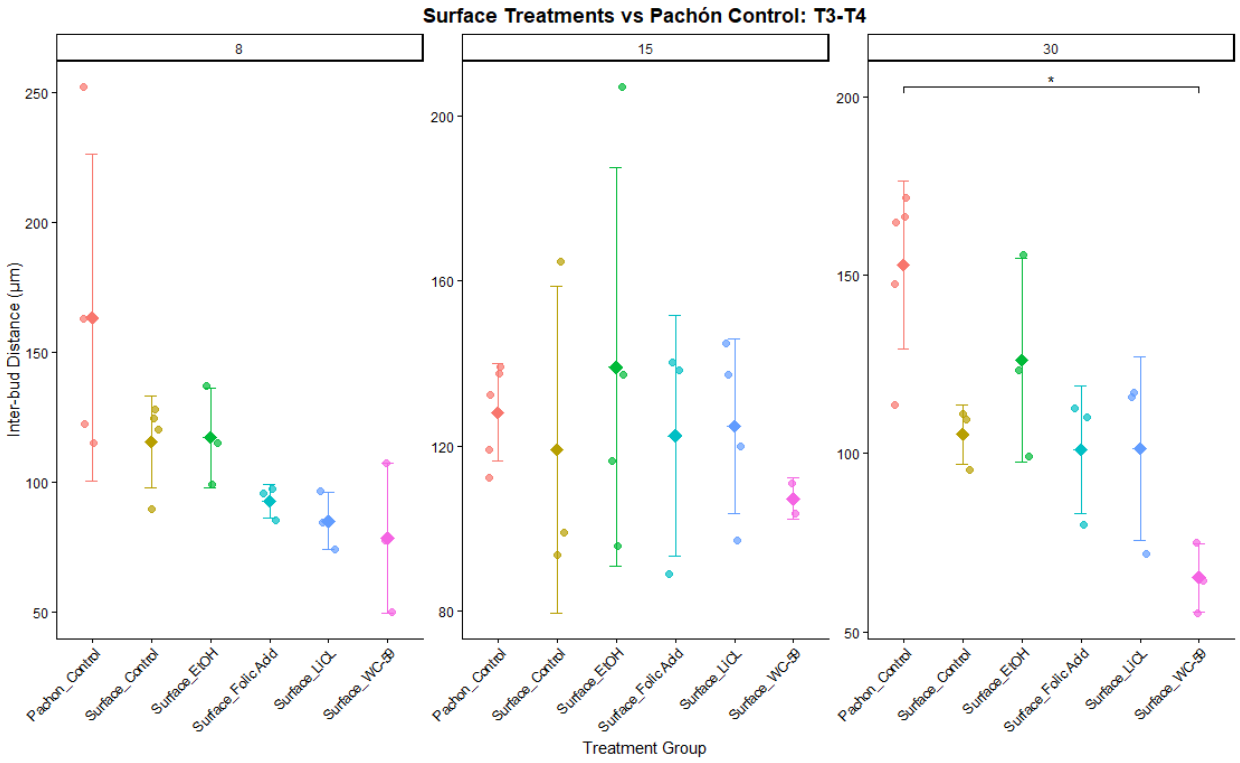

FIGURE 4.18: Bilateral distance between T3-T4 taste bud regions across treatment conditions in Surface fish compared to Pachón cavefish control during larval development. Bilateral distance between T3-T4 taste bud regions was quantified in Surface fish larvae following different treatment conditions (Control, EtOH, folic acid, LiCl, and WC-59) and compared to untreated Pachón cavefish control. Measurements were collected at developmental timepoints of 8, 15, and 30 days post-fertilization. Individual points represent measurements from individual larvae, diamonds indicate the mean, and error bars represent ± standard deviation. Pairwise comparisons were conducted between treatment groups within each developmental stage to assess treatment associated differences in bilateral distance between T3-T4 taste bud regions.

Significance levels: p ≤ 0.05 (*), *p ≤ 0.01 (**), p ≤ 0.001 (***)*, p ≤ 0.0001 (****).

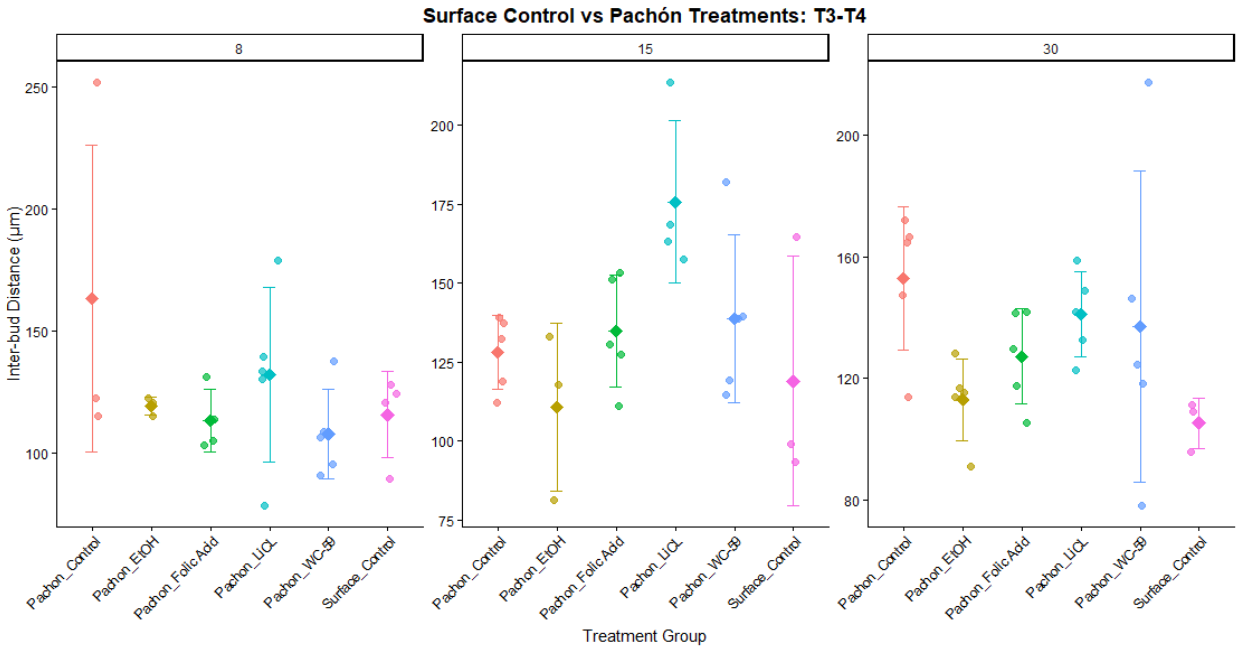

FIGURE 4.19: Bilateral distance between T3-T4 taste bud regions across treatment conditions in Pachón cavefish compared to Surface fish control during larval development. Bilateral distance between T3-T4 taste bud regions was quantified in Pachón cavefish larvae following different treatment conditions (Control, EtOH, folic acid, LiCl, and WC-59) and compared to untreated surface fish control. Measurements were collected at developmental timepoints of 8, 15, and 30 days post-fertilization. Individual points represent measurements from individual larvae, diamonds indicate the mean, and error bars represent ± standard deviation. Pairwise comparisons were conducted between treatment groups within each developmental stage to assess treatment associated differences in bilateral distance between T3-T4 taste bud regions.

Significance levels: p ≤ 0.05 (*), *p ≤ 0.01 (**), p ≤ 0.001 (***)*, p ≤ 0.0001 (****).

Behavioral Assay

Behavioral assays were conducted to examine swimming behavior across treatment groups in SF and Pachón CF during exposure to flavored feed stimuli. Behavioral activity was visualized using heatmaps representing the total area explored within the assay chamber (FIGURE 4.20).

Because heatmap patterns were largely consistent across treatments, representative heatmaps for SF control and Pachón CF control were selected for illustration (FIGURE 4.20). Following a 15-minute acclimatization period, Pachón CF displayed a consistent circling pattern along the perimeter of the Petri dish, indicating repeated edge-associated swimming behavior with periodic changes in swimming speed.

In contrast, SF exhibited more exploratory swimming behavior following acclimatization. SF individuals moved throughout the chamber and displayed intermittent stationary periods, resulting in more dispersed movement patterns compared to Pachón CF.

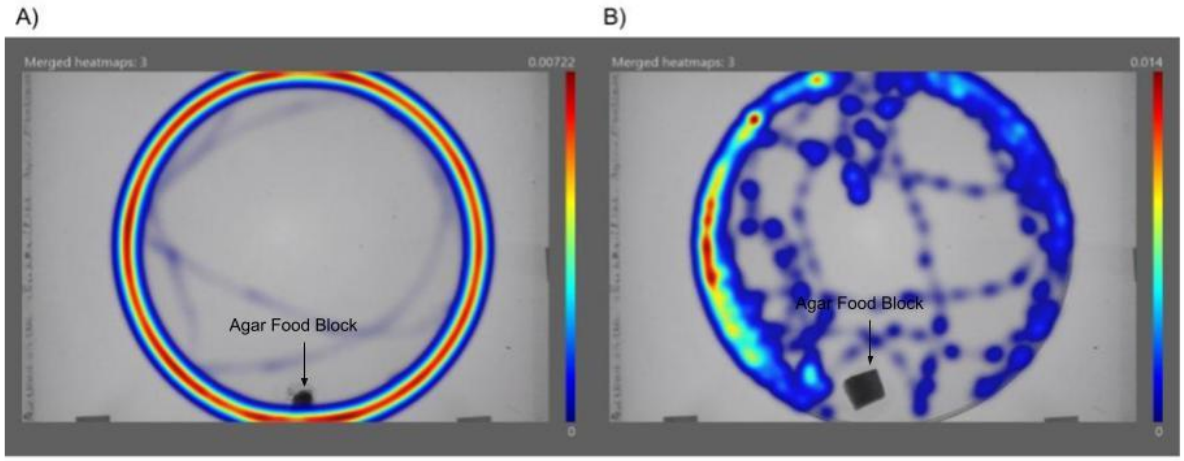

FIGURE 4.20: Behavioral heatmaps showing swimming patterns of Pachón cavefish and surface fish. Heatmaps generated using EthoVision 3.1 tracking software for both A) Pachón Cavefish and B) Surface Fish. Average overall time spent within specific coordinated areas of petri dishes are represented spectrum of colors red to blue, red indicating highest density of time spent of the span of 5 minutes per trial of the course of 3 trials.

Behavioral Assay: Distance from feed in relation towards individual treatments

Average distance from the feed source was measured in SF and Pachón CF across different feeding conditions (control, EtOH, quinine, and sucrose) (FIGURE 4.21).

When comparing SF to Pachón CF across feeding conditions, no statistically significant differences in average distance from the feed were observed. However, SF displayed a broader range of preferred distances and generally maintained greater average distances from the feed source compared to Pachón CF. This pattern reflects the exploratory swimming behavior observed in SF, whereas Pachón CF displayed more consistent circling behavior near the perimeter of the dish.

EtOH treated SF and Pachón CF, results were similar between the two morphs, showing no significant differences between the two (FIGURE 4.22). SF having overall greater distance from feed with greater variance compared to Pachón cave fish.

Folic acid treated SF and Pachón CF, no significant difference was observed between the two morphs (FIGURE 4.23). While on average showing greater variation in average distance within folic acid treated surface morphs compared to CF.

LiCl treated SF and Pachón cave fish results had also showed that average distance from different feeds were not statistically significant between the two morphs (FIGURE 4.24). Overall showing reduced variance in distance within LiCl treated Pachón CF compared to LiCl treated SF.

Observing LiCl treated SF alone, no statistical significance was noted between different feeding types, indicating no differential preference between feeds (FIGURE 4.31).

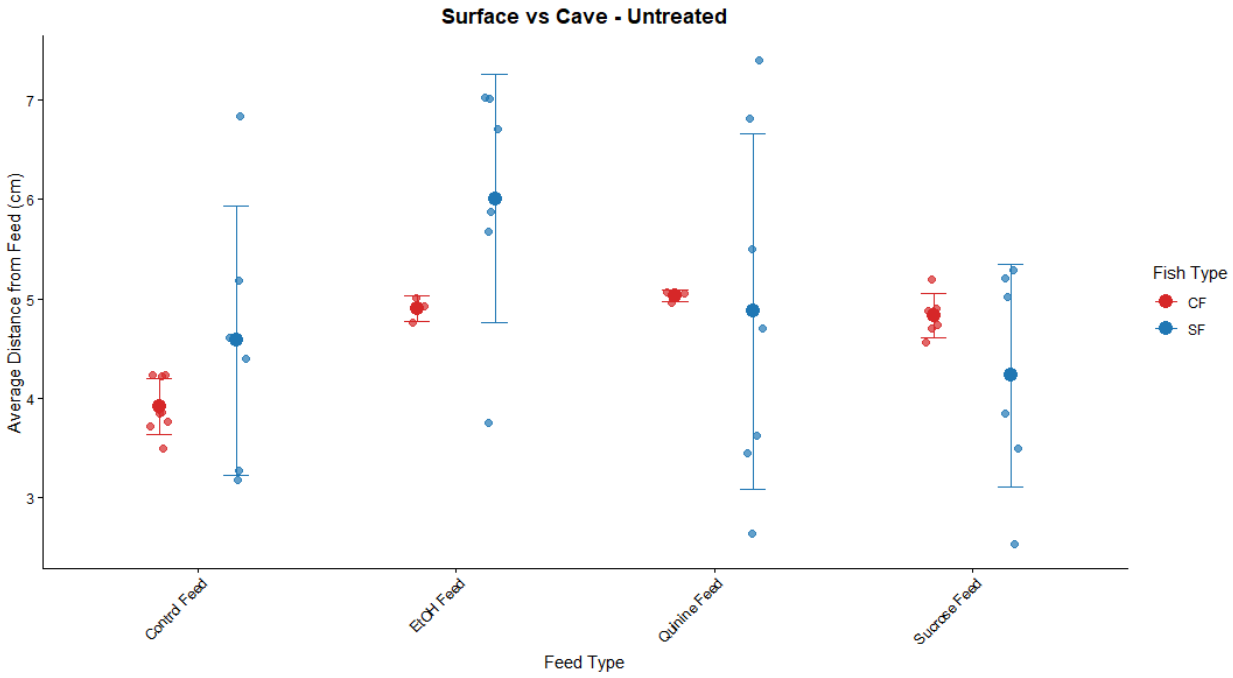

FIGURE 4.21: Chemosensory feeding behavior associated with average distance from feed for untreated surface and cavefish larvae. Average distance associated from feed was measured for untreated surface fish and cavefish under different feeding types (Control, EtOH, Quinine and Sucrose feeds). Individual points represent measurements from individual trials, diamonds indicate the mean, and error bars represent ± standard deviation. Pairwise comparison was conducted between untreated surface fish and cavefish morphs within individual feeding types.

Significance levels: $p \leq 0.05$ (*), $p \leq 0.01$ (**), $p \leq 0.001$ (***), $p \leq 0.0001$ (****).

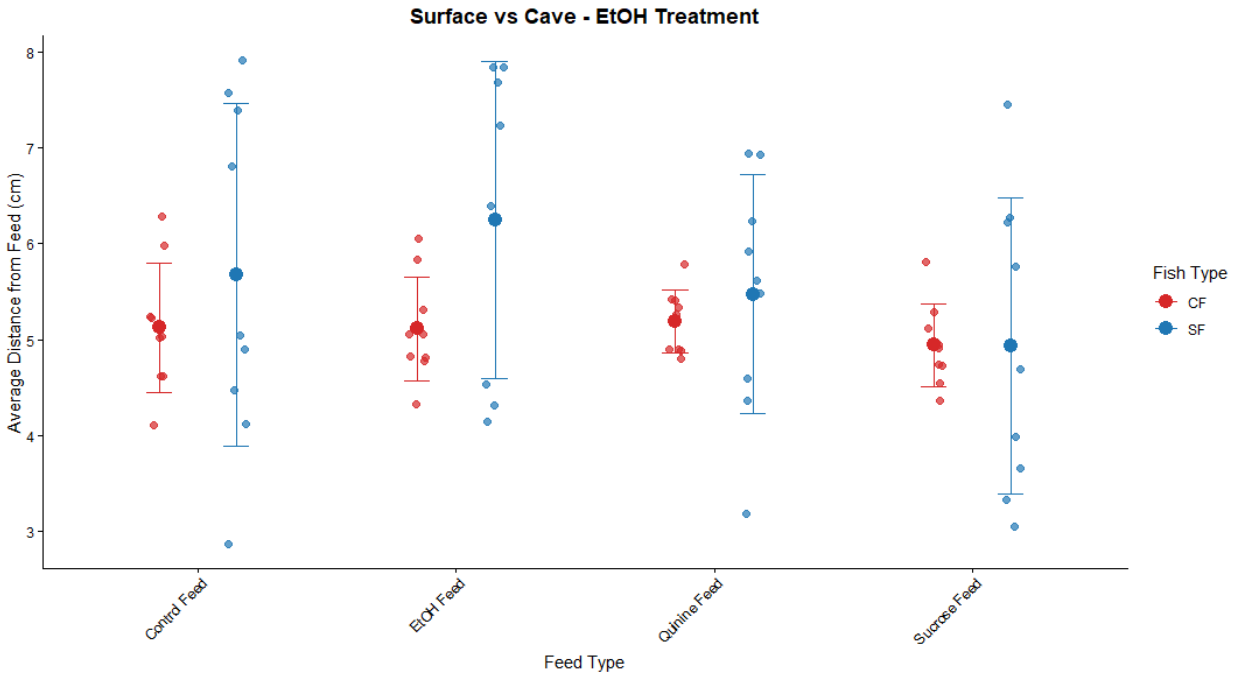

FIGURE 4.22: Chemosensory feeding behavior associated with average distance from feed for EtOH treated surface and cavefish larvae. Average distance associated from feed was measured for EtOH treated surface fish and cavefish under different feeding types (Control, EtOH, Quinine and Sucrose feeds). Individual points represent measurements from individual trials, diamonds indicate the mean, and error bars represent ± standard deviation. Pairwise comparison was conducted between EtOH treated surface fish and cavefish morphs for individual feeding types.

Significance levels: $p \leq 0.05$ (*), $p \leq 0.01$ (**), $p \leq 0.001$ (***), $p \leq 0.0001$ (****).

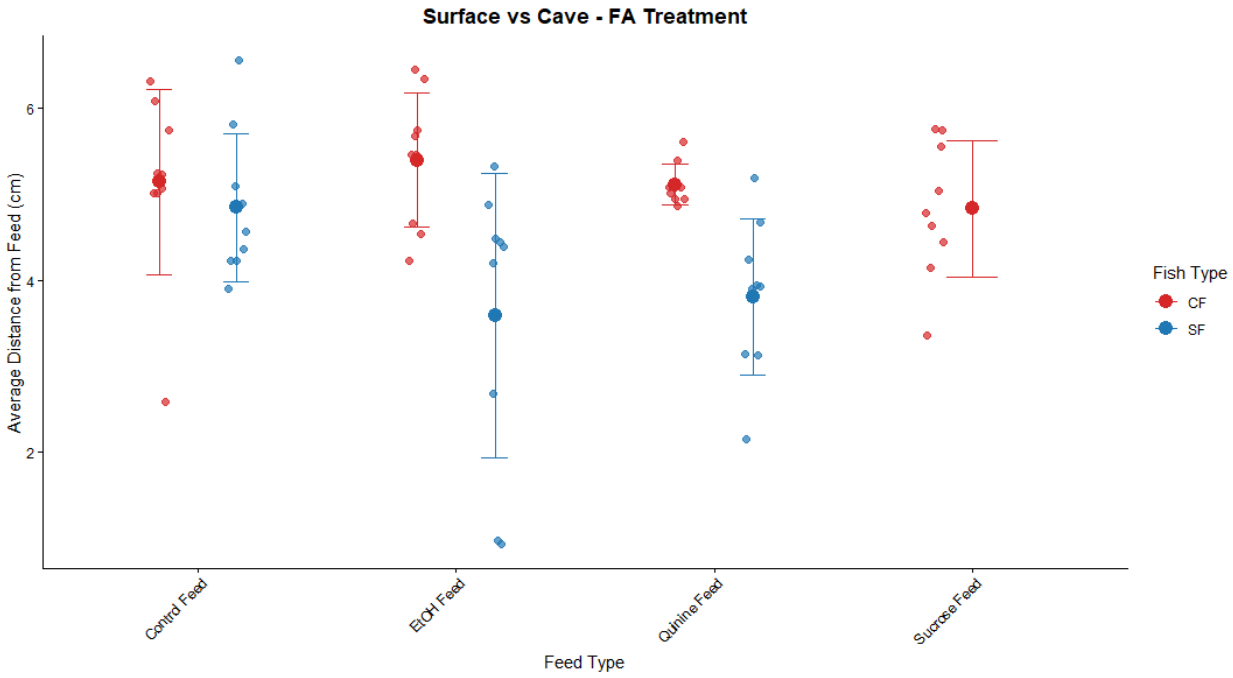

FIGURE 4.23: Chemosensory feeding behavior associated with average distance from feed for folic acid treated surface and cavefish larvae. Average distance associated from feed was measured for folic acid treated surface fish and cavefish under different feeding types (Control, EtOH, Quinine and Sucrose feeds). Individual points represent measurements from individual trials, diamonds indicate the mean, and error bars represent ± standard deviation. Pairwise comparison was conducted between folic acid treated surface fish and cavefish morphs for individual feeding types.

Significance levels: $p \leq 0.05$ (*), $p \leq 0.01$ (**), $p \leq 0.001$ (***), $p \leq 0.0001$ (****).

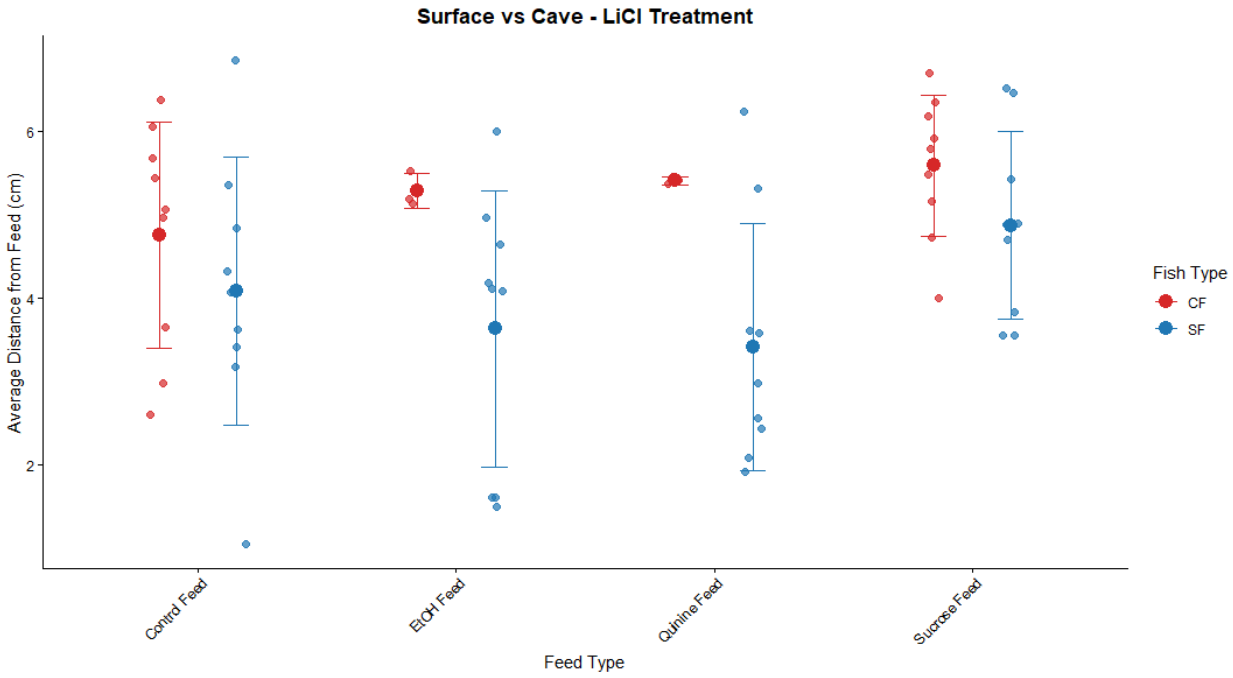

FIGURE 4.24: Chemosensory feeding behavior associated with average distance from feed for LiCl treated surface and cavefish larvae. Average distance associated from feed was measured for LiCl treated surface fish and cavefish under different feeding types (Control, EtOH, Quinine and Sucrose feeds). Individual points represent measurements from individual trials, diamonds indicate the mean, and error bars represent ± standard deviation. Pairwise comparison was conducted between LiCl treated surface fish and cavefish morphs for individual feeding types.

Significance levels: $p \leq 0.05$ (*), $p \leq 0.01$ (**), $p \leq 0.001$ (***), $p \leq 0.0001$ (****).

Behavioral Assay: Distance of individual treatments samples in relation towards feeding type

Average distance from the feed source was measured for individual treatment groups of SF and Pachón CF under different feeding conditions (control, EtOH, quinine, and sucrose).

When comparing SF and Pachón CF within control feeding conditions, no statistically significant differences were observed between morphs across individual treatments (FIGURE 4.25). However, Pachón CF generally maintained shorter average distances from the feed source compared to SF.

When comparing SF and Pachón CF within EtOH feeding conditions, no statistically significant differences were detected between morphs across treatment groups (FIGURE 4.26). SF, however, displayed greater variance in distance from the feed source compared to Pachón CF.

Comparison of SF and Pachón CF within quinine feeding conditions revealed no statistically significant differences between morphs (FIGURE 4.27). SF again displayed greater variance in distance from the feed compared to Pachón CF.

When comparing SF and Pachón CF within sucrose feeding conditions, no statistically significant differences were detected between morphs (FIGURE 4.28). SF again displayed greater variance in average distance from the feed compared to Pachón CF.

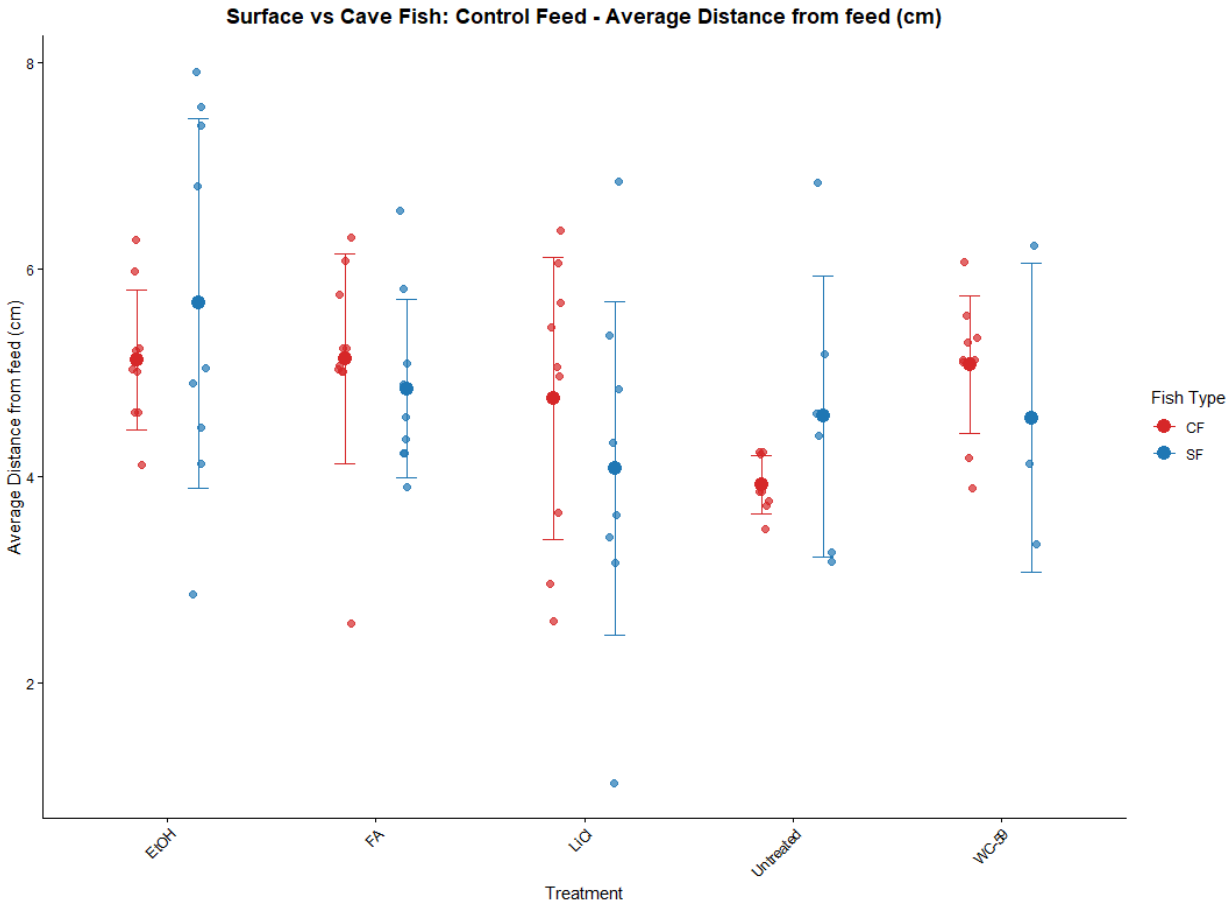

FIGURE 4.25: Chemosensory feeding behavior associated with average distance from control feed across treatment conditions in surface and cave morph larvae. Average distance from control feed was measured for surface fish and cavefish larvae following different treatment conditions (Control, EtOH, FA, LiCl, and WC-59 treatments). Individual points represent measurements from individual trials, diamonds indicate the mean, and error bars represent ± standard deviation. Pairwise comparison was conducted between surface fish and cavefish for control feed.

Significance levels: p ≤ 0.05 (*),p ≤ 0.01 (**),p ≤ 0.001 (***), p ≤ 0.0001 (****).

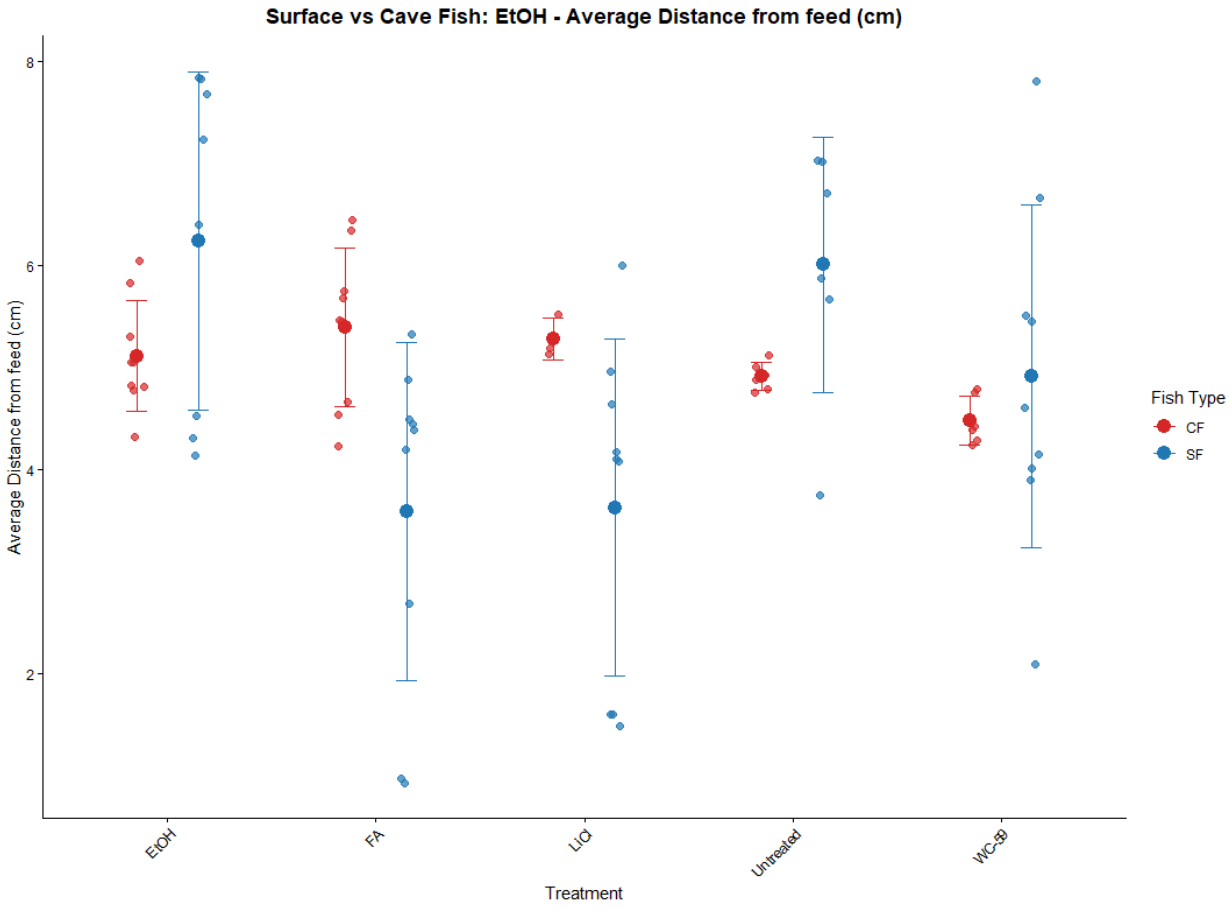

FIGURE 4.26: Chemosensory feeding behavior associated with average distance from EtOH feed across treatment conditions in surface and cave morph larvae. Average distance from EtOH feed was measured for surface fish and cavefish larvae following different treatment conditions (Control, EtOH, FA, LiCl, and WC-59 treatments). Individual points represent measurements from individual trials, diamonds indicate the mean, and error bars represent ± standard deviation. Pairwise comparison was conducted between surface fish and cavefish for EtOH feed.

Significance levels: p ≤ 0.05 (*),p ≤ 0.01 (**),p ≤ 0.001 (***), p ≤ 0.0001 (****).

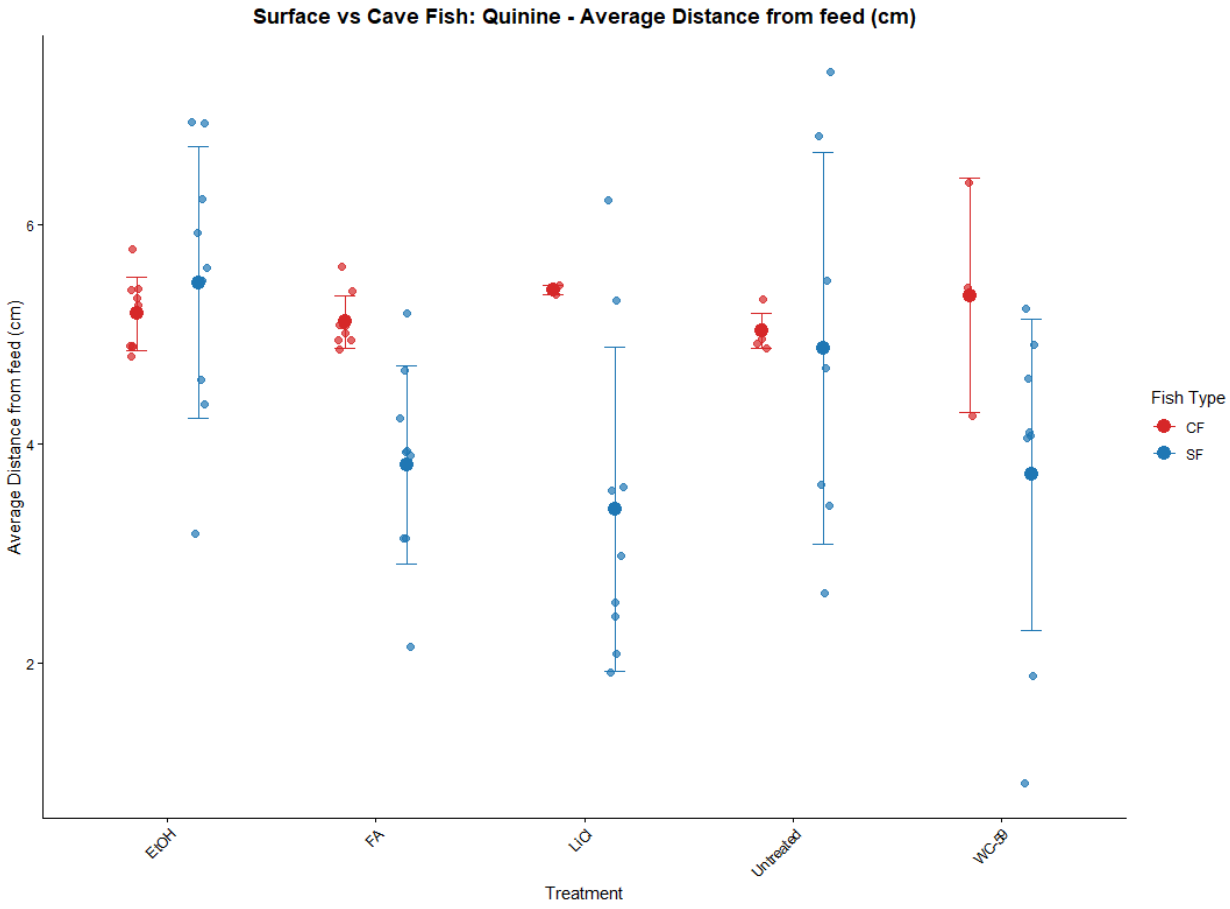

FIGURE 4.27: Chemosensory feeding behavior associated with average distance from quinine feed across treatment conditions in surface and cave morph larvae. Average distance from quinine feed was measured for surface fish and cavefish larvae following different treatment conditions (Control, EtOH, FA, LiCl, and WC-59 treatments). Individual points represent measurements from individual trials, diamonds indicate the mean, and error bars represent ± standard deviation. Pairwise comparison was conducted between surface fish and cavefish for quinine feed.

Significance levels: p ≤ 0.05 (*),p ≤ 0.01 (**),p ≤ 0.001 (***), p ≤ 0.0001 (****).

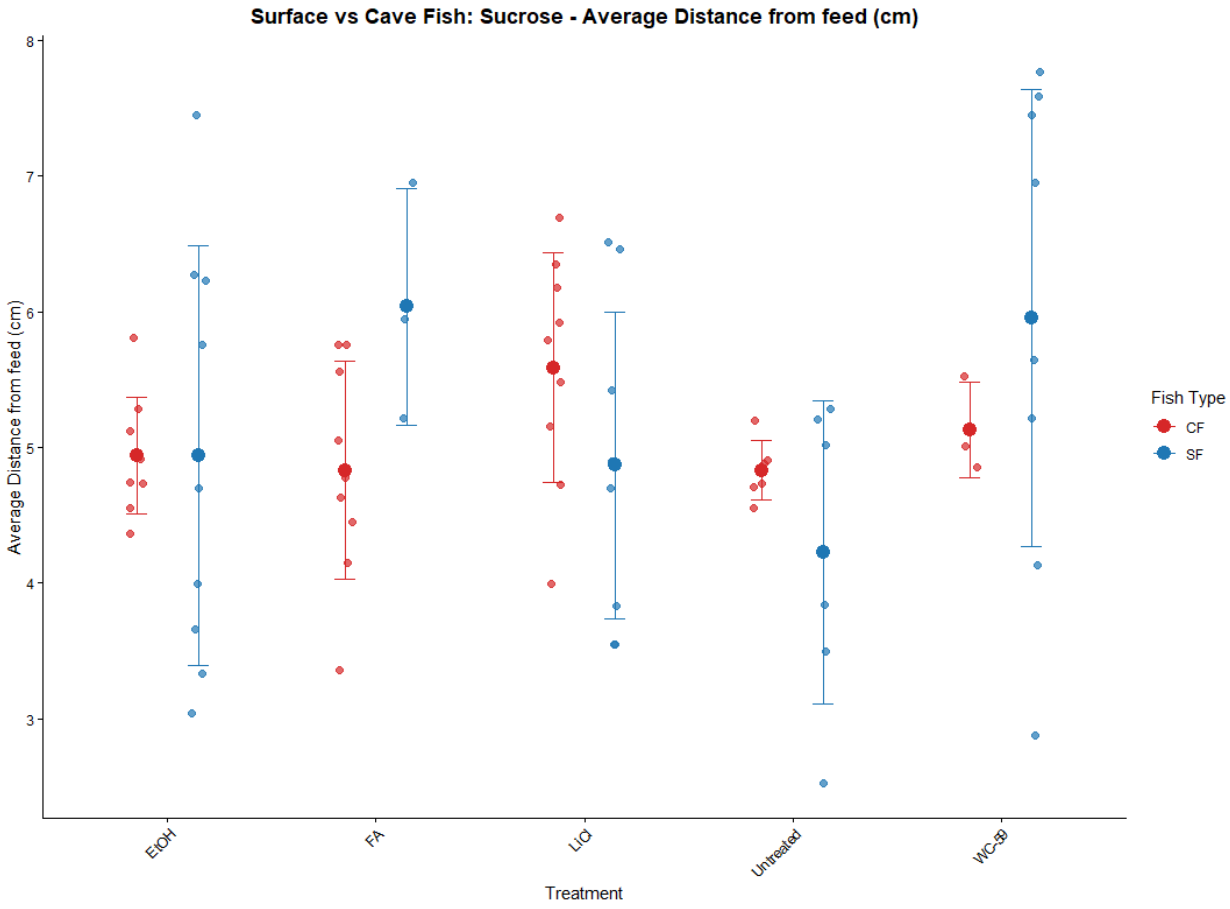

FIGURE 4.28: Chemosensory feeding behavior associated with average distance from sucrose feed across treatment conditions in surface and cave morph larvae. Average distance from sucrose feed was measured for surface fish and cavefish larvae following different treatment conditions (Control, EtOH, FA, LiCl, and WC-59 treatments). Individual points represent measurements from individual trials, diamonds indicate the mean, and error bars represent ± standard deviation. Pairwise comparison was conducted between surface fish and cavefish for sucrose feed.

Significance levels: p ≤ 0.05 (*),p ≤ 0.01 (**),p ≤ 0.001 (***), p ≤ 0.0001 (****).

Behavioral Assay: Time spent near feed per treatments

Average time spent near the feed source was measured for SF and Pachón CF across different feeding conditions (control, EtOH, quinine, and sucrose) and treatment groups (FIGURE 4.29).

When comparing untreated SF and untreated Pachón CF across individual feeding conditions, no statistically significant differences were observed between morphs. However, Pachón CF consistently exhibited reduced variance in the time spent near the feed source compared to SF (FIGURE 4.29).

Similar patterns were observed across all treatment groups. Comparisons between SF and Pachón CF treated with EtOH, folic acid, or LiCl revealed no statistically significant differences in the average time spent near the feed under any feeding condition (FIGUREs 4.30, 4.31, 5.32). Across these treatments, Pachón CF continued to display more consistent behavior with reduced variance relative to SF.

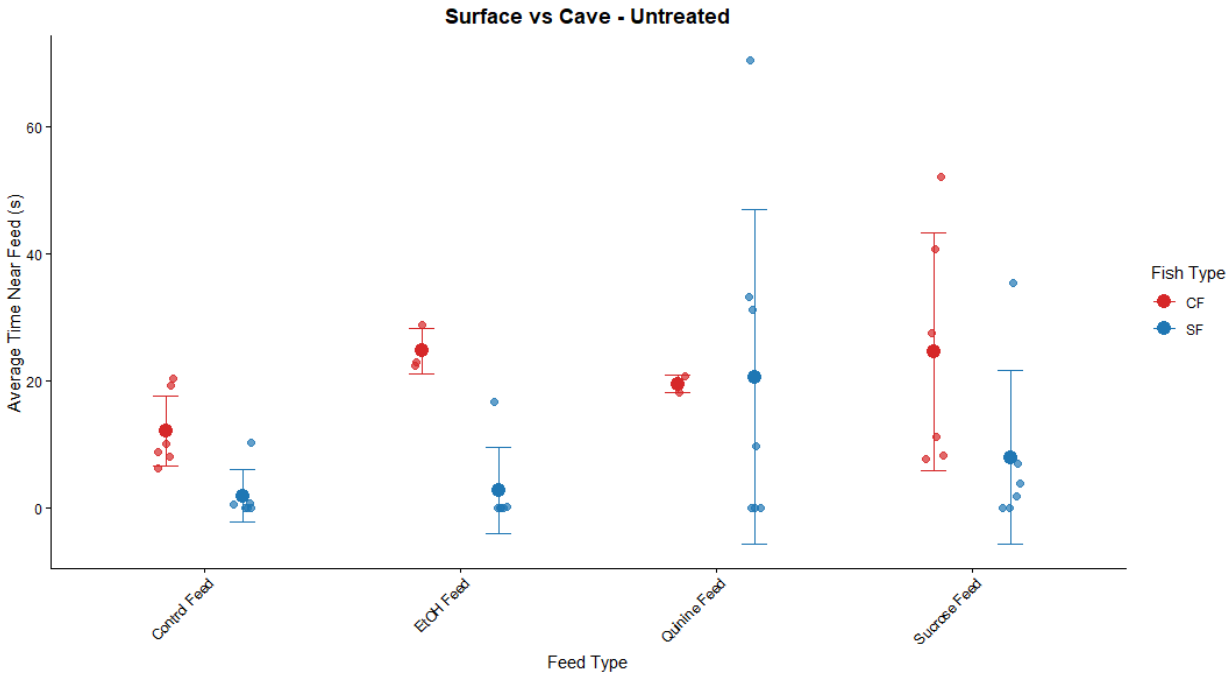

FIGURE 4.29: Chemosensory feeding behavior associated with average time near feed for untreated surface and cavefish larvae. Average time near feed was measured for untreated surface fish and cavefish under different feeding types (Control, EtOH, Quinine and Sucrose feeds). Individual points represent measurements from individual trials, diamonds indicate the mean, and error bars represent ± standard deviation. Pairwise comparison was conducted between untreated surface fish and cavefish morphs for individual feeding types.

Significance levels: $p \leq 0.05$ (*), $p \leq 0.01$ (**), $p \leq 0.001$ (***), $p \leq 0.0001$ (****).

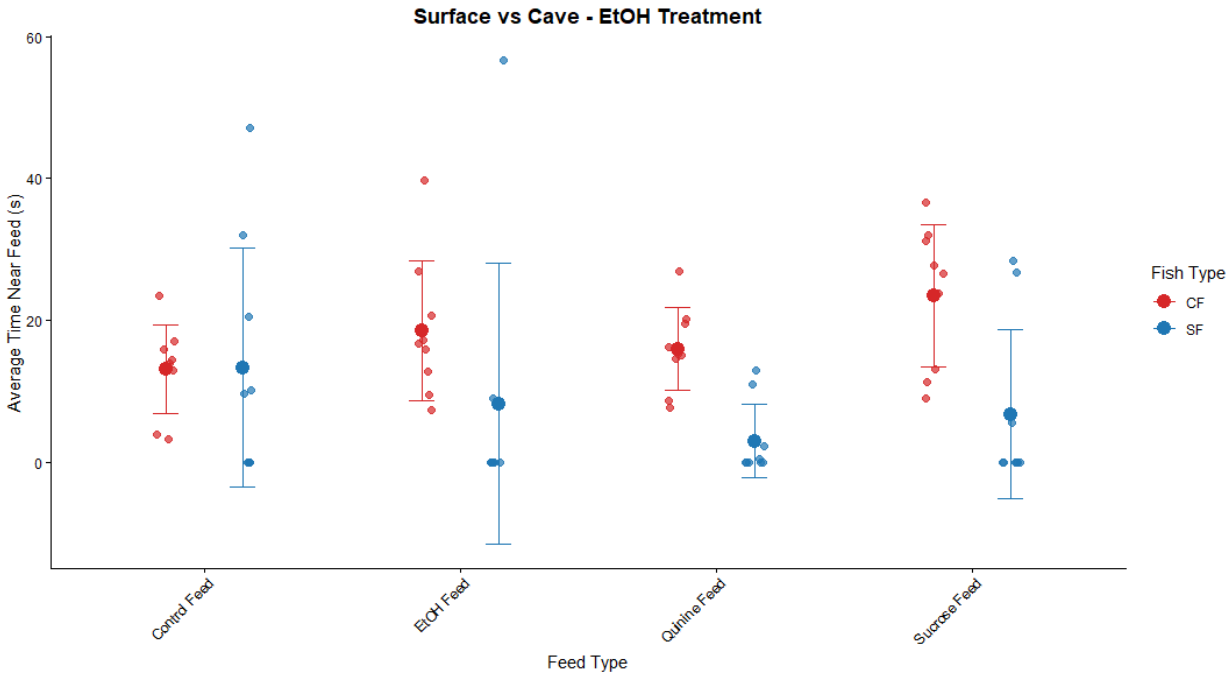

FIGURE 4.30: Chemosensory feeding behavior associated with average time near feed for EtOH treated surface and cavefish larvae. Average time near feed was measured for EtOH treated surface fish and cavefish under different feeding types (Control, EtOH, Quinine and Sucrose feeds). Individual points represent measurements from individual trials, diamonds indicate the mean, and error bars represent ± standard deviation. Pairwise comparison was conducted between EtOH treated surface fish and cavefish morphs for individual feeding types.

Significance levels: $p \leq 0.05$ (*), $p \leq 0.01$ (**), $p \leq 0.001$ (***), $p \leq 0.0001$ (****).

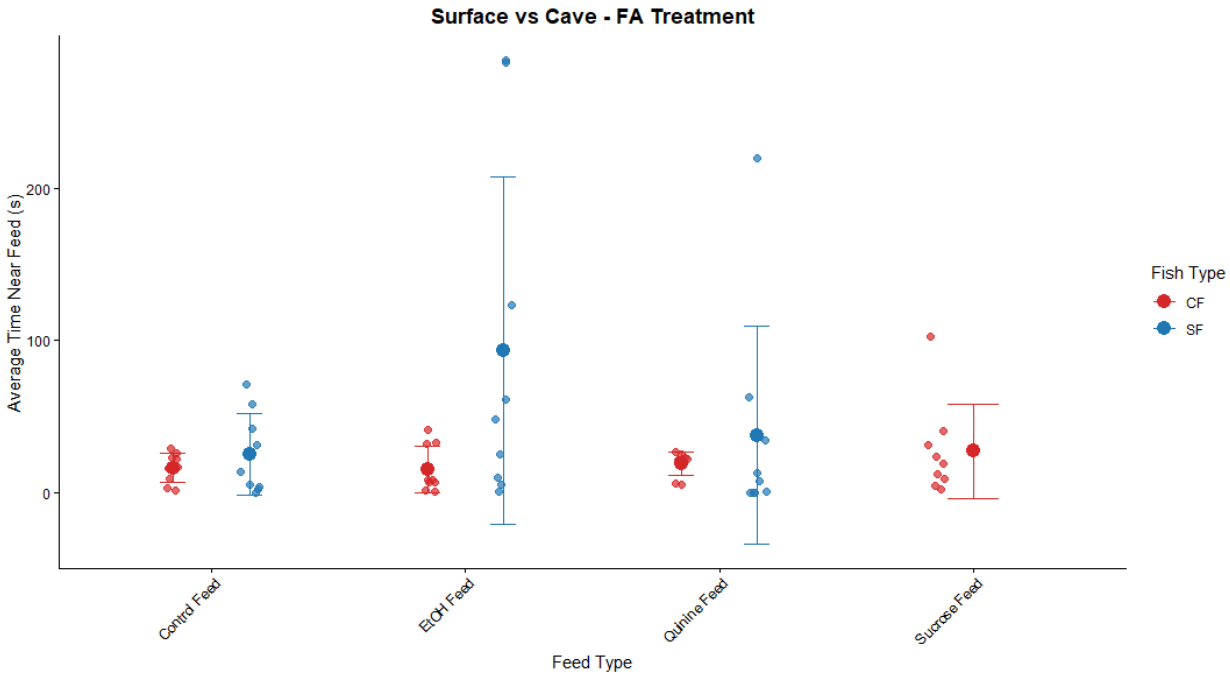

FIGURE 4.31: Chemosensory feeding behavior associated with average time near feed for folic acid treated surface and cavefish larvae. Average time near feed was measured for folic acid treated surface fish and cavefish under different feeding types (Control, EtOH, Quinine and Sucrose feeds). Individual points represent measurements from individual trials, diamonds indicate the mean, and error bars represent ± standard deviation. Pairwise comparison was conducted between folic acid treated surface fish and cavefish morphs for individual feeding types.

Significance levels: $p \leq 0.05$ (*), $p \leq 0.01$ (**), $p \leq 0.001$ (***), $p \leq 0.0001$ (****).

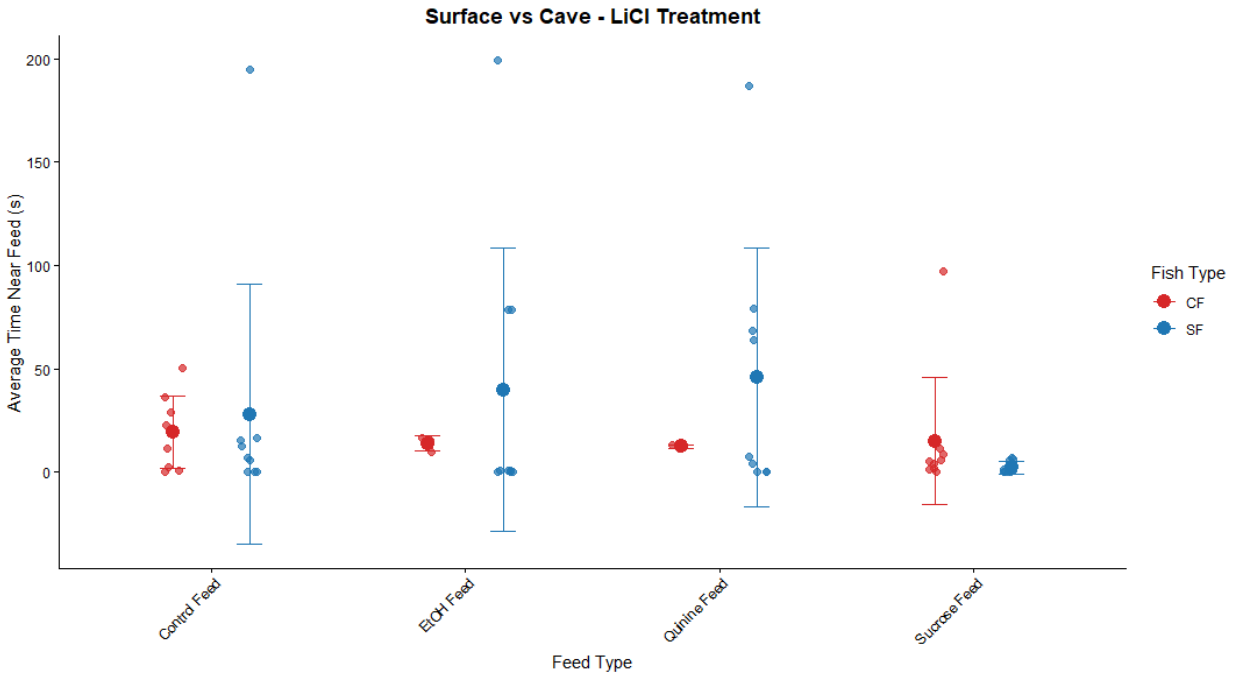

FIGURE 4.32: Chemosensory feeding behavior associated with average time near feed for LiCl treated surface and cavefish larvae. Average time near feed was measured for LiCl treated surface fish and cavefish under different feeding types (Control, EtOH, Quinine and Sucrose feeds). Individual points represent measurements from individual trials, diamonds indicate the mean, and error bars represent ± standard deviation. Pairwise comparison was conducted between LiCl treated surface fish and cavefish morphs for individual feeding types.

Significance levels: $p \leq 0.05$ (*), $p \leq 0.01$ (**), $p \leq 0.001$ (***), $p \leq 0.0001$ (****).

Behavioral Assay: Time of individual treatments in relation towards feeding type

Average time spent near the feed source was analyzed across individual treatments for SF and Pachón CF under different feeding conditions (control, EtOH, quinine, and sucrose).

When observing average time spent near the control feed, no statistically significant differences were detected between SF and Pachón CF (FIGURE 4.33). However, SF displayed greater variance in time spent near the feed compared to Pachón CF.

A similar pattern was observed under EtOH feeding conditions. Comparison between SF and Pachón CF revealed no statistically significant differences in average time spent near the feed (FIGURE 4.34), although SF again displayed greater variance compared to Pachón CF.

Under quinine feeding conditions, no statistically significant differences in average time spent near the feed were observed between SF and Pachón CF (FIGURE 4.35), with SF again exhibiting greater variance.

Finally, when observing time spent near sucrose feed, no statistically significant differences were detected between SF and Pachón CF (FIGURE 4.36). In this condition, Pachón CF displayed slightly greater variance compared to SF.

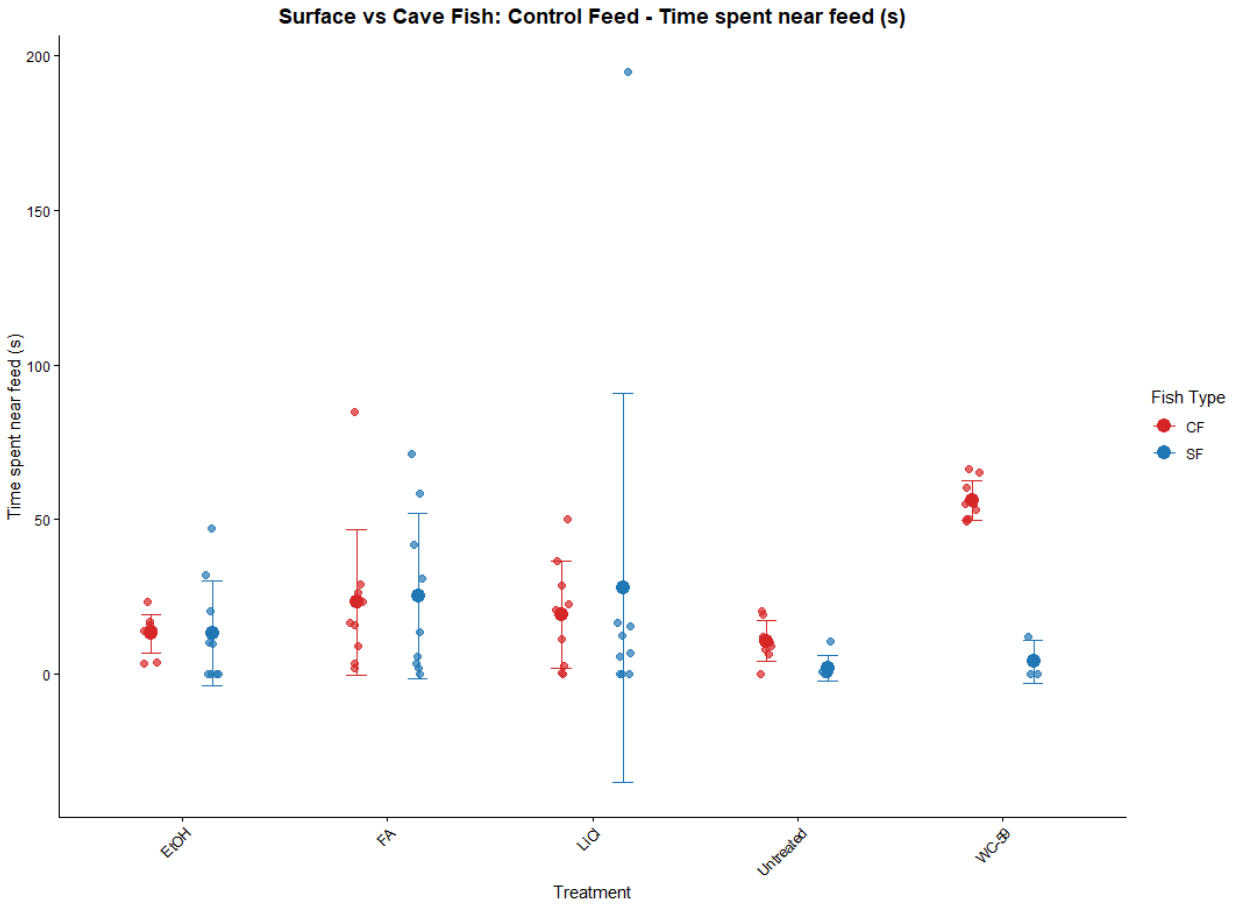

FIGURE 4.33: Chemosensory feeding behavior associated with average time near control feed across treatment conditions in surface and cave morph larvae. Average time near control feed was measured for surface fish and cavefish larvae following different treatment conditions (Control, EtOH, FA, LiCl, and WC-59 treatments). Individual points represent measurements from individual trials, diamonds indicate the mean, and error bars represent ± standard deviation. Pairwise comparison was conducted between surface fish and cavefish for control feed.

Significance levels: $p \leq 0.05$ (*),$p \leq 0.01$ (**),$p \leq 0.001$ (***), $p \leq 0.0001$ (****).

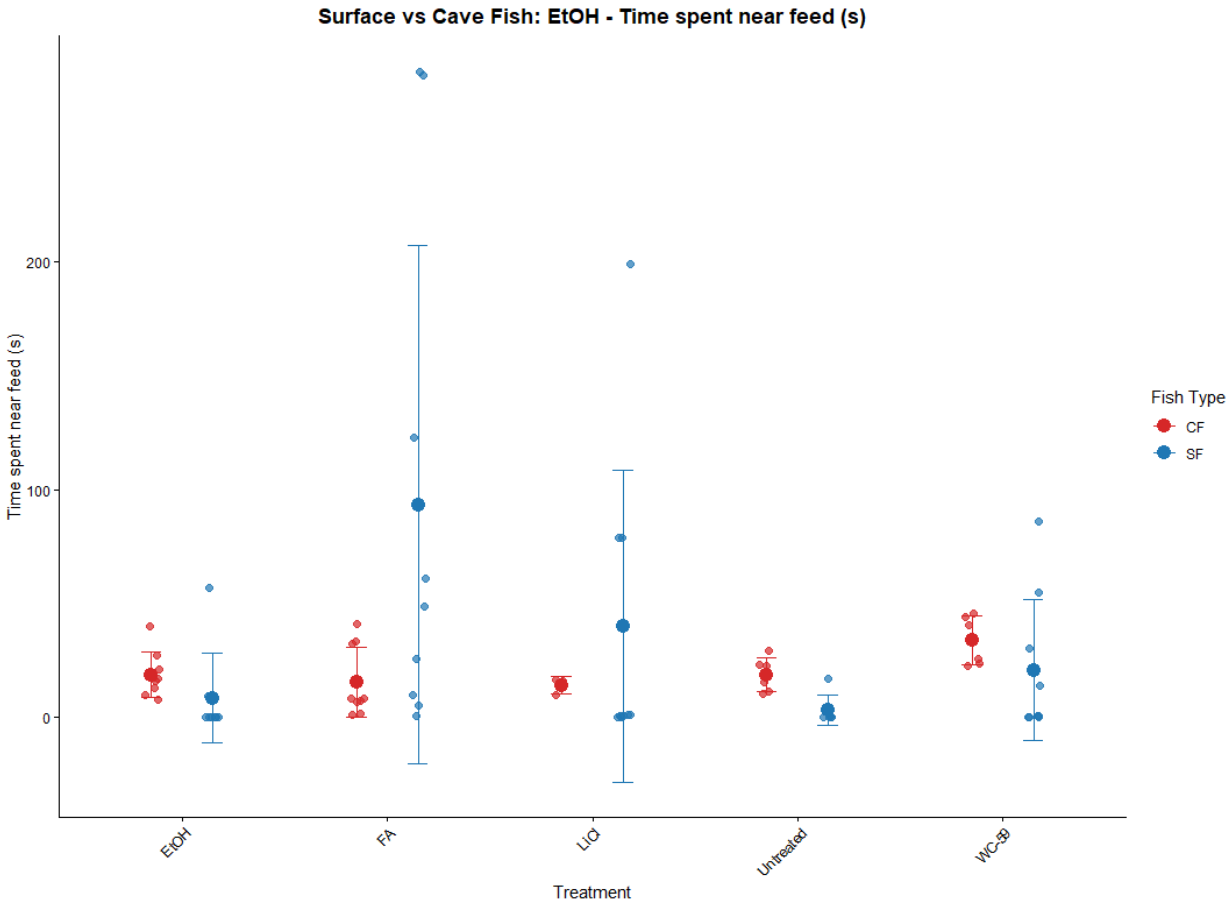

FIGURE 4.34: Chemosensory feeding behavior associated with average time near EtOH feed across treatment conditions in surface and cave morph larvae. Average time near EtOH feed was measured for surface fish and cavefish larvae following different treatment conditions (Control, EtOH, FA, LiCl, and WC-59 treatments). Individual points represent measurements from individual trials, diamonds indicate the mean, and error bars represent ± standard deviation. Pairwise comparison was conducted between surface fish and cavefish for EtOH feed.

Significance levels: $p \leq 0.05$ (*),$p \leq 0.01$ (**),$p \leq 0.001$ (***), $p \leq 0.0001$ (****).

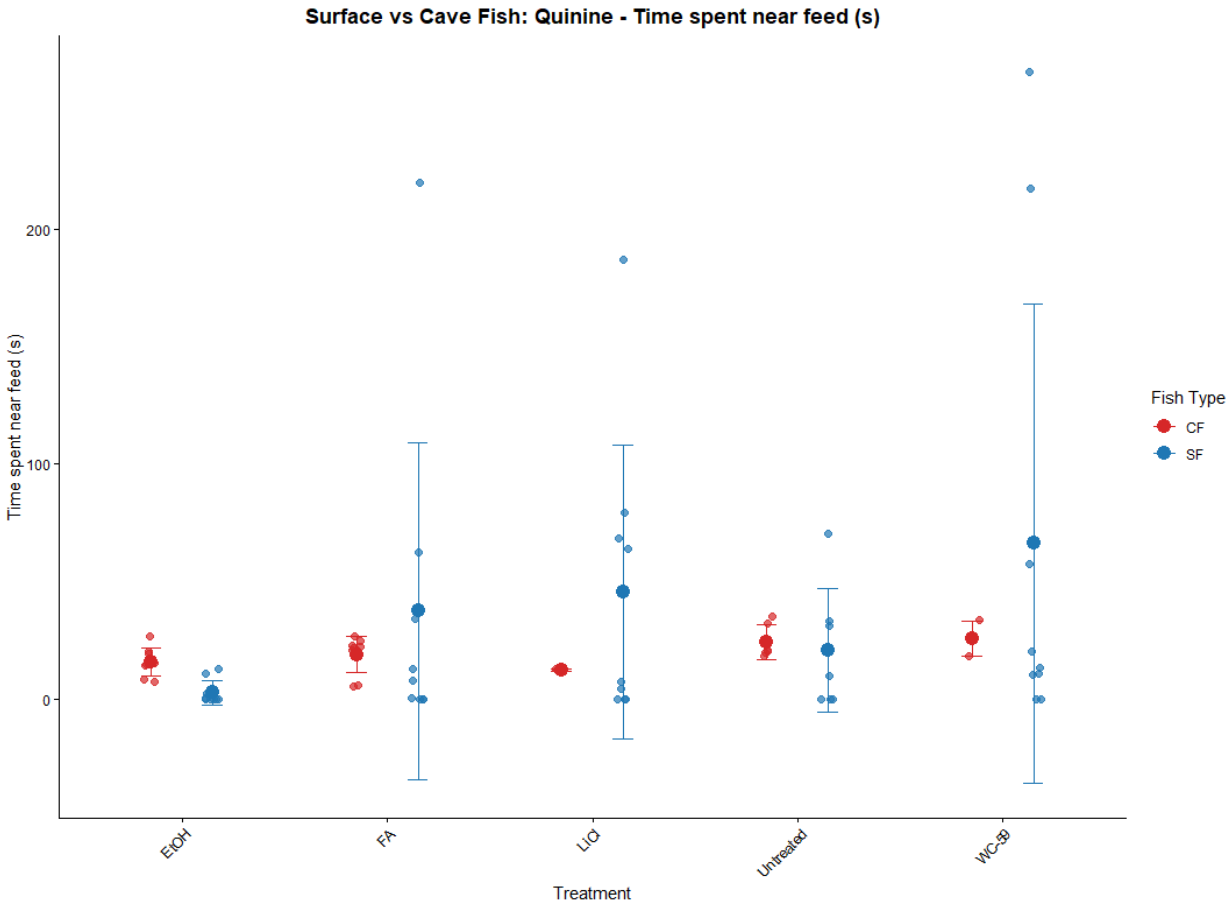

FIGURE 4.35: Chemosensory feeding behavior associated with average time near quinine feed across treatment conditions in surface and cave morph larvae. Average time near quinine feed was measured for surface fish and cavefish larvae following different treatment conditions (Control, EtOH, FA, LiCl, and WC-59 treatments). Individual points represent measurements from individual trials, diamonds indicate the mean, and error bars represent ± standard deviation. Pairwise comparison was conducted between surface fish and cavefish for quinine feed.

Significance levels: p ≤ 0.05 (*),p ≤ 0.01 (**),p ≤ 0.001 (***), p ≤ 0.0001 (****).

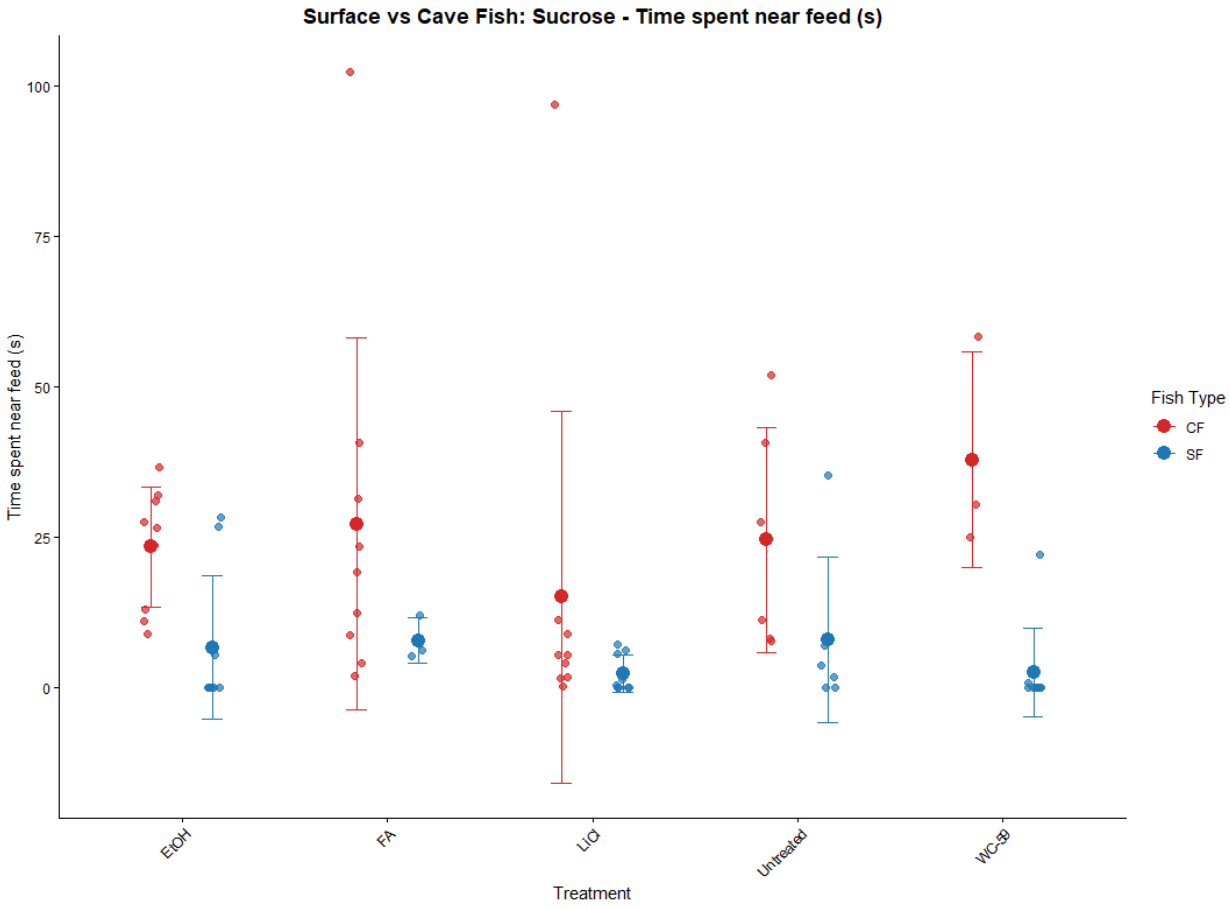

FIGURE 4.36: Chemosensory feeding behavior associated with average time near sucrose feed across treatment conditions in surface and cave morph larvae. Average time near sucrose feed was measured for surface fish and cavefish larvae following different treatment conditions (Control, EtOH, FA, LiCl, and WC-59 treatments). Individual points represent measurements from individual trials, diamonds indicate the mean, and error bars represent ± standard deviation. Pairwise comparison was conducted between surface fish and cavefish for sucrose feed.

Significance levels: p ≤ 0.05 (*),p ≤ 0.01 (**),p ≤ 0.001 (***), p ≤ 0.0001 (****).

Behavioral Assay: Velocity per treatments for feeding type

Average swimming velocity was measured for SF and Pachón CF across different feeding conditions (control, EtOH, quinine, and sucrose) and treatment groups.

When comparing untreated SF and untreated Pachón CF across feeding conditions, no statistically significant differences in average velocity were detected between morphs (FIGURE 4.37). However, Pachón CF generally exhibited slightly higher average velocities compared to SF, while SF displayed greater variance in swimming velocity across samples.

A similar pattern was observed when comparing EtOH treated SF and Pachón CF. No statistically significant differences were detected between morphs across feeding conditions, although EtOH treated Pachón CF again exhibited slightly higher average velocities than SF (FIGURE 4.38).

When comparing folic acid treated SF and Pachón CF, no statistically significant differences in velocity were detected between morphs across feeding conditions. Pachón CF continued to exhibit slightly higher average velocities compared to SF (FIGURE 4.39).

Finally, when examining LiCl treated groups, no statistically significant differences in average velocity were observed between SF and Pachón CF across feeding conditions (FIGURE 4.40).

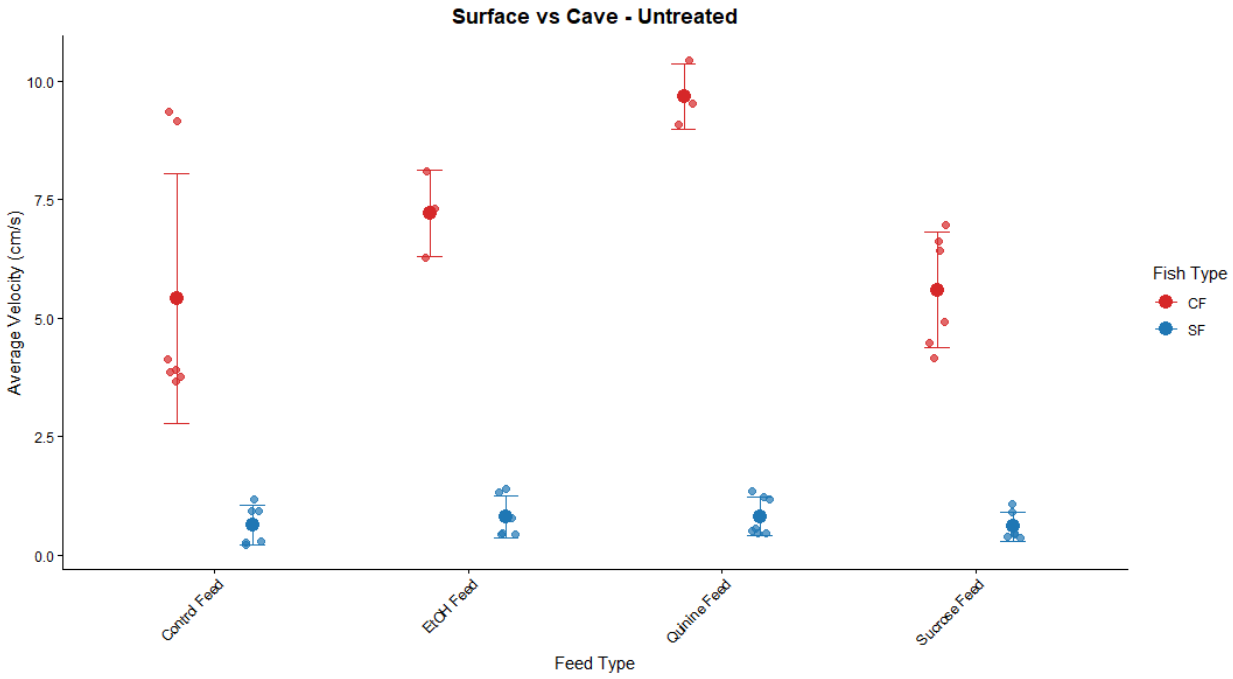

FIGURE 4.37: Chemosensory feeding behavior associated with average velocity of untreated surface and cavefish larvae. Average swimming velocity during feeding trials was measured for surface fish and cavefish under different feeding types (Control, EtOH, Quinine and Sucrose feeds). Individual points represent measurements from individual trials, diamonds indicate the mean, and error bars represent ± standard deviation. Pairwise comparison was conducted between untreated surface fish and cavefish morphs within individual treatment types.

Significance levels: $p \leq 0.05$ (*), $p \leq 0.01$ (**), $p \leq 0.001$ (***), $p \leq 0.0001$ (****).

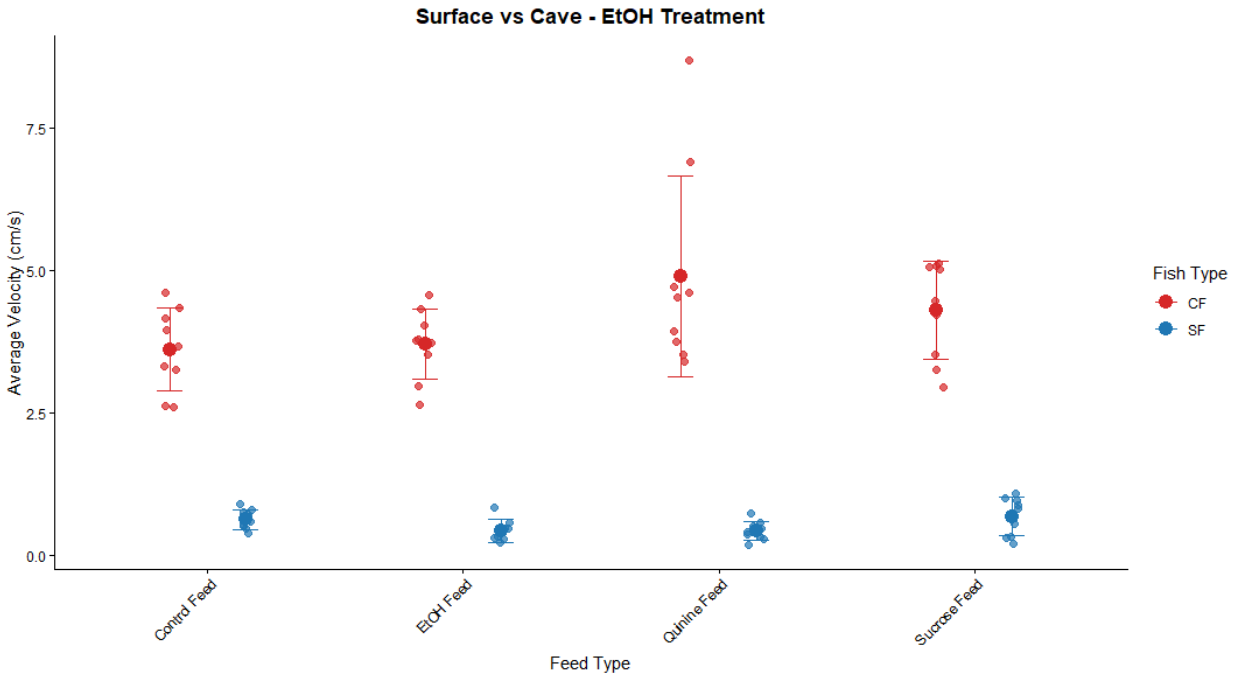

FIGURE 4.38: Chemosensory feeding behavior associated with average velocity of EtOH treated surface and cavefish larvae. Average swimming velocity during feeding trials was measured for EtOH treated surface fish and cavefish under different feeding types (Control, EtOH, Quinine and Sucrose feeds). Individual points represent measurements from individual trials, diamonds indicate the mean, and error bars represent ± standard deviation. Pairwise comparison was conducted between EtOH treated surface fish and cavefish for individual feeding type.

Significance levels: $p \leq 0.05$ (*), $p \leq 0.01$ (**), $p \leq 0.001$ (***), $p \leq 0.0001$ (****).

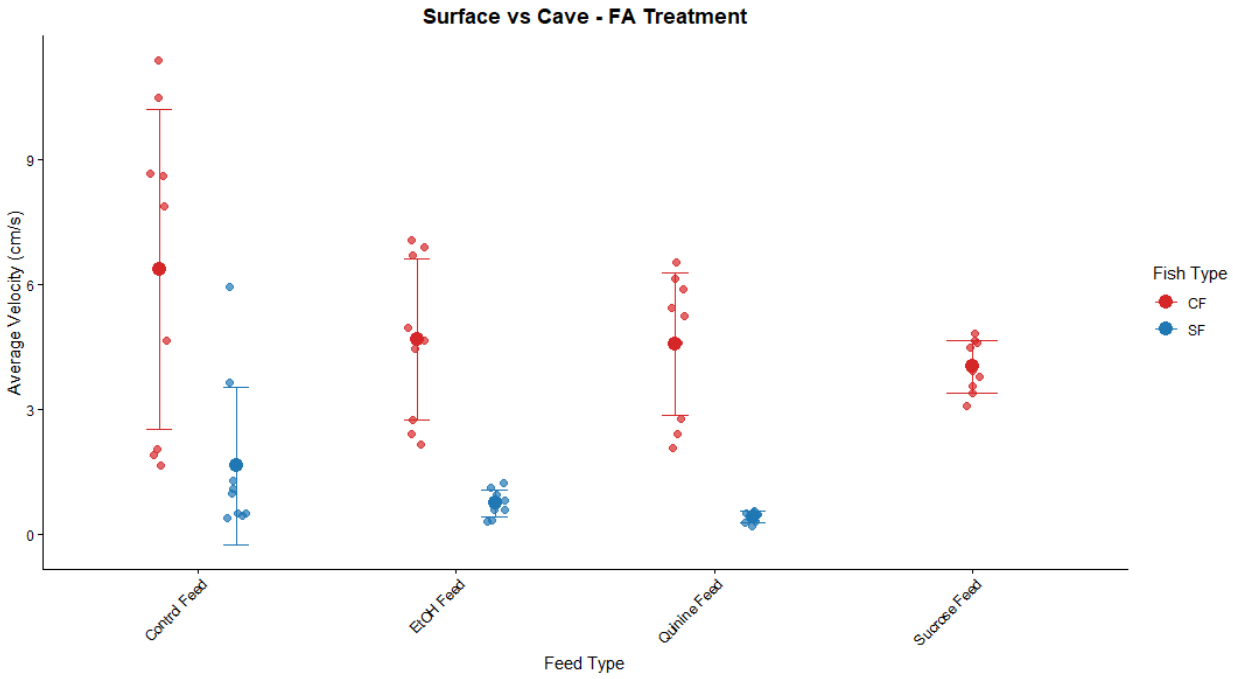

FIGURE 4.39: Chemosensory feeding behavior associated with average velocity of folic acid treated surface and cave morph larvae. Average swimming velocity during feeding trials was measured for folic acid treated surface fish and cavefish under different feeding types (Control, EtOH, Quinine and Sucrose feeds). Individual points represent measurements from individual trials, diamonds indicate the mean, and error bars represent ± standard deviation. Pairwise comparison was conducted between untreated surface fish and cavefish for individual feeding type.

Significance levels: $p \leq 0.05$ (*),$p \leq 0.01$ (**),$p \leq 0.001$ (***), $p \leq 0.0001$ (****).

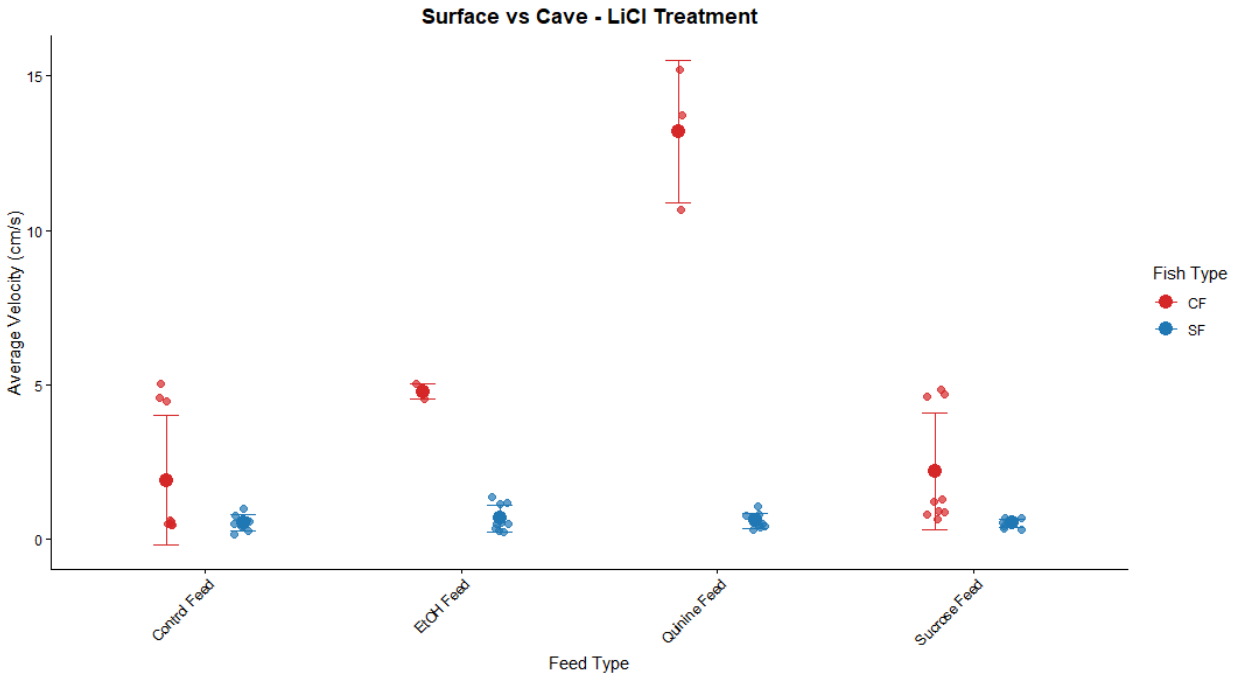

FIGURE 4.40: Chemosensory feeding behavior associated with average velocity of LiCl treated surface and cavefish larvae. Average swimming velocity during feeding trials was measured for EtOH treated surface fish and cavefish under different feeding types (Control, EtOH, Quinine and Sucrose feeds). Individual points represent measurements from individual trials, diamonds indicate the mean, and error bars represent ± standard deviation. Pairwise comparison was conducted between surface and cave morphs within individual feeding type. Pairwise comparison was conducted for LiCl treated surface fish between individual feeding type.

Significance levels: $p \leq 0.05$ (*), $p \leq 0.01$ (**), $p \leq 0.001$ (***), $p \leq 0.0001$ (****).

Behavioral Assay: Velocity per treatments comparing feed type towards individual treatments

Average swimming velocity was compared between individual treatment groups of SF and Pachón CF across different feeding conditions (control, EtOH, quinine, and sucrose).

When comparing average velocity between SF and Pachón CF across individual treatments, no statistically significant differences were observed between the two morphs (FIGURE 4.41). However, Pachón CF generally exhibited slightly higher average velocities compared to SF.

A similar pattern was observed under EtOH feeding conditions. No statistically significant differences in velocity were detected between SF and Pachón CF across treatments (FIGURE 4.42).

Under quinine feeding conditions, average velocities were comparable between SF and Pachón CF, with no statistically significant differences observed between morphs (FIGURE 4.43).

Under sucrose feeding conditions, no statistically significant differences in velocity were detected between SF and Pachón CF (FIGURE 4.44), although SF generally displayed lower average velocities compared to CF.

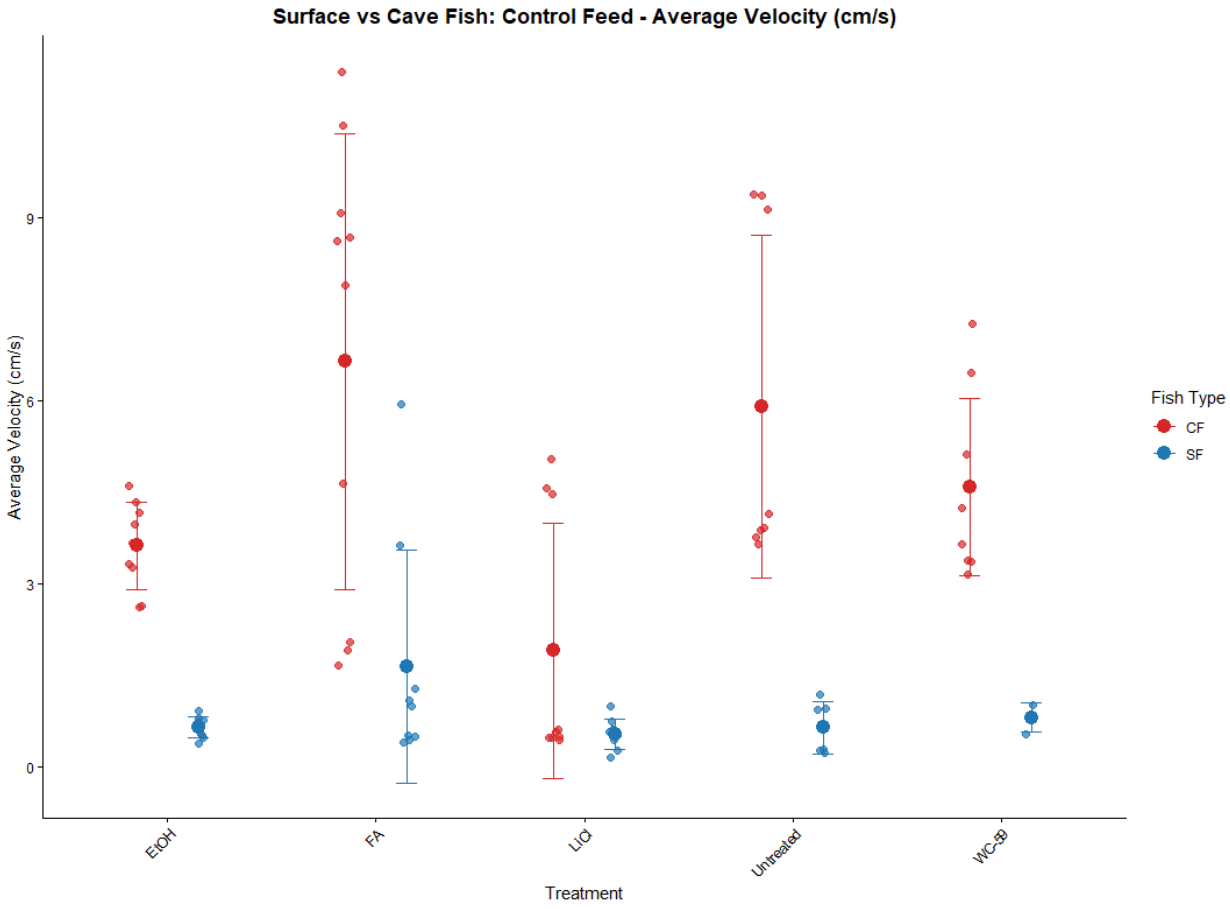

FIGURE 4.41: Chemosensory feeding behavior associated with average velocity within control feed across treatment conditions in surface and cave morph larvae. Average velocity within control feeding trials was measured for surface fish and cavefish larvae following different treatment conditions (Control, EtOH, FA, LiCl). Individual points represent measurements from individual trials, diamonds indicate the mean, and error bars represent ± standard deviation. Pairwise comparison was conducted between surface fish and cavefish for control feed.

Significance levels: p ≤ 0.05 (*),*p ≤ 0.01 (**),p ≤ 0.001 (***),* p ≤ 0.0001 (****).

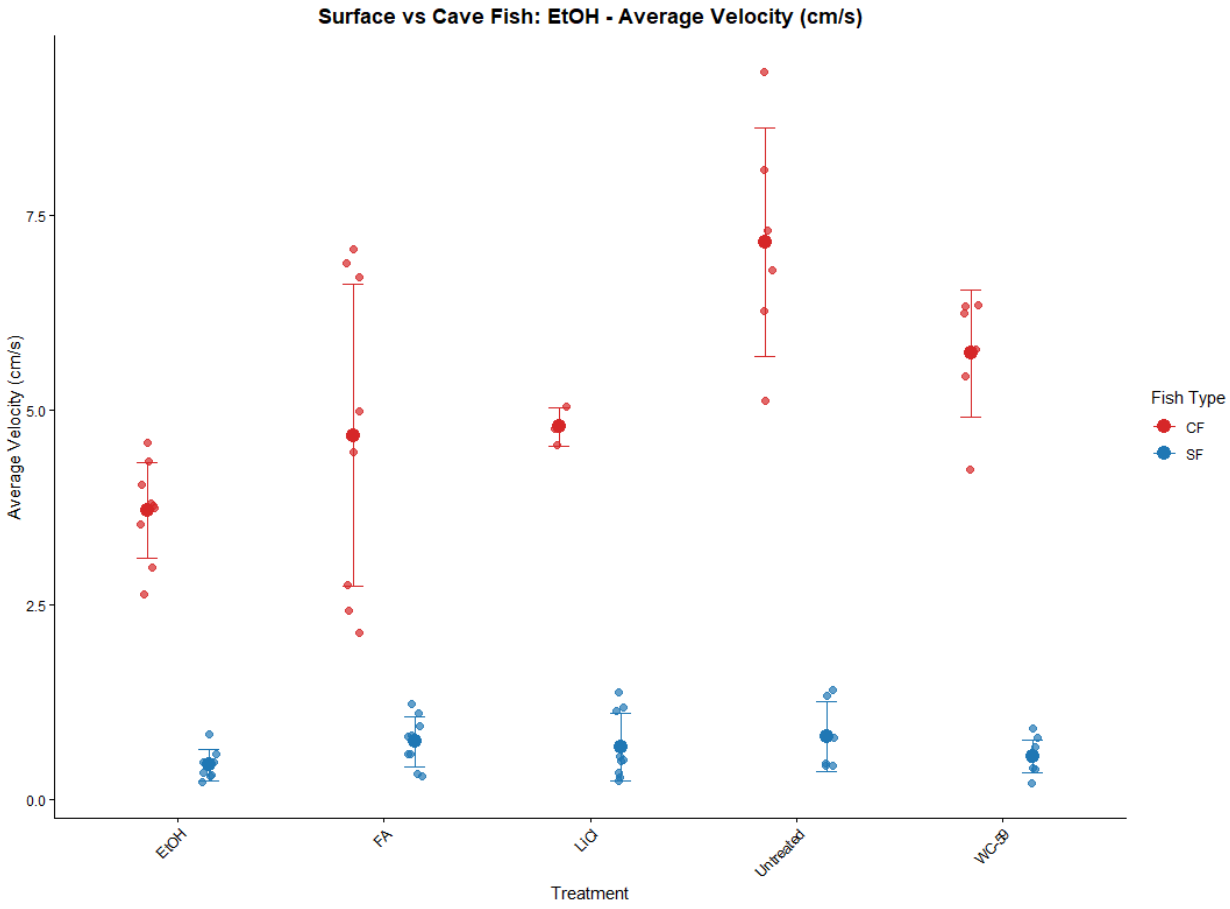

FIGURE 4.42: Chemosensory feeding behavior associated with average velocity within EtOH feed across treatment conditions in surface and cave morph larvae. Average velocity within EtOH feeding trials was measured for surface fish and cavefish larvae following different treatment conditions (Control, EtOH, FA, LiCl, and WC-59 treatments). Individual points represent measurements from individual trials, diamonds indicate the mean, and error bars represent ± standard deviation. Pairwise comparison was conducted between surface fish and cavefish for EtOH feed.

Significance levels: p ≤ 0.05 (*),*p ≤ 0.01 (**),p ≤ 0.001 (***),* p ≤ 0.0001 (****).

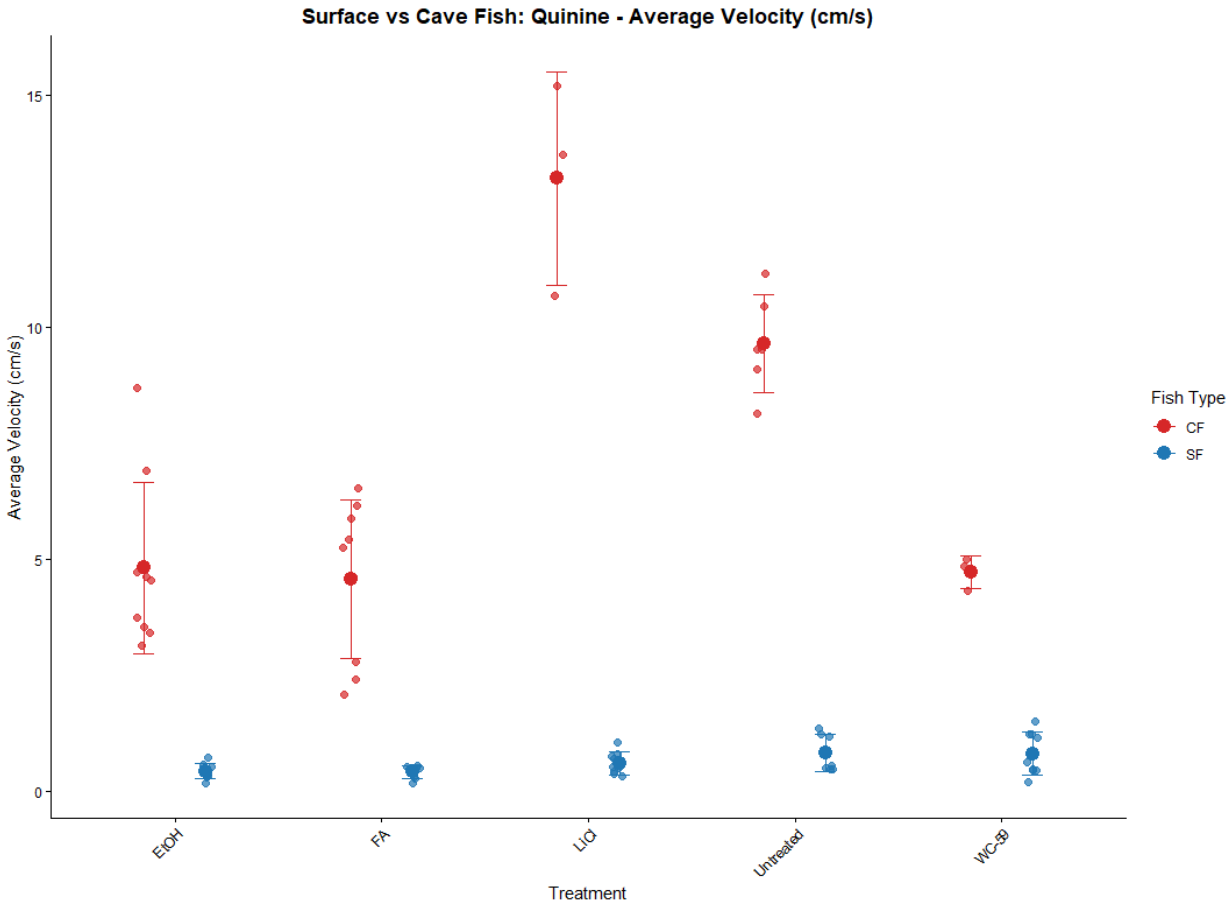

FIGURE 4.43: Chemosensory feeding behavior associated with average velocity within Quinine feed across treatment conditions in surface and cave morph larvae. Average velocity within quinine feeding trials was measured for surface fish and cavefish larvae following different treatment conditions (Control, EtOH, FA, LiCl, and WC-59 treatments). Individual points represent measurements from individual trials, diamonds indicate the mean, and error bars represent ± standard deviation. Pairwise comparison was conducted between surface fish and cavefish for Quinine feed.

Significance levels: p ≤ 0.05 (*),*p ≤ 0.01 (**),p ≤ 0.001 (***),* p ≤ 0.0001 (****).

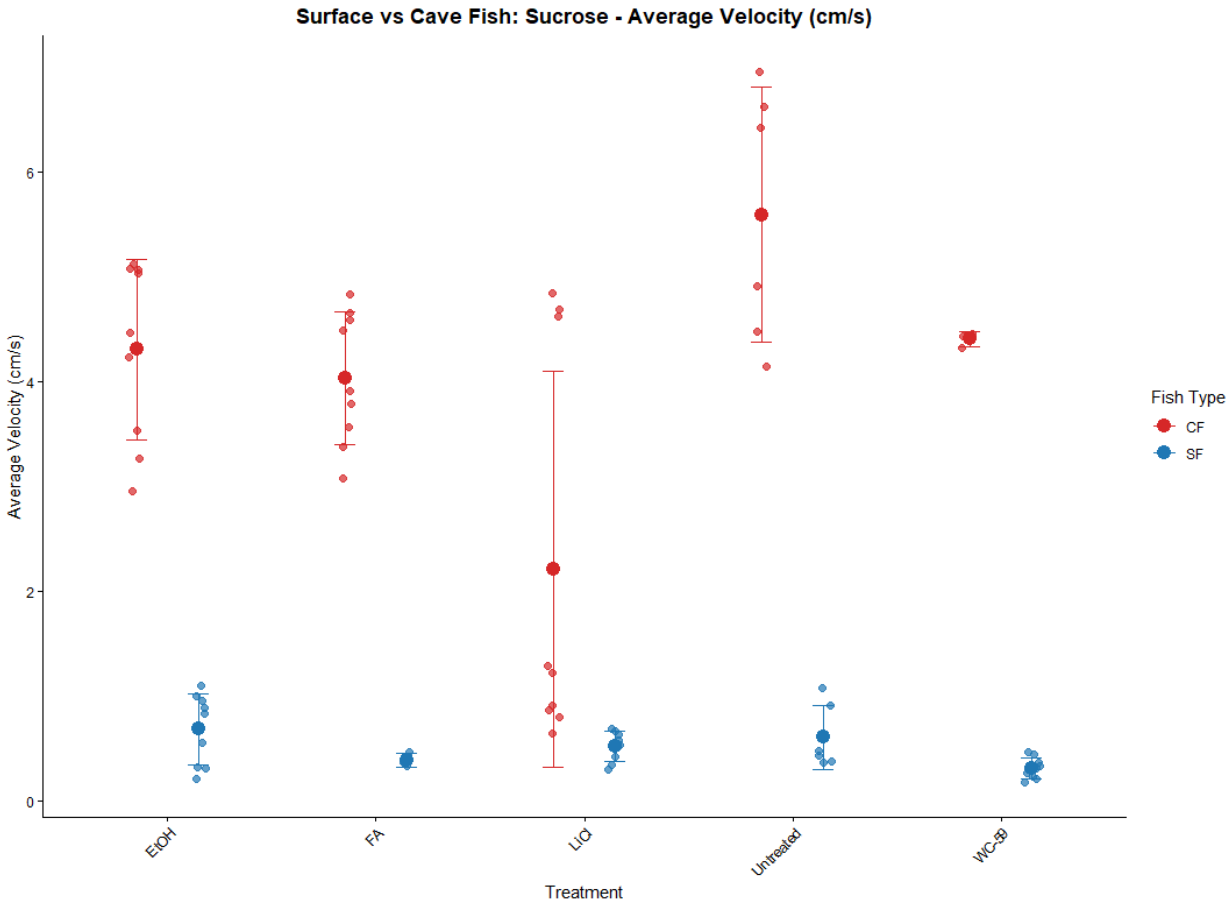

FIGURE 4.44: Chemosensory feeding behavior associated with average velocity within sucrose feed across treatment conditions in surface and cave morph larvae. Average velocity within sucrose feeding trials was measured for surface fish and cavefish larvae following different treatment conditions (Control, EtOH, FA, LiCl, and WC-59 treatments). Individual points represent measurements from individual trials, diamonds indicate the mean, and error bars represent ± standard deviation. Pairwise comparison was conducted between surface fish and cavefish for sucrose feed.

Significance levels: p ≤ 0.05 (*),*p ≤ 0.01 (**),p ≤ 0.001 (***),* p ≤ 0.0001 (****).

Chapter 5: Discussion

Sensory Morphology and Craniofacial Development

The study examined morphological and behavioural differences between SF and Pachón CF morphs of *Astyanax mexicanus*, focusing on taste bud development within the external mandible of the fish and feeding related behaviors during larval development. Quantitative analysis of taste bud number, diameter, and spatial organization revealed consistent developmental differences between the two morphs.

Although early developmental stages showed relatively similar numbers of taste buds between the two morphs, later developmental stages demonstrated expanded gustatory morphology within Pachón CF. CF frequently exhibited increased taste bud diameter and greater spacing between taste bud containing regions compared with SF. Similar expansions of non-visual sensory systems have been documented in cave populations of *Astyanax mexicanus*[70].

Such modifications are commonly thought to be compensatory adaptations associated with regressive eye evolution and life in darkness. CF populations frequently show loss of visual sensory systems together with expansion of mechanosensory neuromasts and gustatory receptors, which are thought to improve detection of environmental cues for the presence of food sources in the absence of visual input[71]. In addition to sensory changes, CF populations also exhibit modifications to craniofacial skeletal structures, including differences in jaw morphology and cranial architecture relative to SF [18,72]. Some cave populations have been shown to possess broader craniofacial structures and differences in bite mechanics, suggesting relatively larger or modified jaw structures that may enhance feeding efficiency in cave environments [18,73]. The increased taste bud size and spacing observed in Pachón CF in this study may therefore reflect

an adaptive enhancement of the gustatory sensory system that facilitates efficient food detection within cave environments.

Regional Development of Taste buds

In addition to overall morphological differences, this study examined the spatial organisation of taste bud containing regions (T1–T4) along the external surface of the mandible. Developmental analysis revealed that taste buds emerge sequentially during larval development, with certain regions appearing later in development. Taste bud development followed a region specific temporal sequence across the mandible, with T1, T3, and T4 taste buds first observed at 8 dpf, indicating that these regions represent the earliest detectable sites of gustatory development. This conclusion is supported by the presence of comparable taste bud counts and spatial patterning in SF at the same developmental stage, suggesting that initial taste bud formation is conserved between the two morphs, with divergence occurring later in development. Further support for this temporal sequence is provided by changes in taste bud diameter over time, where T1 taste buds reached a diameter of approximately 50 µm earlier than other regions, indicating earlier maturation. In contrast, T3 and T4 taste buds reached similar diameters at approximately the same developmental stage, suggesting concurrent development, while T2 taste buds appeared last, reaching comparable size only at later time points. This developmental pattern was largely conserved across both morphs, as taste bud diameter changes followed similar trajectories, except for T2, which was absent in SF across all stages examined. The earlier maturation of T1 taste buds may reflect regional differences in the timing of taste bud differentiation, potentially ensuring the early establishment of sensory structures involved in food detection. Conversely, the delayed development of T2 and concurrent maturation of T3 and

T4 suggest that taste bud development is regulated in a region-specific manner rather than occurring uniformly across the oral cavity. The conservation of these developmental trajectories between morphs further suggests that the temporal patterning of taste bud maturation is a robust developmental feature of Astyanax mexicanus.

These findings suggest that regional sensory patterning differs between the two morphs and may involve heterochronic developmental changes. Heterochrony, defined as evolutionary changes in the timing of developmental processes, has been proposed as an important mechanism underlying morphological differences between cave and surface populations of *Astyanax mexicanus* [70]. Alterations in developmental signaling pathways can modify the timing and spatial patterning of craniofacial structures, including sensory tissues.

Changes in craniofacial patterning may influence the distribution of sensory structures such as taste buds across the mandible. Increased spacing between taste bud regions in Pachón CF may increase the sensory coverage of the oral surface, potentially improving the ability to detect chemical cues associated with food sources within the aquatic environment. Studies examining taste bud development in *Astyanax mexicanus* have also demonstrated differences in taste bud patterning between cave and surface morphs, while comparative analyses of craniofacial traits indicate that CF exhibit evolutionary divergence in feeding related cranial structures and bite morphology[18,21,73].Together, these findings suggest that the spatial expansion of gustatory structures observed in this study may reflect broader developmental changes in craniofacial architecture associated with cave adaptation.

While a hypothetical developmental pattern of early taste bud formation between the two morphs can be inferred from these findings, further investigation is required to refine this framework. Future studies should incorporate more closely spaced developmental time points to better resolve the temporal sequence of taste bud emergence. In particular, inclusion of earlier stages prior to 8 dpf, as well as intermediate stages between 15 and 30 dpf, would allow for a more precise characterization of region specific development and the timing of divergence between morphs. Such approaches would strengthen the resolution of this proposed developmental model and provide greater insight into the mechanisms underlying gustatory patterning.

Effects of Chemical Perturbations on Gustatory Development

To investigate developmental mechanisms regulating gustatory sensory patterning and craniofacial development, this study examined the effects of chemical perturbation of the canonical Wnt-signaling pathway known to influence craniofacial and sensory organ development. Treatments included alcohol (EtOH), LiCl, folic acid, and the Wnt signaling inhibitor WC-59. Compounds containing documented effects upon canonical Wnt/β-catenin signaling and neural crest development, both of which play crucial roles in craniofacial morphogenesis and oral sensory tissue formation [49–52,54–58,74].

Canonical Wnt/β-catenin signaling is a key regulatory pathway involved in epithelial–mesenchymal interactions that guide the development of craniofacial structures and sensory organs. In gustatory tissues, Wnt signaling has been shown to initiate taste papilla development and regulate taste bud formation [26,28]. Activation of β-catenin signaling promotes taste papilla

formation, whereas disruption of the pathway can prevent papilla initiation and alter gustatory organ patterning [26]. Because neural crest–derived mesenchyme contributes to the development and structural support of oral tissues, perturbations in Wnt signaling or neural crest cell survival have the potential to influence the formation and spatial organization of taste buds[23,52,58].

Despite the theoretical importance of these pathways in sensory organ development, the treatments applied in this study produced relatively limited and inconsistent effects on taste bud morphology. While some statistically significant differences were detected among treatment groups at specific developmental stages or within individual taste bud regions, these effects were not consistently observed across developmental time points or across the different morphological parameters examined. Instead, the most consistent pattern observed throughout the dataset was the inherent morphological divergence between SF and Pachón CF morphs.

Alcohol exposure is a well established teratogenic factor that can disrupt embryonic development through suppression of canonical Wnt signaling and induction of apoptosis in neural crest cell populations [38,75]. Neural crest cells contribute extensively to craniofacial mesenchyme and are essential for the development of oral tissues and facial structures[52,57]. Consequently, alcohol mediated disruption of neural crest development has been associated with the craniofacial abnormalities characteristic of FASD[34,47,76]. Although alcohol has been shown to reduce β-catenin dependent transcription and impair craniofacial morphogenesis in experimental models, alcohol treatment in the present study produced only modest and inconsistent changes in taste bud morphology across developmental stages[38].

LiCl, in contrast, functions as a pharmacological activator of canonical Wnt signaling by inhibiting GSK-3β, thereby stabilizing β-catenin and promoting transcription of Wnt target genes involved in developmental patterning[49,60]. Activation of Wnt signaling can influence neural crest specification and craniofacial development and therefore might be expected to alter gustatory organ formation[56,58]. However, LiCl treatment did not produce consistent increases in taste bud number or diameter relative to control groups, suggesting that the timing or dosage of Wnt pathway activation may not have been sufficient to substantially alter gustatory development during the stages examined.

Similarly, WC-59 functions as a small molecule inhibitor of Wnt signaling by blocking the acyltransferase Porcupine (PORCN), an enzyme required for Wnt ligand maturation and secretion[61]. Because Wnt signaling is required for taste papilla initiation, inhibition of this pathway could theoretically suppress gustatory organ formation[26]. In the present study, several statistically significant differences were detected in WC-59 treated groups, particularly in later developmental stages; however, these differences were not consistently observed across all morphological measurements, suggesting that inhibition of Wnt signaling produced only modest alterations in taste bud morphology.

Folic acid supplementation was included due to its role in nucleotide synthesis and DNA methylation processes that support normal embryonic development[62,63]. Adequate folate availability is essential for neural crest development and craniofacial morphogenesis, and folate supplementation has been shown to mitigate certain developmental defects associated with environmental teratogens. However, folic acid treatment in this study did not produce consistent changes in taste bud number, diameter, or spatial organization, suggesting that folate

supplementation did not substantially influence gustatory development within the experimental conditions used.

The relatively limited treatment effects observed in this study may reflect the inherent robustness of developmental regulatory networks. Biological systems frequently maintain stable developmental outcomes despite moderate environmental or molecular perturbations, a property referred to as developmental robustness[77]. Signaling pathways such as Wnt interact with multiple regulatory networks during embryogenesis, which can buffer developmental processes against transient perturbations[78,79]. Additionally, gustatory organ patterning may occur within specific developmental windows that were not fully captured within the treatment period examined.

Although treatment effects were generally modest, some morphological differences appeared more frequently within Pachón CF compared with SF. Cave populations of *Astyanax mexicanus* have undergone extensive evolutionary divergence affecting craniofacial structures, sensory systems, and developmental signaling pathways[11,70]. These evolutionary modifications may influence the responsiveness of developmental regulatory networks to environmental or pharmacological perturbations. However, because treatment effects in the present study were relatively limited and inconsistent, further investigation would be required to determine whether CF exhibit increased developmental sensitivity to signaling pathway disruption.

Morph-Specific Chemosensory Behavior in *Astyanax mexicanus*

The behavioral assays conducted in this study examined whether developmental exposure to pharmacological modulators of Wnt signaling (LiCl and WC-59), folic acid supplementation, or

alcohol altered chemosensory driven feeding behavior in surface and cave morphs of *Astyanax mexicanus*. Across multiple feeding stimuli, including control agar, sucrose, alcohol, and quinine, no statistically significant treatment effects were detected for time spent near feed, distance to feed, or locomotor velocity. Instead, behavioral patterns were largely consistent across treatment conditions. Suggesting that short-term developmental perturbations of Wnt signaling and related pathways did not produce measurable changes in chemosensory driven feeding engagement under the experimental conditions used and that most consistent behavioral differences observed in the dataset reflected inherent divergence between surface and cave morphotypes.

The absence of strong treatment, behavioral effects may reflect the inherent robustness of developmental systems controlling feeding behavior. Neural circuits regulating sensory processing and motor output are shaped through complex developmental pathways and may maintain functional stability despite moderate perturbations of individual signaling pathways[77–79]. Although Wnt signaling plays an important role in craniofacial development and sensory organ patterning, alterations to these pathways do not necessarily translate into immediate behavioral differences, particularly when compensatory developmental mechanisms can maintain overall sensory function[49–51].

Despite the lack of treatment related behavioral differences, morph-specific behavioral tendencies were observed. SF exhibited greater variability in spatial distribution and exploratory movement throughout the behavioral arena. This pattern may reflect the ecological context in which surface populations evolved. Surface dwelling *Astyanax mexicanus* inhabit riverine environments where prey detection often relies on the integration of multiple sensory

modalities, particularly visual cues combined with olfactory and gustatory information[11,70]. Under experimental conditions where visual cues were limited, SF may therefore exhibit more variable exploratory behavior rather than consistent localization near chemical feeding stimuli.

Some SF showed trends toward increased engagement near alcohol or quinine containing feeds relative to sucrose or control agar. However, these differences were not statistically significant and should therefore be interpreted cautiously. Teleost fishes possess complex gustatory and olfactory receptor systems capable of detecting a wide variety of chemical cues, including bitter compounds and alcohol related stimuli[45,46]. Behavioral responses to these compounds may therefore involve exploratory investigation rather than clear preference patterns, particularly when stimuli are presented in simplified laboratory contexts.

In typical experimental systems, developmental EtOH exposure has been shown to alter chemosensory responses rather than directly induce feeding preference changes. Studies demonstrate that early EtOH exposure can reduce aversion to bitter compounds such as quinine and increase behavioral acceptance of EtOH associated sensory cues[80–82]. These effects are attributed to experience dependent plasticity in gustatory and olfactory pathways, resulting in altered hedonic evaluation of chemical stimuli. As such, organisms exposed to EtOH during development often display increased engagement with otherwise aversive stimuli, reflecting changes in chemosensory processing rather than true preference.

Within this context, the trends observed in SF toward increased interaction with EtOH and quinine containing stimuli may reflect subtle modulation of chemosensory responsiveness or reduced aversion, rather than selective feeding preference. However, the lack of statistical

significance suggests that such effects are either modest in magnitude or dependent on exposure timing, dosage, or duration, which are known to influence EtOH induced chemosensory plasticity in other systems[80,83].

In contrast, cave morphs displayed relatively consistent engagement with all feed types across treatment conditions. This lack of clear preference patterns may reflect an opportunistic feeding strategy adapted to subterranean environments. Cave ecosystems are characterized by the absence of primary productivity and irregular food input, conditions that favor generalist feeding strategies capable of responding broadly to potential food signals[70]. Under these ecological constraints, responding to any available chemical cue may be advantageous compared with selective discrimination among specific food sources.

Numerous studies have demonstrated that CF possess enhanced non-visual sensory systems that support food detection in complete darkness. These adaptations include increased numbers of taste buds, expansion of bitter taste receptor gene families, and enhanced chemosensory sensitivity relative to surface morphs[20,21,39]. Additionally, CF exhibit enhanced mechanosensory lateral line systems that allow them to detect water movement associated with potential prey[71]. Together, these sensory adaptations allow CF to detect weak or diffuse food signals within complex cave environments.

Patterns of locomotor activity observed in this study were also consistent with previously reported CF behaviors. Cave morphs generally exhibited higher locomotor velocities and more persistent movement throughout the behavioral arena compared with SF. Increased locomotor activity has been described in CF populations and is thought to facilitate food searching in

environments where resources are sparse and unpredictably distributed[70,71]. Persistent exploratory movement may therefore increase encounter rates with food signals detected through chemosensory or mechanosensory pathways.

SF, in contrast, showed lower average locomotor velocities and more intermittent movement patterns. This behavior may reflect their continued reliance on visual cues for prey localization. In natural surface environments, visual information plays a central role in prey detection and feeding behavior. When visual cues are absent or reduced, SF may exhibit less directed feeding behavior, resulting in increased variability in spatial distribution relative to feeding stimuli.

Taken together, these findings support an ecological framework in which the two morphotypes exhibit distinct feeding strategies shaped by their evolutionary environments. SF appear to retain flexible sensory discrimination associated with visually guided feeding strategies, whereas CF display persistent locomotion and broad responsiveness to potential food cues. These differences likely reflect evolutionary adaptation to contrasting environments characterized by abundant visual information in surface habitats and perpetual darkness and limited resources in cave systems.

Importantly, these morph-specific behavioral patterns remained stable across all pharmacological treatments examined. The lack of consistent treatment effects suggests that the neural circuits governing chemosensory driven feeding behavior in *Astyanax mexicanus* are relatively robust to moderate developmental perturbations of Wnt signaling pathways. Although the treatments applied in this study may influence aspects of sensory organ development, the

behavioral outcomes measured here appear to be primarily shaped by evolutionary adaptation rather than acute pharmacological manipulation.

FASD-Relevant Interpretation of Ethanol and Folic Acid Effects

EtOH exposure was included in this study as a model of FASD, given its well established effects on CNCC development and craniofacial morphogenesis. Previous studies have demonstrated that EtOH exposure induces apoptosis in neural crest cell populations and disrupts their migration, contributing to the craniofacial abnormalities observed in FASD[76,84] .These effects are partly mediated through disruption of canonical Wnt/β-catenin signaling, where EtOH exposure alters intracellular calcium signaling and destabilizes β-catenin, reducing transcriptional activity required for normal craniofacial development[76].Based on these findings, EtOH treatment in the present study was expected to produce measurable alterations in gustatory development.

However, the relatively limited and inconsistent effects observed suggest that the experimental conditions did not strongly disrupt the developmental processes underlying taste bud formation. One important factor is the timing of exposure. In this study, treatment was administered at approximately 10 hpf, representing a restricted developmental window. In contrast, EtOH exposure in human FASD typically occurs chronically across multiple stages of pregnancy. The severity of EtOH induced defects is highly dependent on the timing of exposure, with early developmental stages showing greater sensitivity compared to later stages[85]. As such, the timing and duration of exposure in this model may not fully capture the cumulative effects associated with FASD. This limitation also applies to the other treatments used in this study, including folic

acid and Wnt pathway modulators, as developmental sensitivity to these perturbations is similarly time dependent.

In addition to timing, the modest effects observed suggest that mechanisms beyond neural crest disruption may contribute to craniofacial and sensory development. While neural crest cells play a central role in craniofacial morphogenesis, other processes such as epithelial–mesenchymal interactions and tissue specific signaling networks are also critical for proper development . The absence of strong phenotypic changes in this study may therefore reflect compensatory developmental mechanisms or pathway redundancy that maintain structural integrity despite perturbation.

Folic acid supplementation was examined as a potential mitigating factor, given its role in nucleotide synthesis and methylation processes essential for neural crest development. Previous studies have shown that folate derivatives can reduce EtOH induced defects and improve neural crest cell survival and migration[83].

In the present study, however, folic acid treatment did not produce consistent changes in gustatory morphology, nor did it clearly counteract the modest effects observed with EtOH exposure. This suggests that, under the experimental conditions used, folate supplementation alone was not sufficient to significantly alter developmental outcomes. Together, these findings highlight the importance of exposure timing, dosage, and pathway interactions in determining sensitivity to EtOH and suggest that FASD related mechanisms may not uniformly affect all craniofacial and sensory structures.

Chapter 6: Conclusion

Conclusion

This study shows that differences in gustatory morphology, development, and chemosensory attractive behavior between SF and Pachón CF are consistent and morph dependent. These traits emerge during development and remain stable despite chemical perturbations. Across all analyses, the clearest pattern was the inherent divergence between morphs rather than treatment driven effects.

Gustatory morphology was similar at early stages but diverged over time. CF showed increased taste bud size and greater spatial distribution at later stages. This pattern was supported by region specific development across the mandible. Taste buds appeared sequentially, with T1, T3, and T4 emerging earlier, while T2 appeared later. Notably, T2 was only observed in CF within the stages examined. These findings suggest that differences in timing and spatial organization contribute to distinct sensory structures between morphs.

Chemical perturbations targeting canonical Wnt signaling produced limited and inconsistent effects. Some differences were observed at specific stages, but these were not maintained across time points or regions. Overall, the treatments did not significantly alter taste bud morphology. Similarly, chemosensory attraction behavior was not affected by treatment. There were no consistent changes in time near feed, distance to feed, or locomotor activity.

Instead, behavioral differences were driven by morphotype. SF showed more variable and exploratory movement. CF displayed more consistent engagement with feed and higher locomotor activity. These patterns suggest different feeding strategies that reflect their respective environments.

Together, these results indicate that both morphological and behavioral traits are primarily shaped by developmental processes and evolutionary history. They are not easily altered by short-term pharmacological manipulation. This supports the idea that these systems are relatively robust under the conditions tested.

There are several limitations to consider. The developmental time points used may not capture the earliest stages of taste bud formation. Additional time points would improve resolution of developmental timing. Treatment effects may also depend on dosage and exposure timing, which were limited in this study. Molecular analyses were not included, so underlying mechanisms could not be directly assessed. Techniques such as quantitative PCR or transcriptomic analysis would help link observed phenotypes to gene expression. Finally, behavioral assays were conducted in simplified conditions, which may not reflect natural environments.

Future work should focus on earlier and more detailed developmental sampling. It should also refine treatment conditions to better target key developmental windows. Incorporating molecular approaches will be important for understanding the mechanisms involved. Expanding behavioral assays to more complex environments may also provide further insight into feeding strategies.

Overall, this study demonstrates that sensory morphology and chemosensory attractive behavior in *Astyanax mexicanus* are developmentally regulated and strongly influenced by morphotype. These findings provide a foundation for future studies on the mechanisms underlying sensory evolution.

Appendix:

Appendix A: WHOLE-MOUNT PONCEAU S STAINING PROTOCOL

1 Sample Collection and Preparation

Larval samples of *Astyanax mexicanus* were collected at 8, 15, and 30 dpf and processed immediately for whole-mount staining. Specimens were euthanized using 0.1% MS-222 prior to staining.

2 Preparation of Staining Solution

The staining solution consisted of:

- 0.5% Ponceau S (CAS: 6226-79-5)
- Prepared in 0.3 M trichloroacetic acid (TCA) (Sigma-Aldrich, CAS: 76-03-9)

The solution was adjusted to pH 0.9 using a Fisher Scientific AB150 pH/mV meter.
All staining solution was prepared fresh and maintained at room temperature prior to use.

3 Staining Procedure

1. Following euthanasia, larvae were transferred into the staining solution using a plastic pipette.
2. Individual specimens were immersed in the staining solution for **20 seconds** to allow rapid labeling of external structures.
3. Staining was performed in small volumes to ensure consistent exposure across samples.

4 Washing Procedure

1. Immediately following staining, samples were rinsed in distilled water.
2. Washing was performed for **20 seconds** with gentle agitation to remove excess dye.
3. This step was optimized to reduce background staining while preserving structural contrast.

Appendix B: PREPARATION OF 1% AGAR MOUNTING AND FEEDING BLOCKS

1 Reagents and Materials

- Agar powder
- Distilled water
- 50 mL glass flask or beaker
- Heating source (e.g., hot plate or microwave)
- Stirring rod or magnetic stirrer
- 9 cm diameter Petri dishes
- Cutting tool (e.g., sterile blade or scalpel)
- Chemical stimuli:
    - Sucrose (1 M)
    - Quinine (3 mM)
    - Ethanol (EtOH, 1%)

2 Preparation of 1% Agar Solution

A 1% (w/v) agar solution was prepared as follows:

1. Agar powder was weighed and added to distilled water at a concentration of **1 g per 100 mL**.
2. For standard preparation volumes, **50 mL** of solution was prepared per flask (0.5 g agar in 50 mL distilled water).
3. The mixture was gently stirred to disperse the agar prior to heating.

3 Dissolution and Melting

1. The agar solution was heated using a hot plate or microwave until fully dissolved.
2. The average melting temperature for agar ranged between **85–95°C**.
3. Heating was continued until the solution became clear, indicating complete dissolution of the agar.
4. Care was taken to avoid overheating or excessive evaporation.

4 Cooling and Handling

1. Following dissolution, the agar solution was allowed to cool briefly to a manageable temperature while remaining in liquid form.
2. The solution was used immediately after cooling to prevent premature solidification.

5 Preparation of Feeding Blocks with Chemical Stimuli

Agar-based feeding blocks were prepared using the same 1% agar solution with incorporation of chemical treatments:

1. Following dissolution, chemical stimuli were added to the molten agar prior to solidification to ensure uniform distribution. Final concentrations were:
    - **Sucrose (1 M)**
    - **Quinine (3 mM)**
    - **Ethanol (EtOH, 1%)**
2. Control blocks consisted of unflavoured 1% agar prepared under identical conditions without added stimuli.
3. The treated agar solution was poured into **9 cm diameter Petri dishes** to form a uniform layer.
4. Agar was allowed to fully solidify at room temperature.
5. Solidified agar was cut into **1 cm × 1 cm × 1 cm cubic blocks** using a sterile blade or scalpel.
6. Individual feeding blocks were placed at a fixed position along the edge of each Petri dish during behavioral assays to ensure consistent spatial presentation.

Notes on Consistency

To ensure reproducibility across experiments:

- Agar concentration (1% w/v) was kept constant across all preparations.
- Volume per preparation (50 mL per flask) was standardized.
- Chemical stimuli were added at consistent final concentrations.
- Feeding block dimensions (1 cm^3) and placement within Petri dishes were standardized.
- Heating and cooling conditions were controlled to maintain uniform agar properties.

Appendix C: USE OF ARTIFICIAL INTELLIGENCE (AI) TOOLS

1 AI Assistance Statement

Portions of this thesis were edited for clarity, grammar, and formatting with the assistance of ChatGPT (OpenAI).

2 Scope of Use

AI tools were used solely to support:

- Language editing and sentence clarity
- Formatting of sections (e.g., appendices and protocols)
- Minor restructuring for readability

AI tools were **not used** for:

- Data analysis or statistical calculations
- Generation or interpretation of experimental results
- Creation of FIGUREs, raw data, or primary scientific content

3 Author Responsibility

All scientific content, experimental design, data interpretation, and conclusions presented in this thesis are the sole responsibility of the author. All outputs generated with AI assistance were reviewed, verified, and edited as necessary prior to inclusion.

References:

1. Ericsson, A. C., Crim, M. J. & Franklin, C. L. A Brief History of Animal Modeling. *Mo. Med.* **110**, 201–205 (2013).
2. Barré-Sinoussi, F. & Montagutelli, X. Animal models are essential to biological research: issues and perspectives. *Future Sci. OA* **1**, FSO63 (2015).
3. Perlman, R. L. Mouse models of human disease: An evolutionary perspective. *Evol. Med. Public Health* **2016**, 170–176 (2016).
4. Kaplan, B. L. F. *et al.* Protecting Human and Animal Health: The Road from Animal Models to New Approach Methods. *Pharmacol. Rev.* **76**, 251–266 (2024).
5. Mukherjee, P., Roy, S., Ghosh, D. & Nandi, S. K. Role of animal models in biomedical research: a review. *Lab. Anim. Res.* **38**, 18 (2022).
6. Chang, M. C. J. & Grieder, F. B. The continued importance of animals in biomedical research. *Lab Anim.* **53**, 295–297 (2024).
7. Iwaya, C., Suzuki, A., Shim, J., Kim, A. & Iwata, J. Craniofacial bone anomalies related to cholesterol synthesis defects. *Sci. Rep.* **14**, 5371 (2024).
8. Choi, T.-Y., Choi, T.-I., Lee, Y.-R., Choe, S.-K. & Kim, C.-H. Zebrafish as an animal model for biomedical research. *Exp. Mol. Med.* **53**, 310–317 (2021).
9. Schartl, M. Beyond the zebrafish: diverse fish species for modeling human disease. *Dis. Model. Mech.* **7**, 181–192 (2014).
10. Domínguez-Oliva, A. *et al.* The Importance of Animal Models in Biomedical Research: Current Insights and Applications. *Anim. Open Access J. MDPI* **13**, 1223 (2023).
11. Perera, P. P., Guerra, D. P. & Riddle, M. R. The Mexican Tetra, Astyanax mexicanus, as a Model System in Cell and Developmental Biology. *Annu. Rev. Cell Dev. Biol.* **39**, 23–44 (2023).

12. Cobham, A. E. *et al.* Cave adaptation favors aging resilience in the Mexican tetra. *Npj Metab. Health Dis.* **3**, 33 (2025).
13. Borowsky, R. Restoring sight in blind cavefish. *Curr. Biol.* **18**, R23–R24 (2008).
14. Atukorala, A. D. S., Bhatia, V. & Ratnayake, R. Craniofacial skeleton of MEXICAN tetra (Astyanax mexicanus): As a bone disease model. *Dev. Dyn.* **248**, 153–161 (2019).
15. Bilandžija, H. *et al.* Phenotypic plasticity as a mechanism of cave colonization and adaptation. *eLife* **9**, e51830.
16. Simon, V. *et al.* Comparing growth in surface and cave morphs of the species Astyanax mexicanus: insights from scales. *EvoDevo* **8**, 23 (2017).
17. Gross, J. B. & Powers, A. K. A Natural Animal Model System of Craniofacial Anomalies: The Blind Mexican Cavefish. *Anat. Rec.* **303**, 24–29 (2020).
18. Powers, A. K. *et al.* Genetic mapping of craniofacial traits in the Mexican tetra reveals loci associated with bite differences between cave and surface fish. *BMC Ecol. Evol.* **23**, 41 (2023).
19. Goel, G., Sanghai, N., Tranmer, G. K. & Atukorallaya, D. Spatial Distribution and Temporal Dynamics of Neomycin-Induced Neuromast Cell Damage and Regeneration in the Mexican tetra (Astyanax mexicanus). *Cells* **14**, 1680 (2025).
20. Shiriagin, V. & Korsching, S. I. Massive Expansion of Bitter Taste Receptors in Blind Cavefish, Astyanax mexicanus. *Chem. Senses* **44**, 23–32 (2019).
21. Varatharasan, N., Croll, R. P. & Franz-Odendaal, T. Taste bud development and patterning in sighted and blind morphs of Astyanax mexicanus. *Dev. Dyn. Off. Publ. Am. Assoc. Anat.* **238**, 3056–3064 (2009).
22. Chandrashekar, J., Hoon, M. A., Ryba, N. J. P. & Zuker, C. S. The receptors and cells for mammalian taste. *Nature* **444**, 288–294 (2006).

23. Liu, H.-X., Komatsu, Y., Mishina, Y. & Mistretta, C. M. Neural crest contribution to lingual mesenchyme, epithelium and developing taste papillae and taste buds. *Dev. Biol.* **368**, 294–303 (2012).
24. Beites, C. L., Kawauchi, S., Crocker, C. E. & Calof, A. L. Identification and molecular regulation of neural stem cells in the olfactory epithelium. *Exp. Cell Res.* **306**, 309–316 (2005).
25. Zhang, J. *et al.* Sour Sensing from the Tongue to the Brain. *Cell* **179**, 392-402.e15 (2019).
26. Liu, F. *et al.* Wnt-beta-catenin signaling initiates taste papilla development. *Nat. Genet.* **39**, 106–112 (2007).
27. Hall, J. M. H., Bell, M. L. & Finger, T. E. Disruption of sonic hedgehog signaling alters growth and patterning of lingual taste papillae. *Dev. Biol.* **255**, 263–277 (2003).
28. Iwatsuki, K. *et al.* Wnt signaling interacts with Shh to regulate taste papilla development. *Proc. Natl. Acad. Sci.* **104**, 2253–2258 (2007).
29. Piarowski, C. M., Isner, T. J. & Barlow, L. A. Developing and regenerating a sense of taste. *Curr. Top. Dev. Biol.* **165**, 353–404 (2025).
30. Silva, P., Azimian Zavareh, P. & Atukorallaya, D. Teleost Fish as Model Animals to Understand Alcohol Teratology. in *Fetal Alcohol Spectrum Disorder: Advances in Research and Practice* (eds Chudley, A. E. & Hicks, G. G.) 31–48 (Springer US, New York, NY, 2022). doi:10.1007/978-1-0716-2613-9_3.
31. Youngentob, S. L. & Glendinning, J. I. Fetal ethanol exposure increases ethanol intake by making it smell and taste better. *Proc. Natl. Acad. Sci. U. S. A.* **106**, 5359–5364 (2009).
32. Hannigan, J. H., Chiodo, L. M., Sokol, R. J., Janisse, J. & Delaney-Black, V. Prenatal alcohol exposure selectively enhances young adult perceived pleasantness of alcohol odors. *Physiol. Behav.* **148**, 71–77 (2015).

33. Duko, B. *et al.* Prenatal alcohol exposure and offspring subsequent alcohol use: A systematic review. *Drug Alcohol Depend.* **232**, 109324 (2022).

34. Riley, E. P., Infante, M. A. & Warren, K. R. Fetal alcohol spectrum disorders: an overview. *Neuropsychol. Rev.* **21**, 73–80 (2011).

35. Jones, KennethL. & Smith, DavidW. RECOGNITION OF THE FETAL ALCOHOL SYNDROME IN EARLY INFANCY. *The Lancet* **302**, 999–1001 (1973).

36. Boggs, K. *et al.* Contribution of Underlying Connective Tissue Cells to Taste Buds in Mouse Tongue and Soft Palate. *PLOS ONE* **11**, e0146475 (2016).

37. Gundogan, F. *et al.* Chronic Prenatal Ethanol Exposure Disrupts WNT Signaling In Adolescent Cerebella. *J. Clin. Exp. Pathol.* **3**, 1–11 (2013).

38. Flentke, G. R., Garic, A., Amberger, E., Hernandez, M. & Smith, S. M. The Calcium-Mediated Repression of β-Catenin and Its Transcriptional Signaling Mediates Neural Crest Cell Death in an Avian Model of Fetal Alcohol Syndrome. *Birt. Defects Res. A. Clin. Mol. Teratol.* **91**, 591–602 (2011).

39. Bibliowicz, J. *et al.* Differences in chemosensory response between eyed and eyeless Astyanax mexicanus of the Rio Subterráneo cave. *EvoDevo* **4**, 25 (2013).

40. Piekarski, N., Gross, J. B. & Hanken, J. Evolutionary innovation and conservation in the embryonic derivation of the vertebrate skull. *Nat. Commun.* **5**, 5661 (2014).

41. Noden, D. M. & Schneider, R. A. Neural Crest Cells and the Community of Plan for Craniofacial Development. in *Neural Crest Induction and Differentiation* (ed. Saint-Jeannet, J.-P.) 1–23 (Springer US, Boston, MA, 2006). doi:10.1007/978-0-387-46954-6_1.

42. Sharpe, P. T. Dental mesenchymal stem cells. *Development* **143**, 2273–2280 (2016).

43. Raterman, S. T., Metz, J. R., Wagener, F. A. D. T. G. & Von den Hoff, J. W. Zebrafish Models of Craniofacial Malformations: Interactions of Environmental Factors. *Front. Cell Dev. Biol.* **8**, 600926 (2020).

44. Bloomquist, R. F. *et al.* Coevolutionary patterning of teeth and taste buds. *Proc. Natl. Acad. Sci. U. S. A.* **112**, E5954-5962 (2015).

45. Roper, S. D. & Chaudhari, N. Taste buds: cells, signals and synapses. *Nat. Rev. Neurosci.* **18**, 485–497 (2017).

46. Doty, R. L. Treatments for smell and taste disorders: A critical review. *Handb. Clin. Neurol.* **164**, 455–479 (2019).

47. Popova, S., Dozet, D., Shield, K., Rehm, J. & Burd, L. Alcohol's Impact on the Fetus. *Nutrients* **13**, 3452 (2021).

48. Lussier, A. A. *et al.* DNA methylation as a predictor of fetal alcohol spectrum disorder. *Clin. Epigenetics* **10**, 5 (2018).

49. Komiya, Y. & Habas, R. Wnt signal transduction pathways. *Organogenesis* **4**, 68–75 (2008).

50. Liu, J. *et al.* Wnt/β-catenin signalling: function, biological mechanisms, and therapeutic opportunities. *Signal Transduct. Target. Ther.* **7**, 1–23 (2022).

51. Clevers, H. & Nusse, R. Wnt/β-catenin signaling and disease. *Cell* **149**, 1192–1205 (2012).

52. Mayor, R. & Theveneau, E. The neural crest. *Development* **140**, 2247–2251 (2013).

53. Hari, L. *et al.* Lineage-specific requirements of beta-catenin in neural crest development. *J. Cell Biol.* **159**, 867–880 (2002).

54. Alam, S., Duncan, D. & Hasan, S. Profilin and Non-Canonical Wnt Signaling: Coordinating Cytoskeletal Dynamics from Development to Disease. *J. Dev. Biol.* **13**, 31 (2025).

55. De Calisto, J., Araya, C., Marchant, L., Riaz, C. F. & Mayor, R. Essential role of non-canonical Wnt signalling in neural crest migration. *Dev. Camb. Engl.* **132**, 2587–2597 (2005).

56. Maj, E. *et al.* Controlled levels of canonical Wnt signaling are required for neural crest migration. *Dev. Biol.* **417**, 77–90 (2016).

57. LaBonne, C. Vertebrate Development: Wnt Signals at the Crest. *Curr. Biol.* **12**, R743–R744 (2002).

58. Ji, Y., Hao, H., Reynolds, K., McMahon, M. & Zhou, C. J. Wnt Signaling in Neural Crest Ontogenesis and Oncogenesis. *Cells* **8**, 1173 (2019).

59. Groenewald, W., Lund, A. H. & Gay, D. M. The Role of WNT Pathway Mutations in Cancer Development and an Overview of Therapeutic Options. *Cells* **12**, (2023).

60. Klein, P. S. & Melton, D. A. A molecular mechanism for the effect of lithium on development. *Proc. Natl. Acad. Sci. U. S. A.* **93**, 8455–8459 (1996).

61. Proffitt, K. D. *et al.* Pharmacological inhibition of the Wnt acyltransferase PORCN prevents growth of WNT-driven mammary cancer. *Cancer Res.* **73**, 502–507 (2013).

62. Blom, H. J., Shaw, G. M., den Heijer, M. & Finnell, R. H. Neural tube defects and folate: case far from closed. *Nat. Rev. Neurosci.* **7**, 724–731 (2006).

63. Ly, A., Hoyt, L., Crowell, J. & Kim, Y.-I. Folate and DNA Methylation. *Antioxid. Redox Signal.* **17**, 302–326 (2012).

64. Bhatia, V. *et al.* Extraoral expression and characterization of bitter taste receptors in Astyanax mexicanus (Mexican tetra fish). *FASEB BioAdvances* **4**, 574–584 (2022).

65. Hinaux, H. *et al.* A Developmental Staging Table for *Astyanax mexicanus* Surface Fish and Pachón Cavefish. *Zebrafish* **8**, 155–165 (2011).

66. Koontz, A., Urrutia, H. A. & Bronner, M. E. Making a head: Neural crest and ectodermal placodes in cranial sensory development. *Semin. Cell Dev. Biol.* **138**, 15–27 (2023).

67. Robea, M. A., Petrovici, A., Ureche, D., Nicoara, M. & Ciobica, A. S. Histopathological and Behavioral Impairments in Zebrafish (Danio rerio) Chronically Exposed to a Cocktail of Fipronil and Pyriproxyfen. *Life* **13**, 1874 (2023).

68. Lemly, A. D. & Smith, R. J. F. A behavioral assay for assessing effects of pollutants on fish chemoreception. *Ecotoxicol. Environ. Saf.* **11**, 210–218 (1986).

69. Kowalko, J. E. *et al.* Convergence in feeding posture occurs through different genetic loci in independently evolved cave populations of Astyanax mexicanus. *Proc. Natl. Acad. Sci. U. S. A.* **110**, 16933–16938 (2013).

70. Jeffery, W. R. Regressive Evolution in *Astyanax* Cavefish. *Annu. Rev. Genet.* **43**, 25–47 (2009).

71. Yoshizawa, M., Gorički, Š., Soares, D. & Jeffery, W. R. Evolution of a Behavioral Shift Mediated by Superficial Neuromasts Helps Cavefish Find Food in Darkness. *Curr. Biol.* **20**, 1631–1636 (2010).

72. Atukorala, A. D. S., Bhatia, V. & Ratnayake, R. Craniofacial skeleton of MEXICAN tetra (Astyanax mexicanus): As a bone disease model. *Dev. Dyn.* **248**, 153–161 (2019).

73. Powers, A. K., Berning, D. J. & Gross, J. B. Parallel evolution of regressive and constructive craniofacial traits across distinct populations of Astyanax mexicanus cavefish. *J. Exp. Zoolog. B Mol. Dev. Evol.* **334**, 450–462 (2020).

74. Hari, L. *et al.* Lineage-Specific Requirements of β-Catenin in Neural Crest Development. *J. Cell Biol.* **159**, 867–880 (2002).

75. Laksitorini, M. D. *et al.* Impact of Wnt/β-catenin signaling on ethanol-induced changes in brain endothelial cell permeability. *J. Neurochem.* **157**, 1118–1137 (2021).

76. Smith, S. M., Garic, A., Flentke, G. R. & Berres, M. E. Neural Crest Development in Fetal Alcohol Syndrome. *Birth Defects Res. Part C Embryo Today Rev.* **102**, 210–220 (2014).

77. Kitano, H. Biological robustness. *Nat. Rev. Genet.* **5**, 826–837 (2004).

78. Robustness and Evolvability in Living Systems | Princeton University Press. https://press.princeton.edu/books/paperback/9780691134048/robustness-and-evolvability-in-living-systems (2007).

79. Pigliucci, M. Is evolvability evolvable? *Nat. Rev. Genet.* **9**, 75–82 (2008).

80. Arias, C. & Gabriela Chotro, M. Interactions between prenatal ethanol exposure and postnatal learning about ethanol in rat pups. *Alcohol* **40**, 51–59 (2006).

81. Youngentob, S. L. & Glendinning, J. I. Fetal ethanol exposure increases ethanol intake by making it smell and taste better. *Proc. Natl. Acad. Sci. U. S. A.* **106**, 5359–5364 (2009).

82. Glendinning, J. I. *et al.* Fetal alcohol exposure reduces responsiveness of taste nerves and trigeminal chemosensory neurons to ethanol and its flavor components. *J. Neurophysiol.* **118**, 1198–1209 (2017).

83. Arias, C. & Chotro, M. G. Increased palatability of ethanol after prenatal ethanol exposure is mediated by the opioid system. *Pharmacol. Biochem. Behav.* **82**, 434–442 (2005).

84. Smith, S. M., Garic, A., Berres, M. E. & Flentke, G. R. Genomic factors that shape craniofacial outcome and neural crest vulnerability in FASD. *Front. Genet.* **5**, 224 (2014).

85. Goodlett, C. R. & Horn, K. H. Mechanisms of Alcohol-Induced Damage to the Developing Nervous System. *Alcohol Res. Health* **25**, 175–184 (2001).

86. Hall, B. The Neural Crest and Neural Crest Cells in Vertebrate Development and Evolution. in 159–177 (2009). doi:10.1007/978-0-387-09846-3_5.

87. Shi, Y. *et al.* 5-mehtyltetrahydrofolate rescues alcohol-induced neural crest cell migration abnormalities. *Mol. Brain* **7**, 67 (2014).